

Synthesis of Cadmium Selenide

Quantum Dots and Their Cytotoxicity

A thesis submitted to the University of East Anglia

for the degree of Master of Science by Research

By

Ruoxi Liu

School of Chemistry

University of East Anglia

Norwich NR4 7TJ

October 2013

©This copy of thesis has been supplied on condition that anyone who consults it is understood to recognize that its copyright rests with the author and that use of any information derived there from must be in accordance with current UK Copyright Law. In addition, any quotation or extract must include full attribution.

Declaration

I declare that the work contained in this thesis submitted by me for the degree of Master of science by Research is my own work, except where due reference is made to other authors, and has not previously been submitted by me for a degree at this or any other university.

Ruoxi Liu

Acknowledgement

I would like to thank my supervisors Dr. Yimin Chao and Dr. Yongping Bao for their esteemed supervision, inspiration and constructive criticism throughout my research work.

I also thank Dr. Qi Wang, Mr Shane Ashby, Mr Jason Thomas, MS Wei Wang and all the members in both Dr. Chao's and Dr. Bao's research groups for their support.

I am one of the co-authors for a manuscript, "protective effect of sulforaphane on CdSe quantum dot-induced cytotoxicity in human hepatocytes", which has been submitted to Free Radical Biology and Medicine (2014).

Abstract

Cadmium selenide (CdSe) nanoparticles (NPs) have applications in biomedical, biochemistry, bioimaging areas through different methods such as cell labelling and drug delivery (Chapter 1). This study aims to test the optical and biological properties of CdSe NPs so that its applications can be improved in these areas in the future.

Three types of CdSe NPs have been synthesised using a wet chemical method with the molar ratio of Cd:Se 10:1, 4:1 and 1:1. The observed luminescence of the CdSe NPs was strong and stable. The maxima PL spectrum peak of the CdSe (10:1) nanoparticles was around 590 nm and the ultraviolet-visible absorption (UV-Vis) spectrum showed a peak between 530-550 nm. The photoluminescence peak of CdSe (4:1) was the same as CdSe (10:1) and the UV-Vis spectrum showed a peak at about 550 nm. The aging studies indicate that sodium citrate (a stabiliser) could enhance the stability of the CdSe NPs. For example, the CdSe NPs with 0.2% sodium citrate were more stable than 0.05% (Chapter 3). Using this property, more stable encapsulated drugs could be made in the future to improve the clinical treatment method (Chapter 1).

Cell toxicity of the CdSe NPs was evaluated through the use of 3-(4,5-Dimethylthiazol-2-yl)-2,5-diphenyltetrazolium bromide (MTT) assay. The MTT results show that the more Cadmium ions accumulated in HHL-5 cells, the greater the cell toxicity is. The results (keeping the cadmium level constant) also indicate that CdSe NPs with a cadmium to selenite ratio with 10:1 (CdSe (10:1)) had the strongest toxicity in HHL-5 cell of all these three kinds of CdSe NPs tested. Conversely, the CdSe (1:1) has the lowest toxicity among all. The results indicated that the toxicity of the cadmium were very obvious so that we need to avoid accumulation of cadmium in clinical. In addition, the confocal images in MCF-7 cells also reflect the relative toxicities of the CdSe NPs. The results of the confocal images indicated that the higher concentrations of the CdSe NPs in the cells, the greater the observed toxicity is.

Moreover, all the experiments in this study (aging, TEM, quantum yield, MTT, confocal) are surrounding 9 kinds of CdSe NPs without any other parameters, which are novel and unique.

Table of contents

CHAPTER 1. INTRODUCTION AND GENERAL BACKGROUND

1.1	Nanoparticles and their applications	1
1.1.1	Optical characteristics of Nanoparticles and their applications	4
1.1.2	Nanotoxicity and applications	5
1.2	Quantum dots and their applications	6
1.2.1	Optical properties of Quantum dots and their applications.....	7
1.2.2	Cytotoxicity of Quantum dots and their application	9
1.3	Cadmium selenide nanoparticles and their applications	10
1.3.1	Optical properties and applications of CdSe NPs	12
1.3.2	The cytotoxicity of CdSe NPs and their applications.....	15
1.4	References	16

CHAPTER 2. EXPERIMENTAL METHODS

2.1	Synthesis of CdSe Nanoparticles by a microwave-assisted method	29
2.2	Photoluminescence spectroscopy	30
2.3	UV-Vis Spectroscopy	34
2.4	Quantum Yield Measurement	34
2.5	Transmission electron microscopy (TEM)	36
2.6	Cell Culture	37
2.7	MTT Cell Proliferation and Viability Assays	38
2.8	Confocal Laser Scanning Microscopy	39
2.9	Reference	41

CHAPTER 3. SYNTHESIS OF CDSE QUANTUM DOTS AND THEIR OPTICAL PROPERTIES

3.1	The stability and ageing results of the CdSe NPs	43
3.1.1	CdSe NPs (1:1) with 0.05%, 0.1% and 0.2% sodium citrate as stabilizer	44
3.1.2	CdSe NPs (4:1) with 0.05 %, 0.1 % and 0.2 % sodium citrate stabilizer	46
3.1.3	CdSe NPs (10:1) with 0.05 %, 0.1 % and 0.2 % sodium citrate stabilizer	48
3.2	The size of the CdSe NPs	49
3.2.1	Size calculation.....	49
3.2.2	TEM results of CdSe (10:1) with 0.05 %, 0.1 % and 0.2 % sodium citrate as stabilizer.....	51

3.2.3	TEM results of CdSe (4:1) with 0.05 %, 0.1 % and 0.2 % sodium citrate as stabilizer.....	53
3.2.4	TEM results of CdSe (1:1) with 0.05 %, 0.1 % and 0.2 % sodium citrate as stabilizer.....	55
3.3	The Quantum yield of the CdSe NPs	58
3.3.1	CdSe NPs (1:1) with 0.05 %, 0.1 % and 0.2 % sodium citrate stabilize.....	59
3.3.2	CdSe NPs (4:1) with 0.05 %, 0.1 % and 0.2 % sodium citrate stabilizer	63
3.3.3	CdSe NPs (10:1) with 0.05 %, 0.1 % and 0.2 % sodium citrate stabilizer	67
3.4	Reference.....	71

CHAPTER 4. CYTOTOXICITY AND IMAGING IN CELLS

4.1	Cytotoxicity in the immortalised human hepatocytes (HHL-5) cells	76
4.1.1	CdSe NPs (10:1) with 0.1 % and 0.2 % sodium citrate stabiliser	76
4.1.2	CdSe NPs (4:1) with 0.1 % and 0.2 % sodium citrate stabilizer	78
4.1.3	CdSe NPs (1:1) with 0.1 % and 0.2% sodium citrate stabilizer	79
4.2	Confocal Imaging results in MCF-7 cells	80
4.2.1	Confocal imaging of MCF-7 cells with medium control.....	81
4.2.2	Confocal imaging of MCF-7 cells in CdSe (10:1) with 0.1 % sodium citrate as stabilizer with concentration of 10 μ M without dialysis	82
4.2.3	Confocal imaging of MCF-7 cells in CdSe (10:1) with 0.1 % sodium citrate as stabilizer with concentration of 10 μ M after dialysis	83
4.2.4	Confocal imaging of MCF-7 cells in CdSe (10:1) with 0.1 % sodium citrate as stabilizer with concentration of 15 μ M before dialysis	84
4.2.5	Confocal imaging of MCF-7 cells in CdSe (10:1) with 0.1 % sodium citrate as stabilizer with concentration of 15 μ M after dialysis	85
4.3	Reference.....	86

CHAPTER 5. SUMMARY AND FUTURE WORK

5.1	Summary.....	88
5.2	Future work	91
5.3	Reference.....	92

List of Figures

Figure 1.1 particle in the box.....	2
Figure 1.2 The electrostatic repulsion mechanism of sodium citrate and CdSe NPs	12
Figure 2.1 Jablonski diagram. S_0 is the the electronic state (ground state). S_1 is the electronic state (excited state) and number 0-5 are vibrational levels.	30
Figure 2.2 a) Visible spectrum b) An excitation spectrum of the CdSe NPs samples.....	32
Figure 2.3 Diagram to explain how the spectrophotometer works.....	33
Figure 2.4 Quantum yield results of Quinine reference	35
Figure 2.5 24 wells plate plan for confocal microscopy.	40
Figure 2.6 Pick up the slices after 24 hours since the CdSeNPs were added into the cells.	41
Figure 3.1 The ageing spectrum of CdSe NPs (1:1) with 0.05% (A, B), 0.1% (C, D) or 0.2% (E, F) sodium citrate stabilizer.	45
Figure 3.2 The ageing spectrum of CdSe NPs (4:1) with 0.05 % (A, B), 0.1 % (C, D) or 0.2 % (E, F) sodium citrate stabilizer.....	47
Figure 3.3 Graph A, C and E demonstrate the photoluminescence spectrum of CdSe NPs (10:1) with 0.05 %, 0.1 % and 0.2 % sodium citrate stabilizer, respectively. The excitation was 345 nm. Filter cut-off at 390 nm. Graph B, D and F demonstrate the Ultraviolet-visible Spectrum of CdSe NPs (10:1) with 0.05 % , 0.1 % and 0.2 % sodium citrate stabilizer, respectively.	48
Figure 3.4 Quantum Yield results of CdSe (1:1) with 0.05 % , 0.1 % and 0.2 % sodium citrate stabilizer.....	60
Figure 3.5 Quantum Yield results of CdSe (4:1) with 0.05 % , 0.1 % and 0.2 % sodium citrate stabilizer.....	64
Figure 3.6 Quantum Yield results of CdSe (10:1) with 0.05 % , 0.1 % and 0.2 % sodium citrate stabilizer.....	68
Figure 4.1 The effect of CdSe NPs on proliferation of HHL-5 cells.....	76
Figure 4.2 The effect of CdSe NPs on proliferation of HHL-5 cells.....	78
Figure 4.3 The effect of CdSe NPs on proliferation of HHL-5 cells.....	79
Figure 4.4 Confocal Image of MCF-7 cells with medium control only.	81
Figure 4.5 Confocal Image of MCF-7 cells after exposure in 10 μ M CdSeNPs	82
Figure 4.6 Confocal Image of MCF-7 cells after exposure in 10 μ M CdSeNPs (after dialysis)	83
Figure 4.7 Confocal Image of MCF-7 cells after exposure in 15 μ M CdSNPs (before dialysis)	84
Figure 4.8 Confocal Image of MCF-7 cells after exposure in 15 μ M CdSeNPs (after dialysis)	85

List of tables

Table 2.4.1 Linear line absorbance vs integrated intensity of quinine reference	35
Table 3.1.1 The colour and stability of the CdSeNPs.....	43
Table 3.2.1 Diameter value of the CdSeNPs in theory	50
Table 3.2.2 The diameters of CdSe NPs measured by TEM. Mean \pm Standard deviation (SD), n=100.....	56
Table 3.3.1 Linear line absorbance vs integrated intensity of CdSe (1:1) with 0.05 %, 0.1 % and 0.2 % sodium citrate stabiliser.	61
Table 3.3.2 Linear line absorbance vs integrated intensity of CdSe (4:1) with 0.05 %, 0.1 % and 0.2 % sodium citrate stabiliser.	65
Table 3.3.3 Linear line absorbance vs integrated intensity of CdSe (10:1) with 0.05%, 0.1% and 0.2% sodium citrate stabiliser.	69
Table 3.3.4 The summary of quantum yield rate of CdSeNPs.....	70

Abbreviations

CdSe	Cadmium selenium
CO ₂	Carbon dioxide
DAPI	4', 6-diamidino-2-phenylindole
DMEM	Dulbecco's Modified Eagle Medium
DMSO	Dimethyl sulfoxide
DNA	Deoxyribonucleic acid
FBS	Fetal Bovine Serum
H ₂ O	Water or Hydrogen oxide
MTT	(3-(4,5-dimethylthiazol-2-yl)-2,5-diphenyltetrazolium bromide)
NPs	Nanoparticles
PBS	Phosphate buffered saline
PL	Photoluminescence
QD	Quantum dot
QY	Quantum Yield
TEM	Transmission Electron Microscopy
SuperSTEM	Super scanning transmission electron microscope
UV	Ultra Violet

Vis

Visible

Wt

Weight

w/v

Weight to volume ratio

Chapter 1. Introduction and general background

1.1 Nanoparticles and their applications

Over the past century, scientists have made many great voyages of discovery. In 1959 Richard Feynman said that ‘There’s Plenty of Room at the Bottom’, which indicated the potential in atomic and molecular scales, and in nanotechnology.¹ Nanotechnology, nanoparticle (NPs), can be defined as the manipulation of matter with at least one dimension in the nanoscale 1 to 100 nanometers, as defined by National Nanotechnology Initiative.¹ Because of this size range, nanotechnology has a diverse range of applications in many fields, such as energy, surface science, organic chemistry, molecular biology, medical technologies and semiconductor physics.^{2,3}

In nanotechnology, a particle is defined as a small object that behaves as a whole unit with respect to its transport and properties.⁴ Nanoparticles can be made by a wide variety of materials, including metals, semiconductors, organic materials or biomaterials. All these materials can be incorporated into nanomaterials. As defined above, a nanomaterial is a material with at least one external dimension in the nanoscale (1–100 nm); whereas a nanoparticle is defined as a material with all three external dimensions in the nanoscale.⁶

In some materials, when the particle size is reduced, a phenomenon called quantum confinement can be observed. Quantum confinement is the effect which can be observed for some nanomaterials/nanoparticles. When the particles size is similar or smaller than the exciton size this phenomenon will happen and it usually happens in a few nanometers.¹ Quantum confinement effect is the idea behind the “Particle in Box” model; it indicates that once the diameter of the material is of the same magnitude as the wavelength of the electron wave function. When materials are this small (which means

the particle size is similar or smaller than the exciton size, usually happens in a few nanometers), their electronic and optical properties deviate substantially from those of bulk materials.¹ This means that an electron cannot move freely as it in the bulk material so that its optical and electronic properties will be changed. The energy levels can then be modeled using the particle in a box model in which the energy of different states is dependent on the length of the box.¹ The particle in the box model could be explained by the difference between classical and quantum systems. In classical systems, a ball stuck inside a big box so that the particle can move with any speed in the box and it is no more likely to be found at one position than another.¹ By classical mechanics we could roll a particle along the x-axis in this box and predict its position at any later time (Figure 1.1, equation 1.1).¹ The potential energy in this model is given as

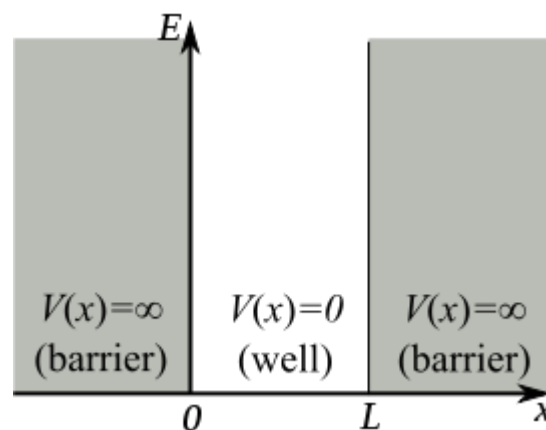


Figure 1.1 particle in the box

$$V(x) = \begin{cases} 0, & 0 < x < L, \\ \infty, & \text{otherwise,} \end{cases} \quad \text{Equation 1.1}$$

Where L is the length of the box and x is the position of the particle within the box. The electron moves between two walls at x=0 and x=L.¹ The potential energy of the particle is

zero between the walls and infinity at the walls. What this statement is saying is that the particle can only be between $x=0$ and $x=L$.¹

However, when the well becomes narrow (usually happens in a few nanometres), the particle could only occupy certain positive energy levels.¹ This means that the observable properties of the particle (such as its energy and position) are related to the mass of the particle and the width of the well.¹ In quantum mechanics, the wavefunction gives the most fundamental description of the behaviour of a particle; the measurable properties of the particle (such as its position, momentum and energy) may all be derived from the wavefunction.¹ For a particle inside the box a free particle wavefunction is appropriate, but since the probability of finding the particle outside the box is zero, the wavefunction must go to zero at the walls (which means $V=0$, equation 1.3).¹ The behaviour of a particle is completely specified quantum mechanically by the Schrödinger equation is given as:

$$\hat{H}\psi = E\psi \quad \text{Equation 1.2}$$

Where \hat{H} is the Hamiltonian that describes the system, and Ψ and E are eigenfunctions and eigenvalues.¹ When the Hamiltonian operator acts on a certain wave function Ψ , and the result is proportional to the same wave function Ψ , then Ψ is a stationary state, and the proportionality constant, E , is the energy of the state Ψ .¹ For any particle, the total energy of that particle is the sum of the kinetic and potential energy.¹

$$-\left[\frac{\hbar^2}{8\pi^2m} \frac{d^2}{dx^2} + V \right] \psi = E\psi \quad \text{Equation 1.3}$$

Where h is Planck's constant, m is the mass of the particle (an electron in this case), and V is the potential energy.¹ In summary, the quantum confinement effect theory explains why nanomaterial such as Ag nanoparticles will lose electric and heat conduction characteristics and become semiconductor.

Semiconductors have become a major interdisciplinary area of science. A semiconductor is a material which has an electrical conductivity between that of a conductor (for instance, copper) and insulator (such as glass).^{9, 10} The conductivity of a semiconductor will change with increasing temperature and shows opposite electrical conductivity characteristics to that of metal.⁹ This characteristic of semiconductors can be useful in a number of applications, for example in the fabrication of thin-film organic electronic devices.^{11, 12}

1.1.1 Optical characteristics of Nanoparticles and their applications

A characteristic of semiconductor nanoparticles is optical fluorescence. Fluorescence is the emission of light by a substance that has absorbed light or other electromagnetic radiation and is a form of luminescence.¹³ Photoluminescence (PL) describes the phenomenon of light emission from any form of matter after the absorption of photons (electromagnetic radiation) and is one of a number of forms of luminescence.¹⁴ According to the quantum size effect theory, when the size of a particle becomes extremely small, and the electronic wave function is confined, quantum-size effects (QSE) are expected to occur. When this happens, changes in the density of states, the transport properties and the optical properties that differ from the bulk material can be observed.¹⁵ Many optical techniques can be used to measure these characteristics of nanoparticles. Nanoparticles composed of different materials will have unique emission wavelengths, excitation

wavelengths and hence varied emission colours. A number of techniques use absorbance, emission or reflectance of light to obtain spectra to help characterize this optical properties.¹⁶⁻²⁴

With the help of Transmission electron microscopy (TEM) and Scanning electron microscopy (SEM), the size and the outline of individual nanoparticles can be measured and seen directly and clearly under the microscope. Due to the booming development of nanotechnology, the original TEM technology has been upgraded to Super STEM. Super STEM can even capture vivid single atom images, a dramatic improvement in image quality of nanoparticles.^{20, 22, 24-27}

1.1.2 Nanotoxicity and applications

In addition to the properties of nanoparticles discussed above, they can also display toxicity, also known as nanotoxicity. Nanotoxicology is the study of the toxicity of nanomaterials. With the rapid development of nanotechnology, the understanding of the nanotoxicity of nanomaterials and nano-enabled products has become more and more important in terms of both human and environmental health and safety. This concept is widely accepted by not only scientists but also by the public.³⁰ As a result the whole area of toxicity of nanoparticles has been and is still actively investigated.³¹

Due to their exciting electrical, optical and physical properties, nanoparticles have a wide range of applications in drug delivery, cancer treatment, diagnostics, photothermal therapy, bioimaging, biosensing, tissue engineering and bioterrorism prevention.^{32, 33} In particular; nanoparticles have a unique advantage in clinical studies due to their size and properties. For example, polymer nanoparticles can be used to encapsulate drugs so that

they can cure and prevent cancer. The tumor microenvironment is a special challenge for drug delivery. In the past, it has been difficult to target the specific tumor cells while ensuring minimal systemic toxicity at the same time. Additionally, due to the lack of specificity, sometimes the drug will damage the healthy cells which surround the tumor cells. However, with the help of nanoscale carriers, it is possible to overcome both systemic and tumor barriers and provide specific and targeted delivery.³⁴

Nanoparticles can be incorporated and incubated with drugs easily within micelles until they are released into the target cells. They also have the ability to stabilize the drugs for a long-term exposure. In this way, nanomedicine can be defined as the primary application of nanotechnology in health.³⁵

Overall, these significant and unique characteristics of nanoparticles have resulted in their great popularity. With the help of nanoparticles, many fields in our life have been improved. However, everything has two sides. Indeed, the benefits of the nanoparticles are huge, but their disadvantages such as pollution, the inhalation of particles³⁶ and nanotoxicity due to accumulated NPs in organs, are issues we need to pay attention to.

1.2 Quantum dots and their applications

Another spectacular development in the microworld was the quantum revolution.³⁷ In 1980, Alexei Ekimov, a Russian solid state physicist discovered semiconductor nanocrystals also known as quantum dots (QDs) or colloidal semiconductor nanocrystals.^{28, 38}

Quantum dots (QDs) are nanometer-scale semiconductor crystals defined as particles with physical dimensions smaller than the exciton Bohr radius of the material.^{39,40} Quantum

dots are semiconductor nanocrystals usually ranging from 2-10 nanometers or more than 50 atoms¹ and they are composed of a hundred to a thousand atoms. These semiconductor materials can be made from an element, such as silicon or germanium, or a compound, such as CdS or CdSe. These small sized particles behave differently and can show some difference in colour, size, and electrical, nonlinear or optical properties when compared to the bulk material. These unique properties of nano sized particles are partly the result of the unusually high surface to volume ratios. These unusual characteristics give quantum dots an unprecedented number of potential applications in all kinds of areas in our life, such as biomedical imaging, electronics, biosensors and many other fields.^{1, 41}

1.2.1 Optical properties of Quantum dots and their applications

The unique optical and electronic properties can give quantum dots some of the benefits over other materials, such as organic dyes, fluorescent proteins and lanthanide chelates.^{39,}
⁴² Most notably, some characteristics which have a significant influence on both fluorophore behavior and applications of quantum dots such as the width of excitation and emission spectra, , photostability and fluorescence lifetime.³⁹

When compared to conventional narrow dyes, QDs have broad absorption and emission spectra which can provide the possibility for excitation of different colours simultaneously.⁴³ Quantum dots can emit photons if excited, the smaller the dot, the higher the energy of the emitted light.⁴³ By using different excitation and emission wavelengths, the full spectrum of colours would be available; this property can be widely used in large screen televisions and cell phones. Based on this quantum electrical characteristic, the electronics industry has been inspired, to use this property. For example, it is possible to make light-emitting diodes (LEDs) and backlights of computers using

quantum dots. Similarly, quantum dots could also be used in solar cells, not only providing a higher quality and efficiency of power generation but also reducing the consumption of non-renewable power sources.⁴⁴

Luminescent semiconductor quantum dots also are being used as a new fluorescent labeling method for use in cell imaging.⁴⁵ They can also be used as probes in transmission electron microscopy (TEM), energy-filtered TEM (EFTEM) and scanning electron microscopy (SEM). A simple way is to use the QDs as TEM tags is to label a nuclear protein on cell sections, allowing fluorescence images to be obtained.⁴⁵ Additionally, the quantum dot probes can also be used in conjunction with immune gold for co-localization of proteins at an ultra-structural level. Further research also shows the potential of QDs together with EFTEM for co-localization of variety of different kinds of proteins.⁴⁵

Photosability is a significant element in most fluorescence applications and give quantum dots an overwhelming advantage over other fluorophores. Quantum dots, as fluorescent probes coated with a suitable chemical shell, can improve the water stability; can enhance the strength of fluorescence, the photostability and other properties of the original QDs, so that these new QDs can work better in the target cells or areas. For example, coating ZnO quantum dots with silica can improve their water stability.⁴⁶ Moreover, graphene quantum dots (GQDs) have a high photostability which can significantly improve the problems such as photobleaching, blinking, low biocompatibility and high toxicity.⁴⁷ Furthermore, the new GQDs have improved properties such as, less negative surface charges so that they are less easily digested by cells, have lower toxicity, and improved photoluminescence.⁴⁷ Last but not least, quantum dots can undergo repeated excitation and still keep a bright fluorescence for hours without any decay of intensity.^{39, 43, 48}

1.2.2 Cytotoxicity of Quantum dots and their application

The cytotoxicity of QDs, has an important influence on cell growth and cell viability, and has been observed in numerous *in vitro* studies.^{39, 53-59} Many factors can affect the toxicity of QDs including their size, capping materials, surface chemistry, coatings, bioactivity and changes to these factors during processing.^{1, 39, 59, 60} Moreover, with the help of quantum dots, the quality of the results by existing techniques can be improved as well such as the confocal microscopy.^{39, 57, 61, 62}

There are many mechanisms which contribute to the cytotoxicity QDs such as the release of toxic free ions and the generation of free radicals. Using different chemical coatings, such as a ZnS shell, of QDs with Cd as a core has been observed to dramatically reduce rates of oxidation and the leakage of Cd ions.^{39, 63, 64}

Because of the numerous types and properties of QDs, they have a wide range of biomedical and biological-applications. QDs encapsulated in special micelles can be used to label individual cells. These encapsulated QDs show stable and nontoxic properties before they adhere to the target cells. With the fluorescence and different colours of the encapsulated QDs, the target cells will be easy to track.³⁹ By doing so, no matter where the target cells go, it can still be found and/or eliminated.

In particular, in clinical applications, if tumor cells are labeled with QDs, it can be easy to detect the degree of aggression and the location of the tumor cells so that they can be eliminated.⁶⁵ In this way, it will significantly improve the efficiency and accuracy of the doses and decrease the consumption of the drug. Therefore, QDs have potential in anticancer therapy and have an inestimable potential in biomedicine and clinical applications in the future.

The effects of quantum dots are not only important in cell tracking where they have already been shown to have an overwhelming advantage over conventional fluorophores due to long fluorescence lifetime and strong photostability but also in *in vivo* animal imaging.

New kinds of QDs (Type II QDs), which use CdTe as a core and CdSe as the shell, can label normal tissues as well as tumour cells. Bioluminescent QDs, which can be absorbed by the digestive system and bring no harm to liver still need to be discovered. Therefore, there are still lots of animal experiments needed to be done before QDs can be used in human body.

In conclusion, some excellent properties of QDs have been discovered and applied in many areas of our lives. More and more people have an awareness of the benefits of QDs. But the disadvantages still need to be considered.

1.3 Cadmium selenide nanoparticles and their applications

Cadmium selenide, as an inorganic compound with the formula CdSe, and is a yellow-orange solid which belongs to a II-VI semiconductor of the n-type (extrinsic semiconductor with a larger electron concentration than hole concentration).^{68, 69} CdSe particles usually less than 10 nm.^{20, 22, 24-27} After the size has been reduced, the CdSe NPs exhibit unique properties that are totally different from the bulk material. This is because of the quantum confinement effect where the size of the particle becomes smaller than the size of the exciton responsible for light emission.^{7, 8} This property of CdSe NPs produces a range of different fluorescence depending on the size of the particle.⁷⁰ CdSeNPs are one of a number of semiconductor nanoparticles types that have attracted increased interest of

scientific community due to their low toxicity and their fluorescence and electronic properties.^{5, 49, 54, 57, 58, 63, 71-78}

There are many ways to synthesize CdSe NPs such as the micro emulsion method,⁷⁹ the hot injection method^{70, 80,81} the ultrasonic assisted ionic liquid method,⁸² and the ultrasonic irradiation method.⁸³ In this study due to the large variety of different kinds of CdSe NPs required, we choose a facile, inexpensive and less hazardous method which can ensure almost complete conversion of the precursors. This is a wet chemical method assisted by microwave-heating.^{64, 84}

These wet chemical methods are a group of methods used for producing nanoparticles and ultra-dispersed inorganic powders from aqueous and non-aqueous solutions. These use a liquid phase as one of the process stages.^{85,86} The uniqueness and advantage of this method is in the small grains produced and the low temperature and the short duration of the phase formation.⁸⁴ Additionally, the equipment and chemicals required for the experiment can be easily found in a biology or chemistry laboratory. The process only requires items such as microwave oven machine, mechanical stirrers, and standard laboratory glassware and chemicals like Cadmium, selenite and sodium citrate can be stored in the laboratory with no inert atmosphere.

There are two stabilizers which can be used to cooperate with particles. One is the ligand stabilizer and the other is the sodium citrate stabilizer. In this study, we synthesized the CdSe NPs with different amounts and levels of sodium citrate as stabilizer. The mechanism about how the sodium citrate could affect the particles is because the weakly coordinating trisodium citrate ligand which stabilizes nanoparticles through electrostatic interactions which is given as below¹:

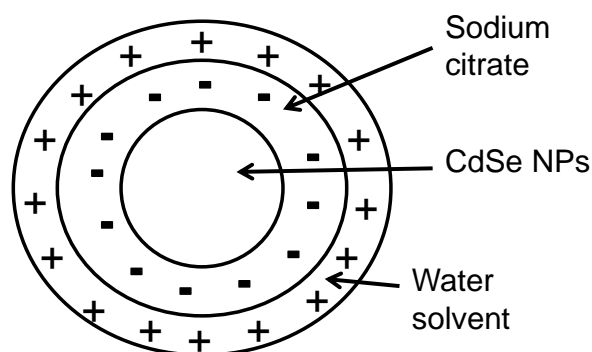


Figure 1.2 The electrostatic repulsion mechanism of sodium citrate and CdSe NPs

The negative sodium citrate ions are filled of the surface of the CdSe NPs which can attract the positive water ions so that the particles could be water soluble.¹ Moreover, when each of this particle close to each other, they will repel because the same polar so that the particles will be separate easily.¹

1.3.1 Optical properties and applications of CdSe NPs

There are different ways to synthesise different kinds of CdSe NPs, some of them are doped or covered with a chemical stabilizer such as sodium citrate⁶⁴ to maintain or improve the stability of the particles. Some studies covered the CdSe core with different kinds of chemical shell such as ZnS or surface capping layer.^{21,87} Some of these studies use exterior elements such as light and heating temperature to change the properties of the CdSe NPs.^{17,20,26,88-90} Indeed, all these methods can affect the optical properties of CdSe NPs and all these methods can have an effect on one or more of the followings four areas: photoluminescence, ultraviolet visible absorption, quantum yield result and the transmission electron microscopy images (visible particle size).

One study prepared CdSe NPs with G4.0-NH₂ PAMAM dendrimers in water and tested how the metallic ions (Zn²⁺, Cd²⁺) affected the photoluminescence (PL) properties of CdSe QDs by spectrophotometric titration. The results show that Zn²⁺ and Cd²⁺ ions can enhance the photoluminescence (PL) intensity of CdSe NPs because they can modify the surface of the particles. Cd²⁺ and Zn²⁺ nanocomposites can emit bright yellow photoluminescence under ultraviolet excitation of 365 nm from an UV LED in the dark. This can be detected with a better resolving rate compared to the old method.⁹¹

Another study synthesized the CdSe NPs via a wet chemical method, using CdSe precursors mixed with hexadecylamine (HDA), tetradecylphosphine oxide (TDPO) and tri-n-octylphosphine oxide (TOPO) as complexing agents in tri-n-butylphosphine (TBP) solvent in the reactor with an argon atmosphere.⁹² By doing so, much larger sized CdSe NPs were produced, with enhanced stability and brighter photoluminescence (by adjusting synthesis temperature and reaction time)⁹² thus enhancing dramatically the potential of these CdSe NPs in biomedical applications such as drug delivery.⁹²

A kind of bowknot-shaped structure formed from individual CdSe NPs which can be affected by ultraviolet (UV) light irradiation has been discovered recently.⁹³ The structural transformation process happens due to the photo corrosion of CdSe NPs under UV light. This study indicates a new technique called photoetching. This technique can affect the transformation process and synthesis of nanoparticles. Therefore, the nanoparticles either irradiated or non-irradiated can be applied in photo electrochemical devices to verify the photovoltaic effect.⁹³

CdSe NPs synthesized in aqueous solutions with sodium citrate as a stabilizer display very low quantum yields initially without the influence of external elements such as light.

However, the quantum yield of CdSe NPs increases sharply under visible light. This leads to aqueous quantum dots with high luminescence that can be applied in biological and many other areas. This study found that the smooth surface of the CdSe core affects the luminescence of the CdSe NPs. If the CdSe core is shielded from photo corrosion, the luminescence of the CdSe NPs will be of greater intensity.⁹⁰

Microwave dielectric heating and irradiation can affect the size and other properties of CdSe NPs. This has been observed in many studies.^{26, 27} CdSe NPs fabricated with different cadmium complexes, such as Cd-Lu, Cd-Myr, Cd-St, Cd-ODPA and Cd-DDPA, under constant parameters which include temperature, ramp, hold, and cooling times lead to different TEM results.²⁷ Even the same CdSe NPs prepared at different temperatures show drastic differences in their photoluminescence and TEM results. These results indicate that at higher temperature, larger particles are obtained and have higher quantum yields.²² Moreover, nanoparticles with a CdSe core and ZnS shell using tetranitro-methane (TNM) as an oxidant surface also lead to different shapes of TEM images.²⁵

Another novel method for the synthesis of CdSe QDs is using a CdSe/CdS core-shell structure with poly(acrylic acid) (PAA) as a capping ligand at 240° C. This can increase the quantum yields by up to 30% and the photoluminescence emission peak could be tuned from 530 to 600 nm by the size of CdSe core. These new CdSe QDs have many excellent properties such as good water solubility, and bright PL emission. These quantum dots can be used as a fluorescence labels for *in vitro* studies.⁹⁴

One of the fundamental goals in biology is to understand the interplay between biomolecules from different cells. To observe these kinds of events, confocal microscopy

is necessary.⁹⁵ Quantum dots like CdSe QDs can emit different colours when stimulated by visible light. Confocal microscopy can observe the fluorescence, colour, distribution and the outline of quantum dots. For example, confocal microscopy can be used to determine the distribution of QDs within polystyrene micro gel particles, dispersed in an organic solvent.⁹⁶ Furthermore, the toxicity of nanoparticles such as CdSe NPs can also be tested by confocal microscopy. By adjusting the parameters of the confocal images and using different dye methods in the cells different materials will emit different colours so that they can be identified easily and clearly under the microscope. These properties of quantum dots have been exploited in biomedical applications.⁹⁷

1.3.2 The cytotoxicity of CdSe NPs and their applications

There are numerous ways to synthesize CdSe NPs to give different kinds of CdSe NPs. Some of them have different chemical layers; some of them are encapsulated within chemical shells.⁹⁸ All these methods make a contribution to enrich the properties of CdSe NPs so that they can be applied in a wide range of areas including biology and biomedicine.

The cytotoxicity and genotoxicity of QDs with a Cadmium selenide/Zinc sulfide (CdSe/ZnS) core/shell for applications in cancer therapy has been discussed recently. Human cancer cells which were treated with CdSe/ZnS QDs and UVB irradiation which lead to a lower cell viability rate and strong phototoxicity. The genotoxicity results indicated that UVB irradiation is the most effective method for increasing the potency of QDs during photodynamic cancer therapy.⁹⁸

The cytotoxicity of different kinds of CdSe QDs varies in different cell lines and can be detected by different techniques. One of the most common techniques used to test for the toxicity in cells is the 3-(4, 5-dimethylthiazol)-2-diphenyltertrazolium bromide (MTT) assay. MTT is pale yellow in solution but produces a dark-blue formazan product with live cells. Besides the MTT assay, there are lots of assays which can test almost every property of the cells. For instance, the genotoxic effects toward cells can be reflected by DNA damage and can be examined by a comet assay.⁹⁹

The toxicity of Caco-2 cells treated by CdSe QDs with ZnS shell and poly-ethylene glycol (PEG) coating has been observed after 24 hours by a MTT assay. The results indicated that the cytotoxicity of CdSe QDs was modulated by surface coating. Initially, PEG coated CdSe QDs had less of an effect on Caco-2 cell viability and attachment. However, acid treatment can damage the surface coating and release Cd ions so that the toxicity of the CdSe QDs will be increased and the cell viability will be reduced sharply.⁶⁴

There are many studies that have already tested different properties of CdSe NPs so far; however, very few of them discussed about the aging and toxicity properties in different ratios of Cadmium to Selenide NPs. This study focuses on optical and biology properties of different ratios of Cd to Se NPs which can help us understand the CdSe NPs better, so that it would be very useful for the clinical research in the future. Overall, the optical properties and biology characteristics of CdSe NPs (QDs) can be applied in numerous areas, in particular in biology, bioimaging and biomedical areas.

1.4 References

1. Bransden, B. H.; Joachain, C. J. Quantum mechanics (2nd ed.). Essex: Pearson Education. 2000.

2. Drexler KE. Engines of Creation: The coming Era of Nanotechnology. USA: Doubleday; 1986.
3. Drexler KE. Nanosystems: Molecular Machinery, Manufacturing, and Computatin. New York: Hign Wiley& Sons; 1992.
4. Granqvist CG, Buhrman RA, Wyns J, Sievers AJ. Far- infrared absorption in ultrafine particles. Physical Review Letters. 1976 1976;37(10):625-629.
5. Buzea C, Pacheco II, Robbie K. Nanomaterials and nanoparticles: Sources and toxicity. Biointerphases. 2007;2(4):MR17-MR71.
6. Mahmoudi M, Hofmann H, Rothen-Rutishauser B, Petri-Fink A. Assessing the In Vitro and In Vivo Toxicity of Superparamagnetic Iron Oxide Nanoparticles. Chemical Reviews. 2012;112(4):2323-2338.
7. Haug H. Quantum Theory of the Optical and Electronic Properties of Semiconductors: World Scientific; 1994.
8. M.Cahay. Quantum confinement VI: Nanostructured Materials and Devices: Proceeding of the international Symposium: The Electrochemical Society; 2001.
9. Yacobi BG. Semiconductor materials: an introduction to basic principles: Springer; 2003.
10. Bangal M, Ashtaputre S, Marathe S, et al. Semiconductor nanoparticles. Hyperfine Interactions. 2005;160(1-4):81-94.
11. Forrest SR. The path to ubiquitous and low-cost organic electronic appliances on plastic. Nature. 2004;428(6986):911-918.
12. Haas B, Beyer A, Witte W, Breuer T, Witte G, Volz K. Application of transmission electron microscopy for microstructural characterization of perfluoropentacene thin films. Journal of Applied Physics. 2011;110(7).

13. F. James Holler DA. Principles Of Instrumental Analysis: Skoog & Stanley R.; 2006.
14. Wilkinson ADMA. Compendium of Chemical Terminology. Oxford: Oxford; 1997.
15. Cornelius TW. Finite and quantum size effects of bismuth nanowires. In Tech, UK 2010.
16. Bardajee GR, Hooshyar Z, Jafarpour F. Antibacterial and optical properties of a new water soluble CdSe quantum dots coated by multidentate biopolymer. Journal of Photochemistry and Photobiology a-Chemistry. 2013;252:46-52.
17. Tian W, Mi W, Tian J, et al. Comparative study on CdSe QDs synthesized from water and ethanol: Hydrogen bond induced particle agglomeration and enhancement on photoluminescence. Analyst. 2013;138(5):1570-1580.
18. Mahmoud WE, Yaghmour SJ, Al-Amri AM. Enhancement of CdSe quantum dots luminescence by calcium ions. Journal of Luminescence. 2013;134:429-431.
19. Chen X, Hutchison JL, Dobson PJ, Wakefield G. Highly luminescent monodisperse CdSe nanoparticles synthesized in aqueous solution. Journal of Materials Science. 2009;44(1):285-292.
20. Zeng R, Shen R. Monitoring of Mn ion ejection from CdSe host lattice. Chemical Physics Letters. 2013;559:50-55.
21. Luo X, Liu P, Nguyen Tam Nguyen T, Farva U, Park C. Photoluminescence Blue-Shift of CdSe Nanoparticles Caused by Exchange of Surface Capping Layer. J Phys Chem C. 2011;115(43):20817-20823.

22. He R, Gu HC. Synthesis and characterization of monodispersed CdSe nanocrystals at lower temperature. *Colloids and Surfaces a-Physicochemical and Engineering Aspects*. 2006;272(1-2):111-116.
23. Hamizi NA, Ying CnS, Johan MR. Synthesis with Different Se Concentrations and Optical Studies of CdSe Quantum Dots via Inverse Micelle Technique. *International Journal of Electrochemical Science*. 2012;7(5):4727-4734.
24. Mahmoud WE, Yaghmour SJ. Synthesis, characterization and luminescence properties of thiol-capped CdSe quantum dots at different processing conditions. *Optical Materials*. 2013;35(3):652-656.
25. Korala L, Brock SL. Aggregation Kinetics of Metal Chalcogenide Nanocrystals: Generation of Transparent CdSe (ZnS) Core (Shell) Gels. *J Phys Chem C*. 2012;116(32):17110-17117.
26. Mahmoud WE, Al-Amri AM, Yaghmour SJ. Low temperature synthesis of CdSe capped 2-mercaptoethanol quantum dots. *Optical Materials*. 2012;34(7):1082-1086.
27. Moghaddam MM, Baghbanzadeh M, Keilbach A, Kappe CO. Microwave-assisted synthesis of CdSe quantum dots: can the electromagnetic field influence the formation and quality of the resulting nanocrystals? *Nanoscale*. 2012;4(23):7435-7442.
28. Ekimov AI, Efros AL, Onushchenko AA. Quantum –size effect in semiconductor (VOL 56, PG 921-924, 1985). *Solid State Communications*. 1993;88(11-12):947-950.
29. Borm PJA. Particle toxicology: From coal mining to nanotechnology. *Inhalation Toxicology*. 2002;14(3):311-324.

30. Sharma M. Understanding the mechanism of toxicity of carbon nanoparticles in humans in the new millennium: A systemic review. *Indian journal of occupational and environmental medicine*. 2010;14(1):3-5.
31. Donaldson K, Stone V, Tran CL, Kreyling W, Borm PJA. *Nanotoxicology. Occupational and Environmental Medicine*. 2004;61(9):727-728.
32. Fisher C, Rider AE, Han ZJ, Kumar S, Levchenko I, Ostrikov K. Applications and nanotoxicity of carbon nanotubes and graphene in biomedicine. *J Nanomater*. 2012.
33. Khlebtsov N, Dykman L. Biodistribution and toxicity of engineered gold nanoparticles: a review of in vitro and in vivo studies. *Chem Soc Rev*. 2011;40(3):1647-1671.
34. Steichen SD, Caldorera-Moore M, Peppas NA. A review of current nanoparticle and targeting moieties for the delivery of cancer therapeutics. *European Journal of Pharmaceutical Sciences*. 2013;48(3):416-427.
35. Liu Y, Miyoshi H, Nakamura M. Nanomedicine for drug delivery and imaging: A promising avenue for cancer therapy and diagnosis using targeted functional nanoparticles. *International Journal of Cancer*. 2007;120(12):2527-2537.
36. Sun QQ, Tan DL, Zhou QP, et al. Oxidative damage of lung and its protective mechanism in mice caused by long-term exposure to titanium dioxide nanoparticles. *J Biomed Mater Res Part A*. 2012;100A(10):2554-2562.
37. University TO. *The quantum world*. Norfolk, UK: Jarrold book printing; 1998.
38. Frigerio C, Ribeiro DSM, Rodrigues SSM, et al. Application of quantum dots as analytical tools in automated chemical analysis: A review. *Analytica Chimica Acta*. 2012;735:9-22.

39. Jamieson T, Bakhshi R, Petrova D, Pocock R, Imani M, Seifalian AM. Biological applications of quantum dots. *Biomaterials*. 2007;28(31):4717-4732.
40. Chan WCW, Maxwell DJ, Gao XH, Bailey RE, Han MY, Nie SM. Luminescent quantum dots for multiplexed biological detection and imaging. *Current Opinion in Biotechnology*. 2002;13(1):40-46.
41. Bruchez M, Moronne M, Gin P, Weiss S, Alivisatos AP. Semiconductor nanocrystals as fluorescent biological labels. *Science*. 1998;281(5385):2013-2016.
42. Wang F, Tan WB, Zhang Y, Fan XP, Wang MQ. Luminescent nanomaterials for biological labelling. *Nanotechnology*. 2006;17(1):R1-R13.
43. Han MY, Gao XH, Su JZ, Nie S. Quantum-dot-tagged microbeads for multiplexed optical coding of biomolecules. *Nature Biotechnology*. 2001;19(7):631-635.
44. boysen E. *Nanotechnology for dummies*. USA; 2011.
45. Nisman R, Dellaire G, Ren Y, Li R, Bazett-Jones DP. Application of quantum dots as probes for correlative fluorescence, conventional, and energy-filtered transmission electron microscopy. *Journal of Histochemistry & Cytochemistry*. 2004;52(1):13-18.
46. Matsuyama K, Ihsan N, Irie K, Mishima K, Okuyama T, Muto H. Bioimaging application of highly luminescent silica-coated ZnO-nanoparticle quantum dots with biotin. *J Colloid Interface Sci*. 2013;399:19-25.
47. Sun HJ, Wu L, Gao N, Ren JS, Qu XG. Improvement of Photoluminescence of Graphene Quantum Dots with a Biocompatible Photochemical Reduction Pathway and Its Bioimaging Application. *Acs Applied Materials & Interfaces*. 2013;5(3):1174-1179.

48. Alivisatos AP. Semiconductor clusters, nanocrystals, and quantum dots. *Science*. 1996;271(5251):933-937.
49. Gerion D, Pinaud F, Williams SC, et al. Synthesis and properties of biocompatible water-soluble silica-coated CdSe/ZnS semiconductor quantum dots. *J Phys Chem B*. 2001;105(37):8861-8871.
50. Pinaud F, Michalet X, Bentolila LA, et al. Advances in fluorescence imaging with quantum dot bio-probes. *Biomaterials*. 2006;27(9):1679-1687.
51. Dahan M, Laurence T, Pinaud F, et al. Time-gated biological imaging by use of colloidal quantum dots. *Optics Letters*. 2001;26(11):825-827.
52. Grecco HE, Lidke KA, Heintzmann R, et al. Ensemble and single particle photophysical properties (Two-Photon excitation, anisotropy, FRET, lifetime, spectral conversion) of commercial quantum dots in solution and in live cells. *Microscopy Research and Technique*. 2004;65(4-5):169-179.
53. Medintz IL, Uyeda HT, Goldman ER, Mattoussi H. Quantum dot bioconjugates for imaging, labelling and sensing. *Nature Materials*. 2005;4(6):435-446.
54. Chen FQ, Gerion D. Fluorescent CdSe/ZnS nanocrystal-peptide conjugates for long-term, nontoxic imaging and nuclear targeting in living cells. *Nano Letters*. 2004;4(10):1827-1832.
55. Clarke SJ, Hollmann CA, Zhang ZJ, et al. Photophysics of dopamine-modified quantumdots and effects on biological systems. *Nature Materials*. 2006;5(5):409-417.
56. Derfus AM, Chan WCW, Bhatia SN. Probing the cytotoxicity of semiconductor quantum dots. *Nano Letters*. 2004;4(1):11-18.

57. Hsieh S-C, Wang F-F, Hung S-C, Chen Y, Wang Y-J. The internalized CdSe/ZnS quantum dots impair the chondrogenesis of bone marrow mesenchymal stem cells. *Journal of Biomedical Materials Research Part B-Applied Biomaterials*. 2006;79B(1):95-101.
58. Kirchner C, Liedl T, Kudera S, et al. Cytotoxicity of colloidal CdSe and CdSe/ZnS nanoparticles. *Nano Letters*. 2005;5(2):331-338.
59. Lovric J, Bazzi HS, Cuie Y, Fortin GRA, Winnik FM, Maysinger D. Differences in subcellular distribution and toxicity of green and red emitting CdTe quantum dots. *Journal of Molecular Medicine-Jmm*. 2005;83(5):377-385.
60. Shiohara A, Hoshino A, Hanaki K, Suzuki K, Yamamoto K. On the cyto-toxicity caused by quantum dots. *Microbiology and Immunology*. 2004;48(9):669-675.
61. Mansson A, Sundberg M, Balaz M, et al. In vitro sliding of actin filaments labelled with single quantum dots. *Biochemical and Biophysical Research Communications*. 2004;314(2):529-534.
62. Zhang TT, Stilwell JL, Gerion D, et al. Cellular effect of high doses of silica-coated quantum dot profiled with high throughput gene expression analysis and high content cellomics measurements. *Nano Letters*. 2006;6(4):800-808.
63. Selvan ST, Tan TT, Ying JY. Robust, non-cytotoxic, silica-coated CdSe quantum dots with efficient photoluminescence. *Adv Mater*. 2005
64. Wang L, Nagesha DK, Selvarasah S, Dokmeci MR, Carrier RL. Toxicity of CdSe Nanoparticles in Caco-2 Cell Cultures. *Journal of nanobiotechnology*. 2008;6:11-Article No.: 11.
65. Wang Y, Yan X-P. Fabrication of vascular endothelial growth factor antibody bioconjugated ultrasmall near-infrared fluorescent Ag₂S quantum dots for

- targeted cancer imaging in vivo. *Chemical Communications*. 2013;49(32):3324-3326.
66. Lim YT, Kim S, Nakayama A, Stott NE, Bawendi MG, Frangioni JV. Selection of quantum dot wavelengths for biomedical assays and imaging. *Molecular imaging*. 2003;2(1):50-64.
67. So MK, Xu CJ, Loening AM, Gambhir SS, Rao JH. Self-illuminating quantum dot conjugates for in vivo imaging. *Nature Biotechnology*. 2006;24(3):339-343.
68. Berger LI. *Semiconductor materials*: CRC Press; 1996.
69. A.F.Wells. *Structural Inorganic Chemistry*: Oxford; 1984.
70. Teranishi T, Nishida M, Kanehara M. Size-tuning and optical properties of high-quality CdSe nanoparticles synthesized from cadmium stearate. *Chem Lett*. 2005;34(7):1004-1005.
71. Chan WH, Shiao NH. Cytotoxic effect of CdSe quantum dots on mouse embryonic development. *Acta Pharmacol Sin*. 2008;29(2):259-266.
72. Gomes SAO, Vieira CS, Almeida DB, et al. CdTe and CdSe Quantum Dots Cytotoxicity: A Comparative Study on Microorganisms. *Sensors*. 2011;11(12):11664-11678.
73. Han D, Song C, Guo G, Li X. Synthesis and fluorescence properties of CdSe/CdS nanoparticles in aqueous media. *Science China Chemistry*. 2010;53(5):1055-1059.
74. Liu W, Zhang SP, Wang LX, et al. CdSe quantum dot (QD)-induced morphological and functional impairments to liver in mice. *plos one*. 2011.
75. Ni T, Nagesha DK, Robles J, Materer NF, Mussig S, Kotov NA. CdS nanoparticles modified to chalcogen sites: New supramolecular complexes,

- butterfly bridging, and related optical effects. *Journal of the American Chemical Society*. 2002;124(15):3980-3992.
76. Rabani E. Structure and electrostatic properties of passivated CdSe nanocrystals. *Journal of Chemical Physics*. 2001;115(3):1493-1497.
77. Zaman MB, Baral TN, Zhang JB, Whitfield D, Yu K. Single-Domain Antibody Functionalized CdSe/ZnS Quantum Dots for Cellular Imaging of Cancer Cells. *J Phys Chem C*. 2009;113(2):496-499.
78. Zheng H, Chen G, Song F, DeLouise LA, Lou Z. The Cytotoxicity of OPA-Modified CdSe/ZnS Core/Shell Quantum Dots and Its Modulation by Silibinin in Human Skin Cells. *Journal of Biomedical Nanotechnology*. 2011;7(5):648-658.
79. Hao EC, Sun HP, Zhou Z, Liu JQ, Yang B, Shen JC. Synthesis and optical properties of CdSe and CdSe/CdS nanoparticles. *Chem Mater*. 1999;11(11):3096-3102.
80. Hambrock J, Birkner A, Fischer RA. Synthesis of CdSe nanoparticles using various organometallic cadmium precursors. *Journal of Materials Chemistry*. 2001;11(12):3197-3201.
81. Capek RK, Lambert K, Dorfs D, et al. Synthesis of Extremely Small CdSe and Bright Blue Luminescent CdSe/ZnS Nanoparticles by a Prefocused Hot-Injection Approach. *Chem Mater*. 2009;21(8):1743-1749.
82. Tong Y, Liao H, Zhang M, Jia J, Jiang S. Synthesis and Fluorescence of Nanoparticles CdSe by Ultrasonic Assisted Ionic Liquid Method. *Fine Chemicals*. 2012;29(5):434-437,457.

83. Behboudnia M, Azizianekalandaragh Y. Synthesis and characterization of CdSe semiconductor nanoparticles by ultrasonic irradiation. *Materials Science and Engineering B-Solid State Materials for Advanced Technology*. 2007;138(1):65-68.
84. Kumar P, Singh K. Synthesis of CdSe Nanoparticles at 50 degrees C by Wet Chemical Method. *Curr Nanosci*. 2010;6(1):89-93.
85. Hornyak;Dutta;Tibbals;Rao. *Introduction to Nanoscience*. USA: CRC press; 2008.
86. S.M.Lindsay. *Introduction to nanoscience*: Oxford; 2010.
87. Fitzmorris BC, Cooper JK, Edberg J, Gul S, Guo J, Zhang JZ. Synthesis and Structural, Optical, and Dynamic Properties of Core/Shell/Shell CdSe/ZnSe/ZnS Quantum Dots. *J Phys Chem C*. 2012;116(47):25065-25073.
88. Ahire JH, Wang Q, Coxon PR, et al. Highly Luminescent and Nontoxic Amine-Capped Nanoparticles from Porous Silicon: Synthesis and Their Use in Biomedical Imaging. *Acs Applied Materials & Interfaces*. 2012;4(6):3285-3292.
89. Brus L. Electronic wave-functions in semiconductor clusters-experiments and theory. *Journal of Physical Chemistry*. 1986, 90(12):2555-2560.
90. Wang Y, Tang ZY, Correa-Duarte MA, et al. Mechanism of strong luminescence photoactivation of citrate-stabilized water-soluble nanoparticles with CdSe cores. *J Phys Chem B*. 2004;108(40):15461-15469.
91. Jin Yu J, Luo Yun J, Xu Guo Z, Yang B. Effects of metallic ions on photoluminescence properties of CdSe/PAMAM nanocomposites and their application in fingerprint detection. In: Wang PC, Ai L, Li YG, Sang XM, Bu JL, eds. *Manufacturing Science and Technology*, Pts 1-3. Vol 295-297; 2011: 900-906.

92. Louh RF, Chang ACC, Wang R, Hsiao CH. Photoluminescence Response and Particle Size Control of CdSe Quantum Dots by Wet Chemical Synthesis for Biomedical Applications. In: Vincenzini P, DeRossi D, eds. Biomedical Applications of Smart Materials, Nanotechnology and Micro/Nano Engineering. Vol 57; 2009: 37-43.
93. Shen YT, Lei D, Feng W. Architectural transformation of the nanoparticle superstructures induced by ultraviolet light irradiation and their application in photoelectrochemical switch devices. *J Mater Chem C*. 2013;1(10):1926-1932.
94. Zhai CX, Zhang H, Du N, et al. One-pot synthesis of biocompatible CdSe/CdS quantum dots and their applications as fluorescent biological labels. *Nanoscale Res Lett*. 2011.
95. de Thomaz AA, Almeida DB, Faustino WM, et al. Study of optically trapped living *Trypanosoma cruzi*/*Trypanosoma rangeli* - *Rhodnius prolixus* interactions by real time confocal images using CdSe quantum dots. In: Dholakia K, Spalding GC, eds. *Optical Trapping and Optical Micromanipulation V*. Vol 7038. Bellingham: Spie-Int Soc Optical Engineering; 2008.
96. Bradley M, Bruno N, Vincent B. Distribution of CdSe quantum dots within swollen polystyrene microgel particles using confocal microscopy. *Langmuir*. 2005;21(7):2750-2753.
97. Hu D, Zhang P, Gong P, et al. A fast synthesis of near-infrared emitting CdTe/CdSe quantum dots with small hydrodynamic diameter for in vivo imaging probes. *Nanoscale*. 2011;3(11):4724-4732.
98. Choi YJ, Kim YJ, Lee JW, Lee Y, Lim YB, Chung HW. Cyto-/Genotoxic Effect of CdSe/ZnS Quantum Dots in Human Lung Adenocarcinoma Cells for Potential

Photodynamic UV Therapy Applications. J Nanosci Nanotechnol. 2012;12(3):2160-2168.

99. Fairbairn DW, Olive PL, Oneill KL. The comet assay- a comprehensive review. Mutation research-reviews in genetic toxicology. 1995, 339(1):37-59.
100. Hornyak;Dutta;Tibbals;Rao, Introduction to Nanoscience. CRC press: USA, 2008.

Chapter 2. Experimental methods

2.1 Synthesis of CdSe Nanoparticles by a microwave-assisted method

The CdSe nanoparticles (CdSe NPs) were synthesized by the microwave heating of an aqueous solution of 0.01M cadmium perchlorate (CdCl_2O_8) as a source of cadmium ions with 0.01 M N, N-dimethyl Selenourea ($\text{C}_3\text{H}_8\text{N}_2\text{Se}$) as a source of selenium ions, in the presence of 0.05, 0.1, 0.2% (w/v) sodium citrate ($\text{Na}_3\text{C}_6\text{H}_5\text{O}_7$) as a stabilizer.¹

Sodium citrate with a weight of 0.0284 gram was dissolved in 45 mL of deionised water, and the pH adjusted to 9.2 using 0.1M NaOH. Sodium citrate with a weight of 0.0568 gram was dissolved in 45 mL of deionised water and the pH adjusted to 9.2 using 0.1M NaOH. Sodium citrate with a weight of 0.1136 gram was dissolved in 45 mL of deionised water and the pH adjusted to 9.2 using 0.1M NaOH. Cadmium perchlorate with the volume of 2mL and 2mL N, N-dimethyl Selenourea were added to the samples and the pH adjusted to 9.2 using 2M NaOH. Next, the mixture of precursors was heated in a conventional 800W microwave oven for 75 seconds and then stored in the dark at room temperature for 2-3 days to give the particles enough time to grow.¹⁻²

CdSe Quantum dots (CdSe QDs) were obtained by increasing the ratio of cadmium to selenium ions. This ratio was changed via the use of 2mL of 0.01, 0.04 and 0.1M cadmium perchlorate giving ratios of 1:1, 4:1 and 10:1 cadmium to selenium respectively. This resulted in average particle sizes of 5.0 nm, 5.8 nm, and 4.9 nm respectively (Chapter 3, Table 3.3). These measurements were made using transmission electron microscopy (TEM), with a sample size of 100 particles per measurement.

2.2 Photoluminescence spectroscopy

Photoluminescence (PL) is a process in which a substance absorbs and then re-radiates photons. This process involves the excitation of an electron to a higher energy state and then a return to a lower energy state accompanied by the emission of a photon (Figure 2.2.1)⁵.

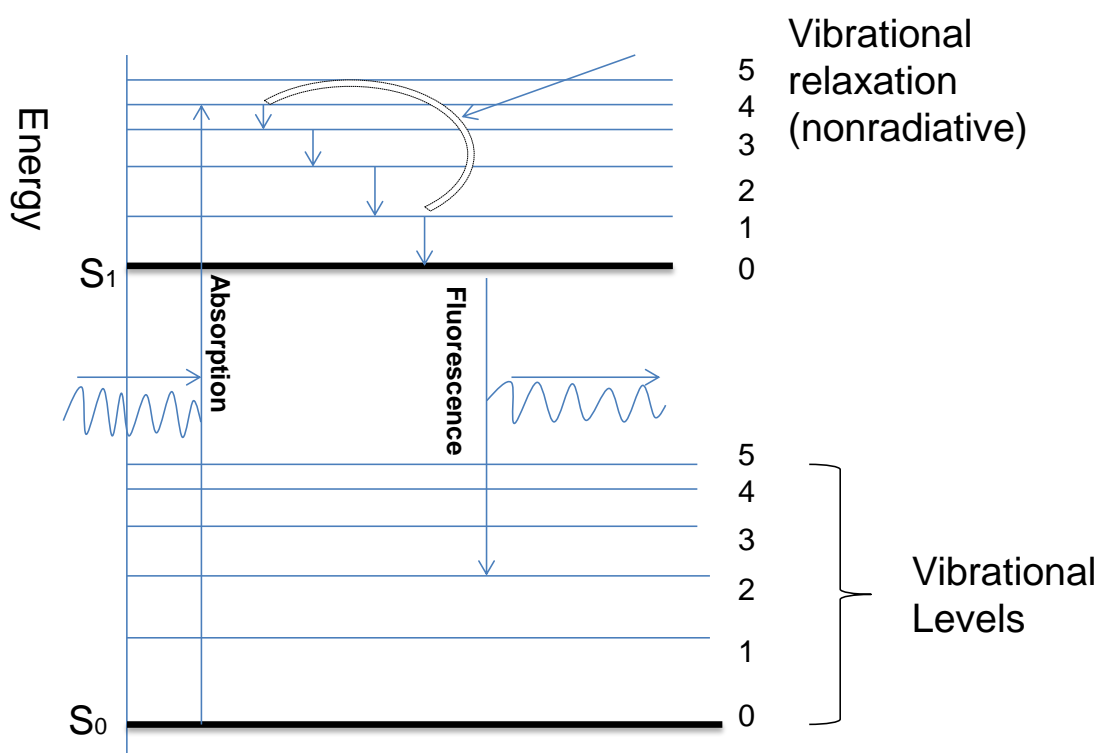


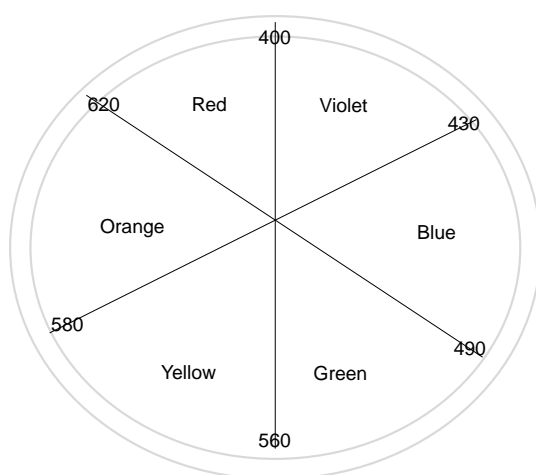
Figure 2.1 Jablonski diagram. S_0 is the the electronic state (ground sate). S_1 is the electronic state (excited state) and number 0-5 are vibrational levels.

The Jablonski diagram shows the sequence of the steps leading to fluorescence (Figure 2.2.1). After the initial absorption, the upper vibrational states undergo radiation less decay; a process called vibrational relaxation.⁵ This energy is given up to the surroundings.⁵ A radiative transition then occurs from the excited state to the ground state (the heavy horizontal lines).⁵ Level spacing decreases as dissociation energy approached.

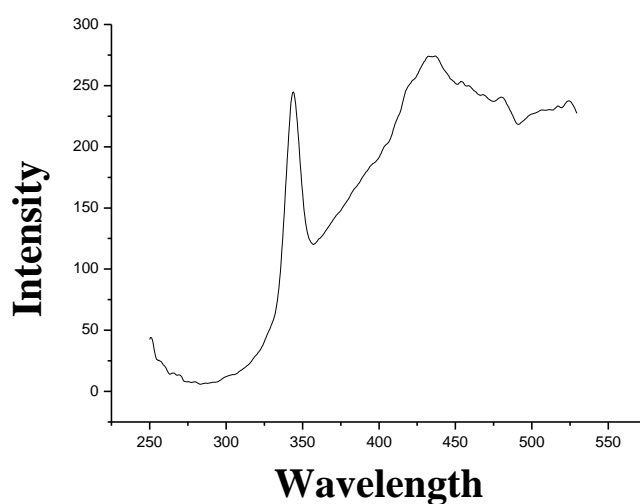
The discrete energy usually become continuous at high enough energies because the

system can no longer exist as a bound state.⁵ The energy become more and more close when it approaches the dissociation energy.⁵ The energy levels after dissociation can take the continuous values with free particles.⁵ This energy separation is 10 to 100 times greater that of the vibrational levels.⁵

The CdSe NPs samples were checked under a UV lamp and the colour of the luminescence was orange. According to the visible spectrum (Figure 2.2.2.a), the peak of the orange should be approximately 550 nm. Therefore, an excitation spectrum scan was taken at emission of 550 nm. The maximum peak in the graph was taken (about 345 nm) as the excitation wavelength of the samples (Figure 2.2.2.b).



a



b

Figure 2.2 a) Visible spectrum b) An excitation spectrum of the CdSe NPs samples

Fluorescence emission spectra of CdSe NPs were recorded in a 10×10 mm quartz cuvette using a Perkin-Elmer LS55 spectrophotometer with the excitation wavelength set at 345 nm (Figure 2.2.3). The emission spectra were corrected using the solvent emission as background.

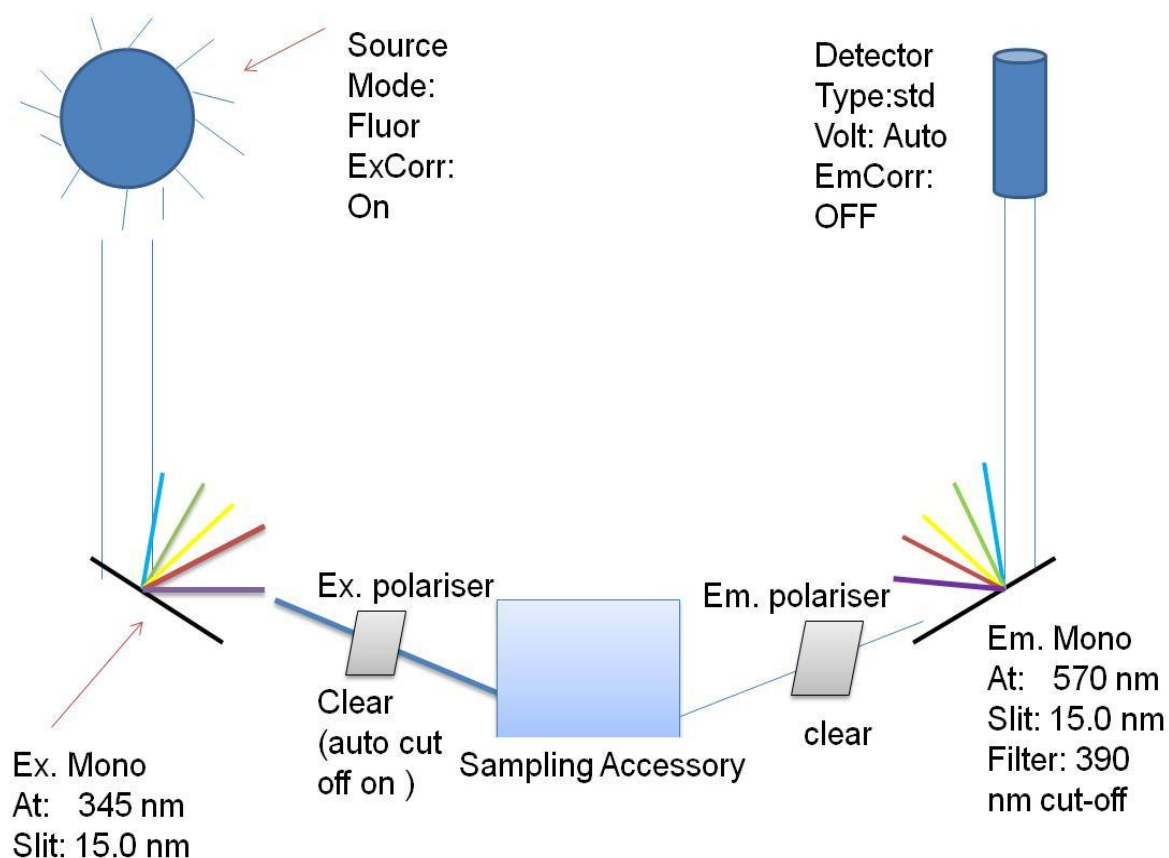


Figure 2.3 Diagram to explain how the spectrophotometer works.

The ageing of the CdSe NPs samples was carried out to be test daily for first week and then once a week last for about three months to see if the curve and the peak of the spectrum changed with time. A pipette was used to transfer an appropriate volume of the CdSe NPs samples from the stock solution to the clean and empty cuvette. This was then covered with the lid. The chamber of the Perkin-Elmer LS55 spectrophotometer was opened and the cuvette was placed in it with the positive side (the side with label) towards the outside of the chamber. The software named FL winlab, was used to set the correct parameters. The emission range of the spectrum was between 300 to 800 nm. The excitation slit of the CdSe NPs samples was 15.0 nm and the emission slit was also 15.0 nm. The scan speed of the samples was 600 nm per minute. The cuvette was cleaned with acetone and nanofiltered water. This process was repeated daily.

2.3 *UV-Vis Spectroscopy*

Ultraviolet–visible spectroscopy (UV) or ultraviolet-visible spectrophotometry refers to absorption spectroscopy or reflectance spectroscopy in the ultraviolet-visible spectral region. Sample absorption spectra were recorded in a 10×10 mm quartz cuvette, and tested using a Perkin-Elmer 35 UV-Vis double-beam spectrophotometer. UV lab software was used to set the appropriate parameters. The scan range was between 200-800 nm with a 600 nm/min rate. A blank (the solvent of the sample) was scanned, the cuvette was then washed with acetone and nanofiltered water, a sample from the stock solution was added to the cuvette and a spectrum was taken.

2.4 *Quantum Yield Measurement*

The quantum yield (QY) is the ratio of emission photons over the total number of photons absorbed by the sample. The most reliable method for recording QY is the comparative method documented by Williams,⁶ which use standard samples with known QY values. This method compares the integrated fluorescence intensity and the absorption for an unknown sample and standard at absorbance between 0.1 and 0.01.

Basically, a quinine reference which the quantum yield rate was already known by us was used as a standard reference (Figure 2.4.1, Table 2.4.1).¹⁰ The stock solution of the samples was dilute to different concentrations and the absorbance from each of these was measured. And then the PL emission against all these concentrations was measured. All the data were then being plotted and the gradient was abstained by the computer. These data were then compared with the quinine reference so that the quantum yield of the samples could be worked out.

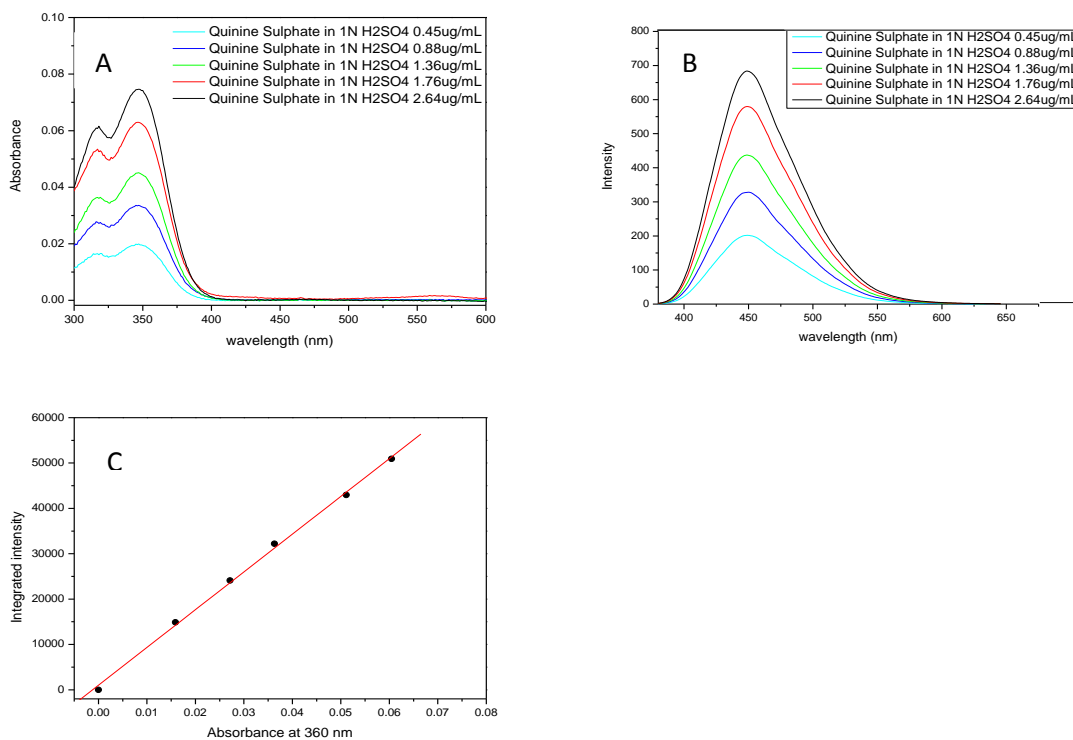


Figure 2.4 Quantum yield results of Quinine reference

Table 2.4.1 Linear line absorbance vs integrated intensity of quinine reference

Quinine Sulphate in 1N H ₂ SO ₄ (µg/mL)	Absorbance at 360 nm	Integrated intensity
0.45	0.015890	14860
0.88	0.027140	24104
1.36	0.036320	32216
1.76	0.051120	42939
2.64	0.060470	50924

One or two drops of Quinine sulphate were added to pre-prepare 0.1M H₂SO₄ in a cuvette. The cuvette was shaken several times and then UV-Vis spectrum was taken over the wavelength range between 200-800 nm. CdSe NPs stock solution were diluted with water and stored in a 10 × 10 mm quartz cuvette. The diluted solution of CdSe NPs was tested using the same process as used for the quinine sulphate reference. The slope from the

scatter plot of absorption against integrated intensity was used to calculate the quantum yield by using the equation below.

$$Q = Q_R \left(\frac{Grad}{Grad_R} \right) \left(\frac{\eta^2}{\eta_R^2} \right)$$

In this equation, Q is the quantum yield; η is the refractive index of the solvent. Grad is the gradient from the plot of integrated fluorescence intensity and absorbance. The subscript R means the reference fluorophore of a known quantum yield.¹⁰

2.5 Transmission electron microscopy (TEM)

Transmission electron microscopy (TEM) is a microscopy technique whereby a beam of electrons is transmitted through an extremely thin specimen, interacting with the specimen as it passes through. Ernst Abbe originally proposed that the ability to resolve detail in an object was limited by the wavelength of the light used.⁷ The first TEM was built by Max Knoll and Ernst Ruska in 1931.⁷

A JOEL 2000EX with the accelerating voltage at 200 kV was used to obtain TEM images.

The grids used in this study were Agar scientific- S160, carbon film, 200 meshes.

Initially, the samples were placed in a sonic bath to separate aggregated particles. Otherwise, the particles on the film would be too dense and it would be difficult to find clear well separated particles. In order to separate these particles completely, an ultrasonic time of at least 1 minute was required. After comparison of the dilute samples and the stock solutions, it was obvious that the former one gave better images; The Cu thin specimen grid was dipped into the CdSe NPs stock solution and the grid was placed on a filter paper, and then left for a few seconds; if the concentration was not high enough, more samples was dropped on the Cu grid.

To get an accurate average particle size more particles were measured from different images. Once some particles were found, the final images were adjusted using the contrast scale, to highlight the particles and dim the background of the image. In order to get a reliable and representative result, at least 100 particles were measured to obtain the standard deviation and the average size of the particles.

2.6 Cell Culture

The immortalised human hepatocytes (defined as HHL-5) cell line was kindly supplied by Dr. Arvind Patel, Medical Research Council (MRC) Virology Unit (Glasgow, UK).

Human hepatocytes (HHL-5) have the highest capacity for binding hepatitis C virus (HCV), Virus-like particles (VLPs) compare to other cell lines such as Huh-7 and HepG2. Therefore, this cell line is likely to be very valuable in the viral receptor attachment and entry process.³ The main reason why we chose HHL-5 was that CdSe NPs can cause liver damage. Acute hepatotoxicity involves two pathways, one for the initial injury produced by direct effects of cadmium and the other for the subsequent injury produced by inflammation. Primary injury appears to be caused by the binding of Cd²⁺ to sulfhydryl groups on critical molecules in mitochondria.⁴

The HHL-5 cells were routinely cultured in Dulbecco's modified essential medium (DMEM) supplemented with 10 % fetal bovine serum (FBS), 1 % Penicillin/Streptomycin (P/S, 5000u) and 1 % L-Glutamine (200mM) at 37 °C in an incubator which has humidified atmosphere with 5 % carbon dioxide. Cells (1 × 10⁶ cells) were cultured in the 75 cm³ flask. The medium was changed every 2-3 days and checked under a microscope to see if the cells achieve 70% -80% confluences.

After the cells reached 70% -80% confluences, the old medium was discarded and removed by a 10mL pipette. Cells were washed twice by pre-warmed PBS by gently pipetting PBS into the flask then carefully mixed by tilting the flask from one side to the other twice.

2mL of pre-warmed Trypsin/EDTA were added to dispatch the cells. Ensuring the film of Trypsin/EDTA came into contact with the whole cell surface by tilting the dish twice. Excess Trypsin/EDTA was removed using a pipette, and the culturing dish was placed in the incubator at 37 °C for 10 min until the cells detached. The cells were dislodged by gently tapping on the side of the flask/dish and were then checked under a microscope. Trypsin was deactivated and diluted by the addition of 10 mL of warm fresh DMEM medium to the flask. The cells were centrifuged at 1000rpm for 5 min. Gently and carefully the supernatant was discarded, and the sedimented cells were mixed in 10 mL of pre-warmed DMEM medium. After cell counting under the microscope, the cells were diluted to reasonable concentration, for instance, 5000 cells/ well for a 96 well plate. The outer wells of the 96 wells plates were filled with 100 μ L phosphate buffered saline (PBS) to limit cell wells from drying out.

2.7 MTT Cell Proliferation and Viability Assays

The MTT (3-(4, 5-dimethylthiazol-2-yl)-2, 5-diphenyltetrazolium bromide) assay was used to evaluate the cell proliferation and cell viability in the presence of the CdSe NPs. MTT assay is a colorimetric assay for measuring the activity of cellular enzymes that reduce the tetrazolium dye. Succinate dehydrogenase in the mitochondria of the living cells can convert MTT to a water-insoluble crystalline blue violet formazan and deposit on the cells, while dead cells cannot perform this process. Dimethyl sulfoxide (DMSO)

can dissolve the formazan in the cell; its optical absorption can then be measured by using a microplate reader. The number of living cells can be judged by the absorbance value (OD value), the larger the OD value is, and the stronger the cell activity will be.

The immortalised human hepatocytes (defined as HHL-5) cells were seeded in a 96 well plate at a concentration of 5.0×10^3 cells in a final volume of 100 μL /well. The 96 well plates were kept in an incubator at 37 $^{\circ}\text{C}$ and left in a humid atmosphere containing 5 % carbon dioxide for 48 hours. Then, the cells were treated with CdSe NPs at various concentrations and incubated for a further 24 hours. Next, the medium was removed using a pump followed by the washing of cells with PBS. 100 μL of 10% solution of MTT reagent in media were added to per well of the 96 well plates. This was incubated at 37 $^{\circ}\text{C}$ for 1 hour. The medium was then extracted using a pump and re-suspended of 100 μL /well of DMSO. To ensure the formazan precipitate was dissolved this mixture was pipetted up and down several times for each well. The microplate was read by using 550 nm as a test wavelength and 630 nm as the reference wavelength.

2.8 Confocal Laser Scanning Microscopy

The first purely analogue mechanical confocal microscope was designed and produced by Eggar and Petran in 1967,⁸ and the first commercial confocal laser scanning fluorescence microscopy systems were produced by Bio-Rad Microscopy Ltd.⁸ 24 well cell culture plate (cat No 662 160) was bought from CELLSTAR®, Greiner bio-one UK. The middle square (box) of the standard hemocytometer chamber is 1mm \times 1mm. Usually counted 4-6 box and calculate average number which is the cells number per ml. This middle square area covered at 100 \times microscope magnification (10 \times ocular and 10 \times objective).¹¹

The samples were prepared as follows: cells were cultured on 24 wells plates on slips. Firstly, a cover slip was placed in to each well with a tweezers. Then, 70 % ethanol, 300 μL was added per well. Next, the ethanol was removed and each well was washed with PBS twice and left to dry. The cells were cultured on the slips with a density of 2.0×10^5 /well using 500 μL of medium (Figure 2.8.1).

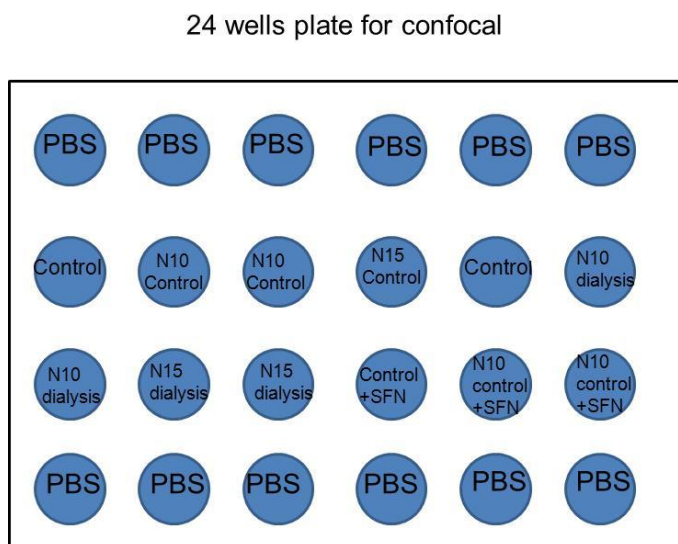


Figure 2.5 24 wells plate plan for confocal microscopy.

After the cells reached 70 % confluence (In cell culture biology, confluence is the term commonly used as a measure of the number of the cells in a cell culture dish or a flask, and refers to the coverage of the dish or the flask by the cells) ⁸ usually after cell culture for about 2-3 days, ⁸ CdSe NPs (10:1) with concentration of 10 μM and 15 μM (N10 and N15 control means the particles without dialysis, N10 and N15 dialysis means the particles were dialysed) were added into the wells (Figure 2.8.1, Figure 2.8.2). The slides were collected after 24 hours after the addition of the CdSe NPs the wells (Figure 2.8.2).

Pick up after 24 hours

	PBS	PBS	PBS	PBS	PBS	PBS
	Control	N10 Control	N10 Control	N15 Control	Control	N10 dialysis
	N10 dialysis	N15 dialysis	N15 dialysis	Media+ DMSO Control	N10 Control+ SFN5	N10 Control+ SFN5
	PBS	PBS	PBS	PBS	PBS	PBS

Figure 2.6 Pick up the slices after 24 hours since the CdSeNPs were added into the cells.

Before picking up cover slips, each well was washed with PBS twice. Then fixed by adding ice-cold methanol, 300 μ L per well and waiting for 5 minutes. Subsequently, PBS was used to wash each well again, DAPI (concentration with 1:5000) 250 μ L per well was added and left for 8 minutes. This was washed with PBS twice; the last wash was kept in the wells. Slowly and smoothly one slip was picked out and dipped into Milli-Q water and then a soft tissue was used wipe off the excess water. 5 μ L mounting gel was added to the slide and the slip was placed on the slide. The slide was left at room temperature for 30 min. Then nail oil was used to fix the slips on to the slide, the slide was covered with film paper and stored in 4 ° C refrigerator. Then the images are recorded under the confocal microscopy.

2.9 Reference

1. Ni, T.; Nagesha, D. K.; Robles, J.; Materer, N. F.; Mussig, S.; Kotov, N. A., CdS nanoparticles modified to chalcogen sites: New supramolecular complexes, butterfly bridging, and related optical effects. *Journal of the American Chemical Society* 2002,124 (15), 3980-3992.

2. Wang, L.; Nagesha, D. K.; Selvarasah, S.; Dokmeci, M. R.; Carrier, R. L., Toxicity of CdSe Nanoparticles in Caco-2 Cell Cultures. *Journal of nanobiotechnology*. 2008.
3. Clayton, R. F.; Rinaldi, A.; Kandyba, E. E.; Edward, M.; Willberg, C.; Klenerman, P.; Patel, A. H., Liver cell lines for the study of hepatocyte functions and immunological response. *Liver international : official journal of the International Association for the Study of the Liver* 2005,25 (2), 389-402.
4. Rikans, L. E.; Yamano, T., Mechanisms of cadmium-mediated acute hepatotoxicity. *Journal of Biochemical and Molecular Toxicology* 2000,14 (2), 110-117.
5. Atkins, P., *The elements of physical chemistry*. Oxford: Oxford, UK, 2001.
6. A. T. R. Williams, S. A. W. a. J. N. M., Relative fluorescence quantum yields using a computer controlled luminescence spectrometer. *Analyst*. 1983.
7. Hornyak; Dutta; Tibbals; Rao, *Introduction to Nanoscience*. CRC press: USA, 2008.
8. Shotton, C. J. R. S. a. D. M., *Confocal Laser Scanning Microscopy*. Information Press Ltd: UK, 1997.
9. Prasad, V.; Semwogerere, D.; Weeks, E. R., Confocal microscopy of colloids. *J Phys-Condens Mat* 2007,19 (11).
10. Ahire JH, Wang Q, Coxon PR, et al. Highly Luminescent and Nontoxic Amine-Capped Nanoparticles from Porous Silicon: Synthesis and Their Use in Biomedical Imaging. *Acs Applied Materials & Interfaces*. 2012;4(6):3285-3292.
11. J.M. Davis. *Basic cell culture*. Oxford, Oxford. 2002.

Chapter 3. Synthesis of CdSe quantum dots and their optical properties

3.1 The stability and ageing results of the CdSe NPs

Most of the papers relating to CdSeNPs have focused on how the band gap, structure or optical properties of CdSe/ZnS nanoparticles change through heating CdSe/ZnS nanocrystal, coating of CdSe NPs or the dissolution of Cadmium ions in different solvents at different temperatures.¹⁻²¹ However, this study focuses on both optical properties and in vitro cytotoxicity of CdSe NPs with differing sodium citrate stabiliser concentrations and ratios of Cadmium to Selenium.

Table 3.1.1 The colour and stability of the CdSeNPs.

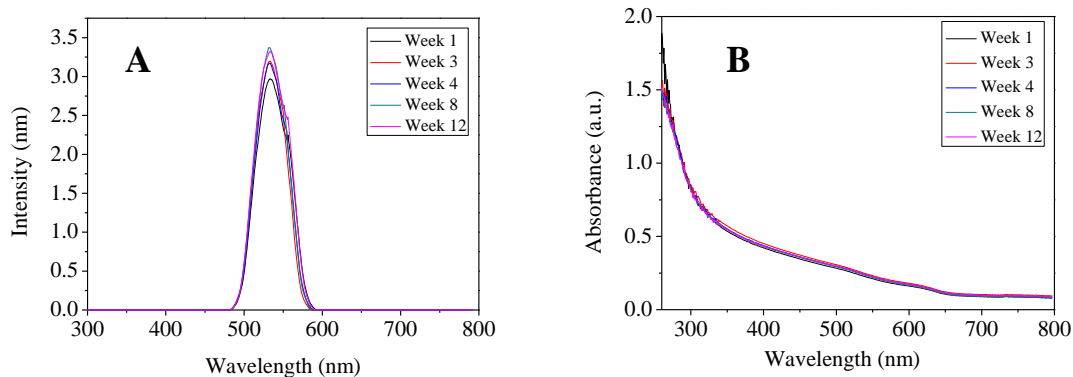
<i>No Sediments days and the colour of samples</i>	Sodium Citrate (%)		
	0.05	0.1	0.2
CdSe (10:1)	40 days (pastel orange)	80 days (orange)	100 days (vivid red)
CdSe (4:1)	30 days (pastel orange)	60 days (pastel red)	90 days (red)
CdSe (1:1)	15 days (light yellow)	20 days (pastel yellow)	30 days (yellow)

If the samples stored longer than the days in table 3.1, it will become unstable and have sediments. The CdSe NPs (10:1) with 0.2% sodium citrate stabiliser have the most stable characteristics (Table 3.1) and deepest colour (Table 3.1). Conversely, CdSe (1:1) with 0.05% sodium citrate stabilizer were the least stable (Table 3.1). Basically, the characteristics of CdSe (10:1) were more stable than CdSe (4:1) while CdSe (4:1) were more stable than CdSe NPs (1:1). Among CdSe NPs (10:1), (4:1) and (1:1), those with 0.2%

of sodium citrate stabilizer were the most stable. In contrast, the samples with 0.05 % sodium citrate as stabilizer were the most unstable (Table 3.1). Therefore, the more sodium citrate stabiliser and Cadmium accumulated in the CdSe NPs, the more stable the particles.

Many papers which relates to photoluminescence spectrum of CdSe NPs do not include ageing studies.¹⁻²¹ The novelty of this study was to focus on the ageing part of the CdSe NPs. CdSe NPs (10:1) with 0.05, 0.1 and 0.2 % sodium citrate, CdSe NPs (4:1) with 0.05, 0.1 and 0.2 % sodium citrate plus CdSe (1:1) with 0.05, 0.1 and 0.2 % sodium citrate were tested on the third day after synthesis (in order to give the particles enough time to grow). Each sample was then tested daily to see if the spectrum changed with time.

3.1.1 CdSe NPs (1:1) with 0.05%, 0.1% and 0.2% sodium citrate as stabilizer



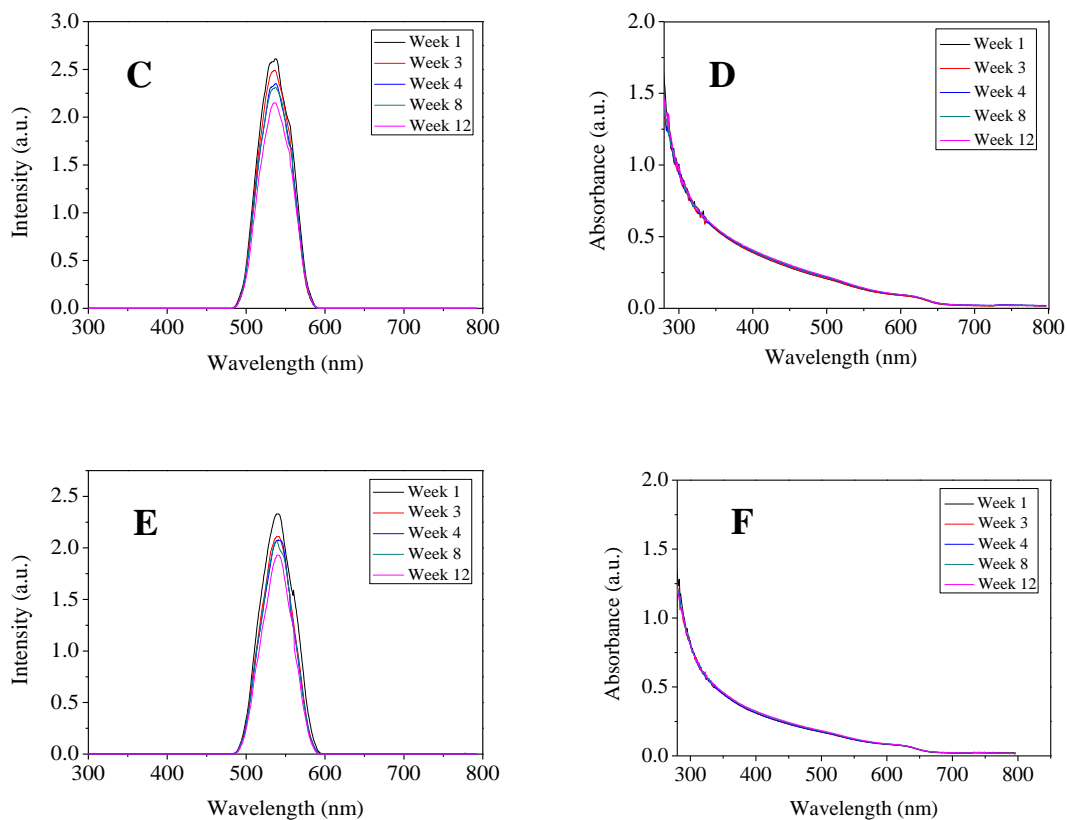


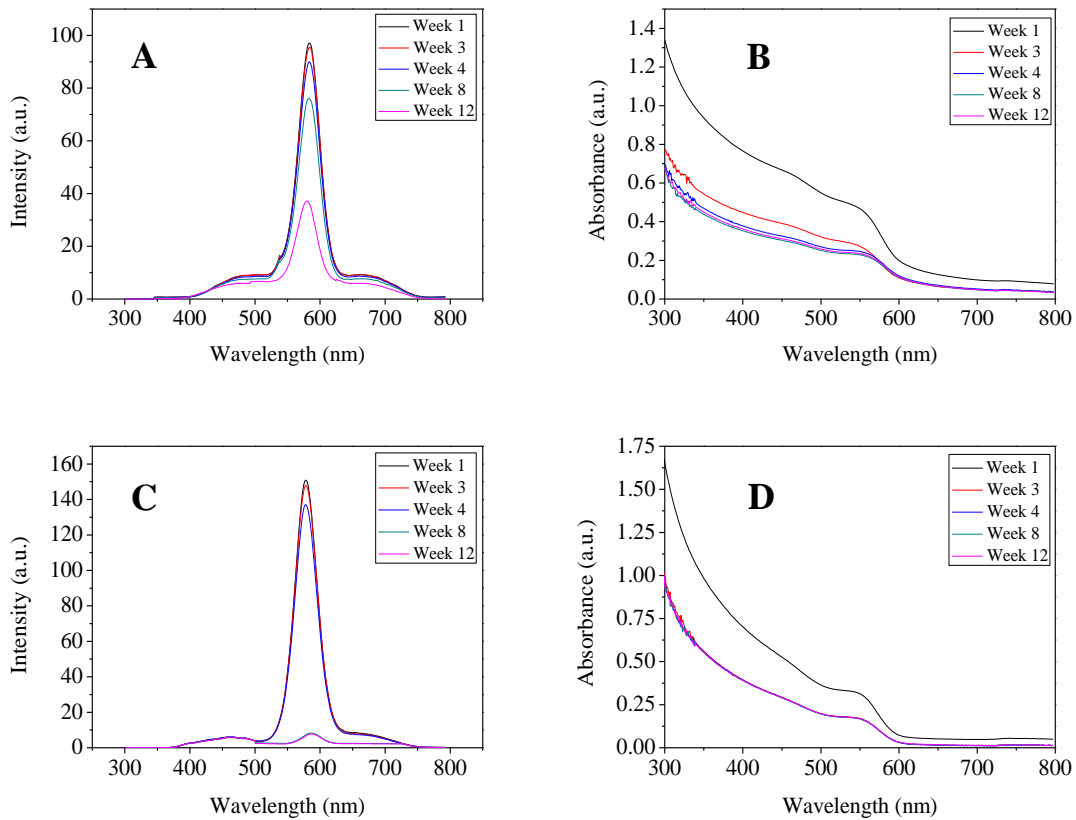
Figure 3.1 The ageing spectrum of CdSe NPs (1:1) with 0.05% (A, B), 0.1% (C, D) or 0.2% (E, F) sodium citrate stabilizer.

Graph A,C and E demonstrate the photoluminescence spectrum of CdSe NPs (1:1) with 0.05 %, 0.1 % and 0.2 % sodium citrate stabilizer, respectively. The excitation was 460 nm. Filter cut-off at 515 nm. Graph B, D and F demonstrate the Ultraviolet-visible Spectrum of CdSe NPs (1:1) with 0.05% , 0.1% and 0.2% sodium citrate stabilizer, respectively.

The peak of the ultraviolet-visible spectrum of CdSe NPs (1:1) with 0.05 %, 0.1 % and 0.2 % sodium citrate as stabilizer were all around 625 nm. The peak of the photoluminescence spectrum of CdSe NPs (1:1) with 0.05 %, 0.1 % and 0.2 % sodium citrate stabilizer were all around 550 nm (Figure 3.1.1). Over the course of a week since the samples were synthesised, it is obvious that the luminescence of the sample was very

stable at least for one month. The fluctuated spectrum of CdSe NPs (1:1) samples probably because the evaporation and sample damage during the experiments (Figure 3.1.1). Nor Aliya Hamizi, et al,⁶ heated the CdSe QD (1:1) solution at 160 °C and tested the PL and UV spectra. The UV-Vis spectrum from this paper was similar to that of the CdSe (1:1) particles in this study.

3.1.2 CdSe NPs (4:1) with 0.05 %, 0.1 % and 0.2 % sodium citrate stabilizer



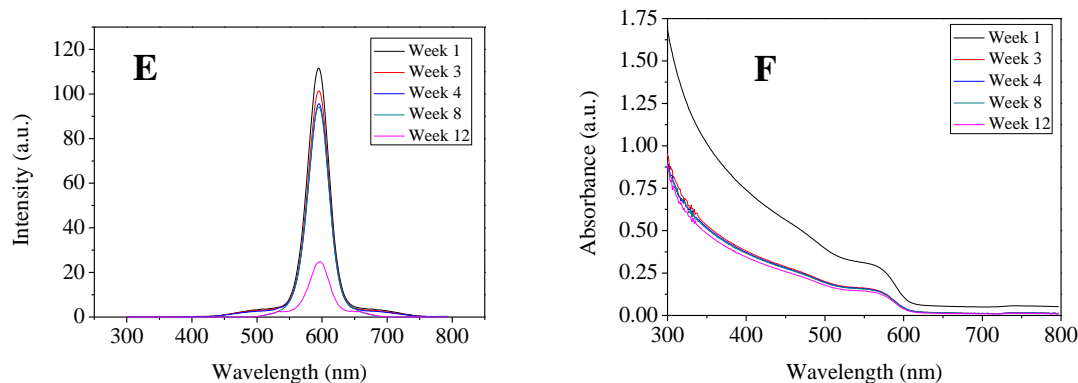


Figure 3.2 The ageing spectrum of CdSe NPs (4:1) with 0.05 % (A, B), 0.1 % (C, D) or 0.2 % (E, F) sodium citrate stabilizer.

Graph A, C and E demonstrate the photoluminescence spectrum of CdSe NPs (4:1) with 0.05 %, 0.1 % and 0.2 % sodium citrate stabilizer, respectively. The excitation was 345nm. Filter cut-off at 390 nm. Graph B, D and F demonstrate the Ultraviolet-visible Spectrum of CdSe NPs (1:1) with 0.05 % , 0.1 % and 0.2 % sodium citrate stabilizer, respectively.

The peak of the photoluminescence spectrum of CdSe (4:1) NPs with 0.05 %, 0.1 % and 0.2 % sodium citrate stabiliser were all around 590 nm (Figure 3.1.2). The peak of the ultraviolet-visible spectrum of CdSe NPs (4:1) with 0.05 %, 0.1 % and 0.2 % sodium citrate stabiliser were all around 550 nm. Over the course of a week since the samples were synthesised, it is obvious that the luminescence of the sample didn't change a lot during the first month. Ruosheng, et al,¹⁴ synthesised Mn: CdSe nanocrystals at 80 °C, 160 °C, 180 °C and 200 °C also got similar PL spectrum results. The trend of the spectrum of CdSe NPs (4:1) with 0.05 %, 0.1 % and 0.2 % sodium citrate stabiliser kept a similar curve during the first months since they were synthesised, the fluctuation of the samples in the spectrum probably because of the evaporation and sample damage during the experiments (Figure 3.1.2).

3.1.3 CdSe NPs (10:1) with 0.05 %, 0.1 % and 0.2 % sodium citrate stabilizer

stabilizer

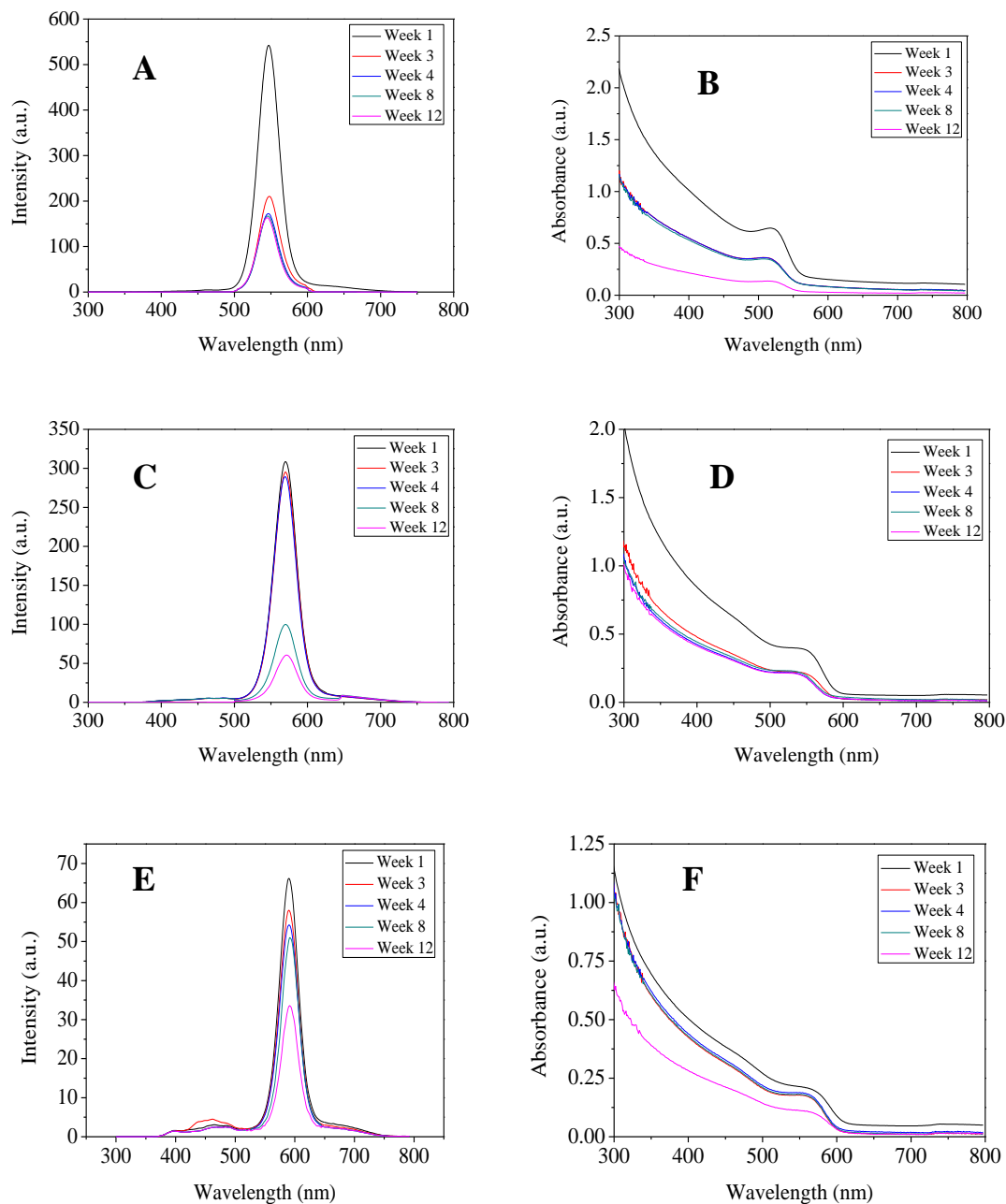


Figure 3.3 Graph A, C and E demonstrate the photoluminescence spectrum of CdSe NPs (10:1) with 0.05 %, 0.1 % and 0.2 % sodium citrate stabilizer, respectively. The excitation was 345 nm. Filter cut-off at 390 nm. Graph B, D and F demonstrate the

Ultraviolet-visible Spectrum of CdSe NPs (10:1) with 0.05 % , 0.1 % and 0.2 % sodium citrate stabilizer, respectively.

The peak of the photoluminescence spectrum of CdSe NPs (10:1) with 0.05 % , 0.1 % and 0.2 % sodium citrate stabilizer were all around 590 nm (Figure 3.1.3). The peak of the ultraviolet-visible spectrum of CdSe NPs (10:1) with 0.05 % , 0.1 % and 0.2 % were all around 550 nm. Xianfeng, et al,¹ heated the 2-MSA-CdSe nanoparticles at 100 °C for 102 hours showing a similar absorption and photoluminescence spectra to this study.

The ageing results show that the CdSe NPs were roughly stable during the first month. Although there were some fluctuations in the graphs it was probably because of sample evaporation, or the consumption and damage of the samples during the experiments. The most stable sample was the sample with 0.2% sodium citrate and the most unstable was the sample with 0.05% sodium citrate (Figure 3.1.1-Figure 3.1.3). Waleed E, et al,¹² synthesised different molar ratios of CdSe:ME in different atmospheres. The particles which were synthesised in nitrogen gas had a higher PL intensity value than those without nitrogen. Ying W, et al,²⁰ exposed the samples to light in air or in nitrogen and got a higher intensity value for the luminescence. However, in this study, all the samples were stored in a dark draw and covered with foil to keep out of the light to ensure the samples were not affected by any other parameters throughout the aging process. Therefore, all the results depict the luminescence of the samples themselves.

3.2 *The size of the CdSe NPs*

3.2.1 Size calculation

According to the effective mass model^{7, 19} the diameter of the CdSe NPs can be calculated by use the formulation below.

$$E_g^{nano} = E_g^{bulk} + \frac{h^2}{8m_0r^2} \left(\frac{1}{m_e^*} + \frac{1}{m_h^*} \right) - \frac{1.8e^2}{4\pi\epsilon\epsilon_0r}$$

Equation 3.2.1

r is the radius of the nanoparticles. The second term is the particle-in-a-box confinement energy for an electron-hole pair in a spherical quantum dot and the third term is the Coulomb attraction between an electron and hole modified by the screening of charges by the crystal. After multiplying by r^2 , this can be rearranged, to the quadratic formula below.

$$r = \frac{-\left(\frac{1.8e^2}{4\pi\epsilon\epsilon_0}\right) + \sqrt{\left(\frac{1.8e^2}{4\pi\epsilon\epsilon_0}\right)^2 + \left(E_g^{nano} - E_g^{bulk}\right) \frac{h^2}{2m_0} \left(\frac{1}{m_e^*} + \frac{1}{m_h^*}\right)}}{2\left(E_g^{nano} - E_g^{bulk}\right)}$$

Equation 3.2.2

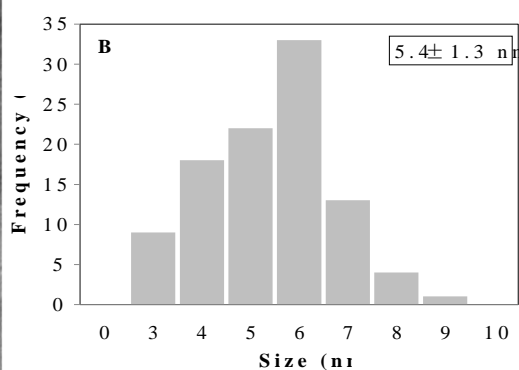
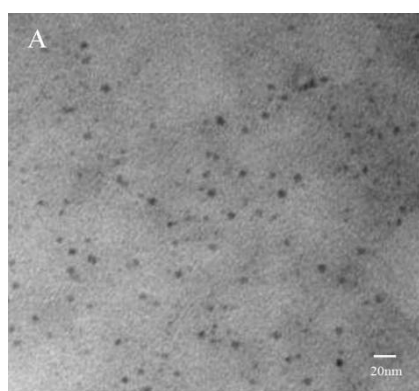
Here, $E_g = hc / \lambda$, $c = 2.998 \times 10^8 \text{ ms}^{-1}$, Band-gap of bulk CdSe: 1.74 eV, Effective masses: $m_e^* = 0.13 m_e$, $m_h^* = 0.6 m_e$, Plank's constant: $h = 6.63 \times 10^{-34} \text{ J}\cdot\text{s}$, Electron mass $m_e = 9.1 \times 10^{-31} \text{ kg}$, Absorption peak wavelengths were different according to different particles. The absorption peak of CdSe NPs (1:1) was at around 550 nm (Figure 3.1.1). The Absorption peak of CdSe NPs (4:1) was at about 590 nm (Figure 3.1.2). The Absorption peak of CdSe NPs (10:1) with 0.05 % sodium citrate stabilizer was at about 550 nm (Figure 3.1.3-A, B), the absorption peak of CdSe NPs (10:1) with 0.1 % sodium citrate as stabilizer was at about 575 nm (Figure 3.1.3-C, D) and the absorption peak of CdSe NPs (10:1) with 0.2 % sodium citrate stabilizer was at about 590 nm (Figure 3.1.3-E, F). The radius times two will be the diameter of the nanoparticles.

Table 3.2.1 Diameter value of the CdSeNPs in theory

Sodium citrate (%)	0.05	0.1	0.2
Ratio (Cd:Se)			
CdSe (10:1)	4.8	5.2	5.6
CdSe (4:1)	5.6	5.6	5.6
CdSe (1:1)	4.8	4.8	4.8

Different size of the particles were synthesised by using of 2 mL of 0.01, 0.04 and 0.1M cadmium perchlorate giving ratios of 1:1, 4:1 and 10:1 cadmium to selenium respectively. This resulted in average particle sizes of 5.0 nm, 5.8 nm, and 4.9 nm respectively (Table 3.3). The real size of the CdSe NPs was very close to the theoretical size (Table 3.2) which means that the real size of the CdSe NPs in table 3.3 was reliable. The diameters of the particles were evaluated using the PL spectra, UV-Vis spectra and were measured using transmission electron microscopy (TEM) imaging.

3.2.2 TEM results of CdSe (10:1) with 0.05 %, 0.1 % and 0.2 % sodium citrate as stabilizer



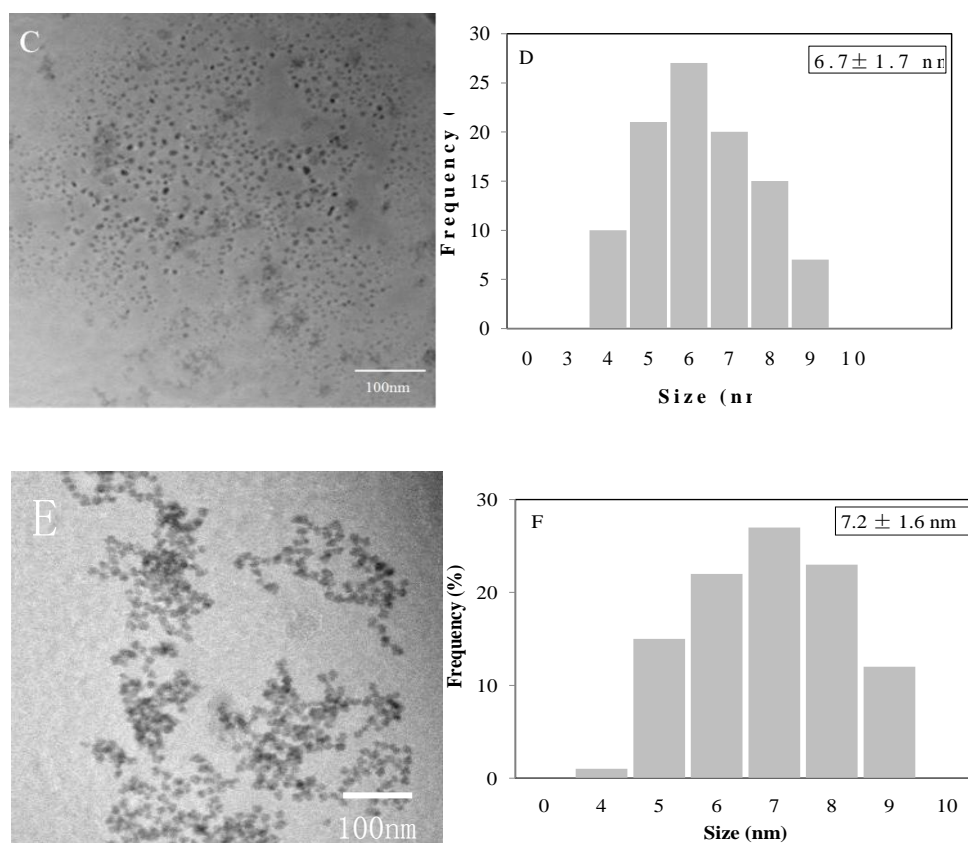


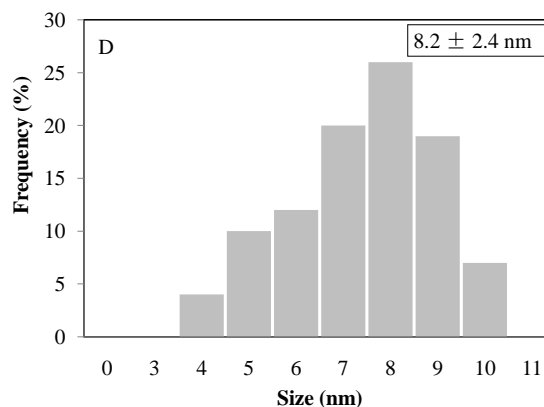
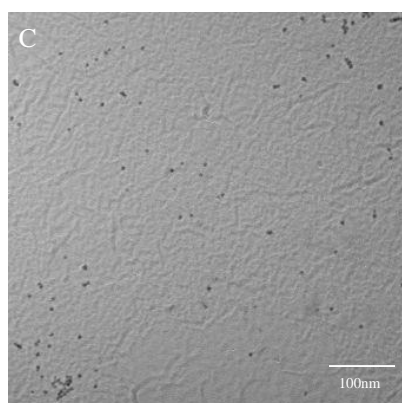
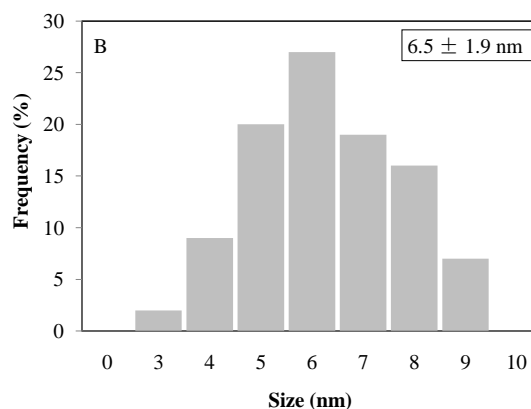
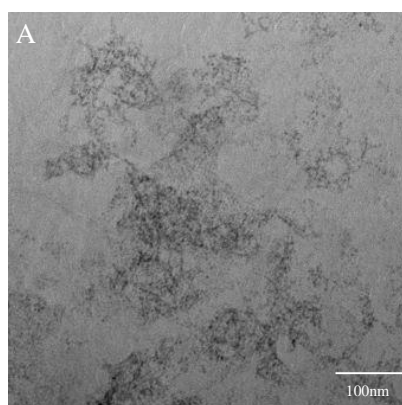
Figure 3.2.2 TEM results of CdSe (10:1) with 0.05 % , 0.1 % and 0.2 % sodium citrate as stabilizer.

Picture A, C, E demonstrate the TEM images of CdSe NPs (10:1) with 0.05 % , 0.1 % and 0.2 % sodium citrate stabilizer, respectively. Picture B, D, F show the size distribution of CdSe NPs (10:1) with 0.05 % , 0.1 % and 0.2 % sodium citrate stabilizer, respectively.

The average size of CdSe NPs (10:1) with 0.05 % , 0.1 % and 0.2 % sodium citrate stabilizer (Figure 3.2.2) was approximately 5.4 ± 1.3 , 6.7 ± 1.7 and 7.2 ± 1.6 nm respectively. Among the 100 particles measured in each picture, a size of about 6.0, 6.0 and 7.0 nm were the most frequently observed with 0.05 % , 0.1 % and 0.2 % sodium citrate as stabilizer, respectively. The TEM images (Figure 3.2.2) also show that the shape of CdSe NPs (10:1) was regular round and separated very well, so they could be easily identified and counted. Mojtaba, *et al.*,¹⁶ heated the CdSe quantum dots with a microwave method to see if the temperature will play an important role in the experiment. After

heating the CdSe quantum dots coated with ODPA nanoparticles, the TEM image showed a similar result to CdSe NPs (10:1) NPs in this study. Waleed E, *et al*,¹² prepared the CdSe quantum dots at different CdSe/Me ratios. A CdSe/Me ratio of 1:3 had a similar TEM image to CdSe (10:1) NPs. However, the TEM images of CdSe (10:1) were much clearer and shows more regular, round particles. This is probably because the stabilizer used and structure of the particles was different.

3.2.3 TEM results of CdSe (4:1) with 0.05 %, 0.1 % and 0.2 % sodium citrate as stabilizer



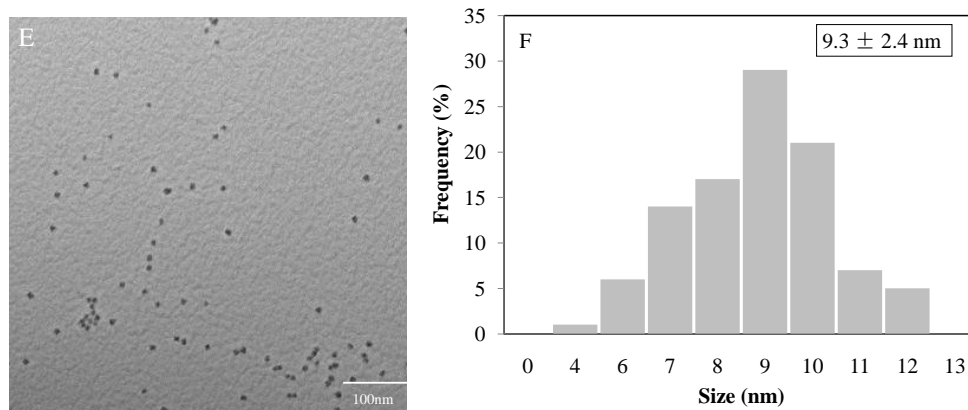


Figure 3.2.3 TEM results of CdSe (4:1) with 0.05 % , 0.1 % and 0.2 % sodium citrate as stabilizer.

Picture A, C, E demonstrate the TEM images of CdSe NPs (4:1) with 0.05 %, 0.1 % and 0.2 % sodium citrate stabilizer, respectively. Picture B, D, F show the size distribution of CdSe NPs (4:1) with 0.05 %, 0.1 % and 0.2 % sodium citrate stabilizer, respectively.

The average size of CdSe NPs (4:1) with 0.05 %, 0.1 % and 0.2 % sodium citrate stabilizer (Figure 3.2.3) was approximately 6.5 ± 1.9 , 8.2 ± 2.4 and 9.3 ± 2.4 nm. Among the 100 particles measured in each picture, a size of about 6.0, 8.0 and 9.0 nm were the most frequently observed with 0.05 %, 0.1 % and 0.2 % sodium citrate as stabilizer, respectively. The TEM image (Figure 3.2.3) also show that the CdSe NPs were round and separated very well, so they could be easily identified and counted. CdSe quantum dots from different cadmium complexes such as Cd-Lu, Cd-DDPA, Cd-Myr, Cd-St also showed similar images; as shown in the paper of Mojtaba,et al.¹⁶ However, the images in this paper were much more dense and clear than CdSe (4:1) NPs. This was probably because the former used different cadmium complexes and the latter just uses the pure elements, cadmium and selenium. Another reason could be that the atmosphere (temperature, ramp, cooling time) was different in these two studies.

3.2.4 TEM results of CdSe (1:1) with 0.05 %, 0.1 % and 0.2 % sodium citrate as stabilizer

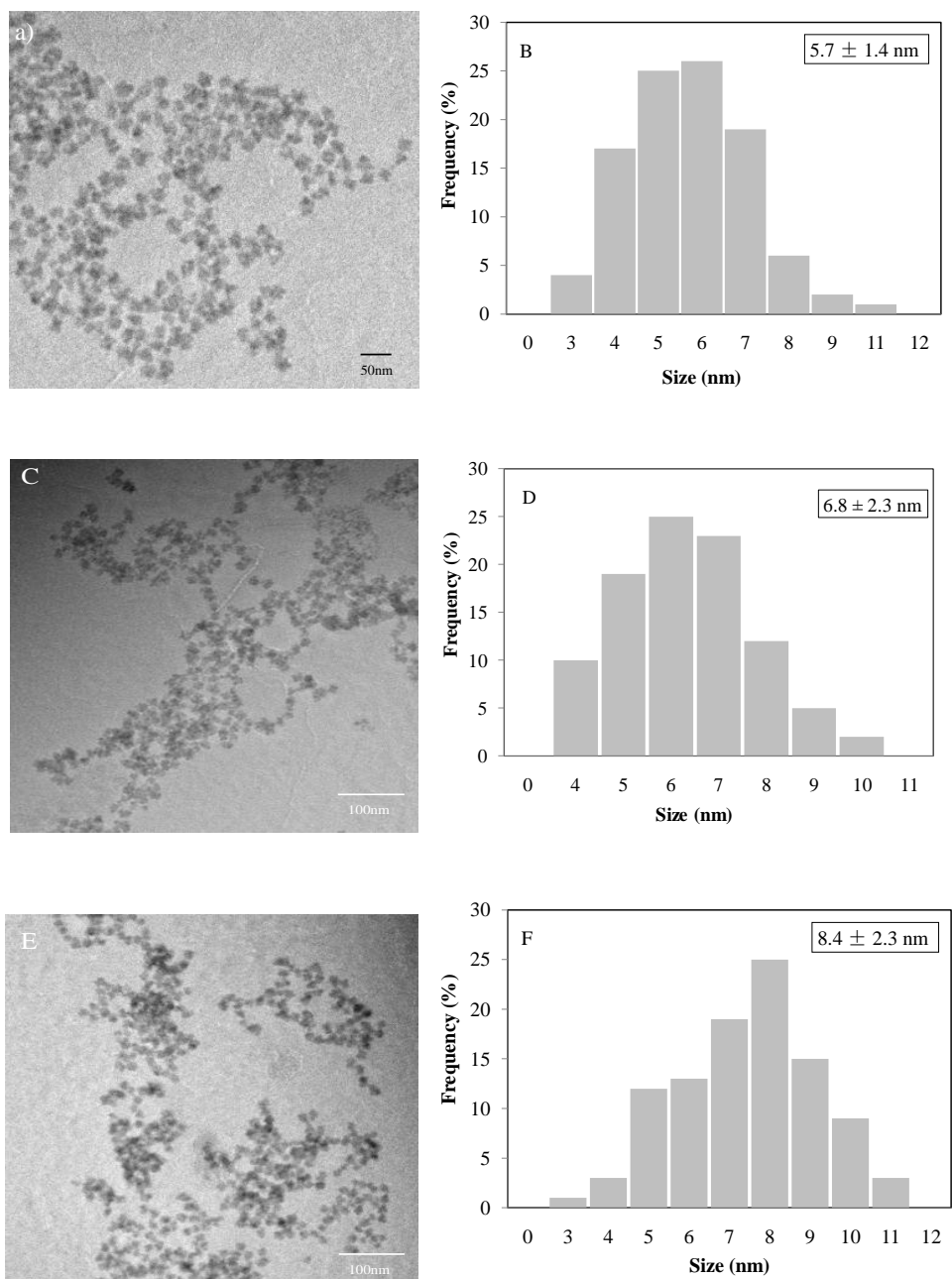


Figure 3.2.4 TEM results of CdSe (1:1) with 0.05 % , 0.1 % and 0.2 % sodium citrate as stabilizer.

Picture A, C, E demonstrate the TEM images of CdSe NPs (1:1) with 0.05 %, 0.1 % and 0.2 % sodium citrate stabilizer, respectively. Picture B, D, F show the size distribution of CdSe NPs (1:1) with 0.05 %, 0.1 % and 0.2 % sodium citrate stabilizer, respectively.

The average size of CdSe NPs (1:1) with 0.05 %, 0.1 % and 0.2 % sodium citrate stabilizer (Figure 3.2.4) was approximately 5.7 ± 1.4 , 6.8 ± 2.3 and 8.4 ± 2.3 nm. Among the 100 particles measured in each picture, a size of about 5.0, 6.0 and 6.0 nm were the most frequently observed with 0.05 %, 0.1 % and 0.2 % sodium citrate as stabilizer, respectively. The TEM image (Figure 3.2.4) also shows that the CdSe NPs were irregular but separated very well, so they could be easily identified and counted. Heating CdSe quantum dots at 170 °C for 50 minutes or use CdSe (ZnS) core (shell) NPs also show similar images, which are explained in papers by Rong He, et al,⁷ and Lasantha, et al.⁹

Table 3.2.2 The diameters of CdSe NPs measured by TEM. Mean \pm Standard deviation (SD), n=100.

Sodium citrate (%) Ratio (Cd:Se)	0.05	0.1	0.2
CdSe (10:1)	5.4 ± 1.3	6.7 ± 1.7	7.2 ± 1.6
CdSe (4:1)	6.5 ± 1.9	8.2 ± 2.4	9.3 ± 2.4
CdSe (1:1)	5.7 ± 1.4	6.8 ± 2.3	8.4 ± 2.3

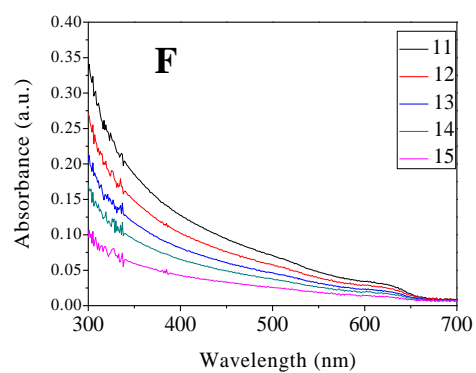
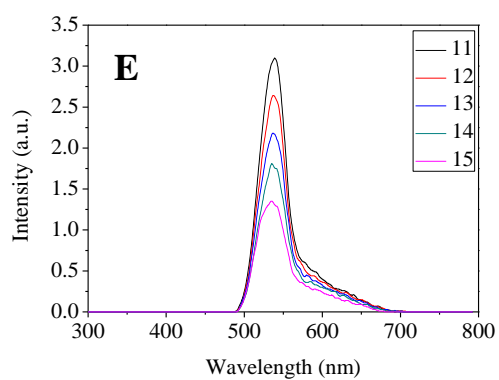
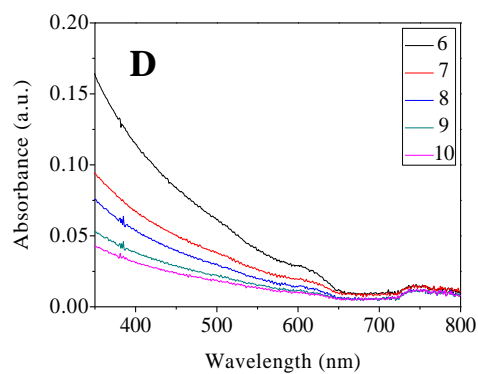
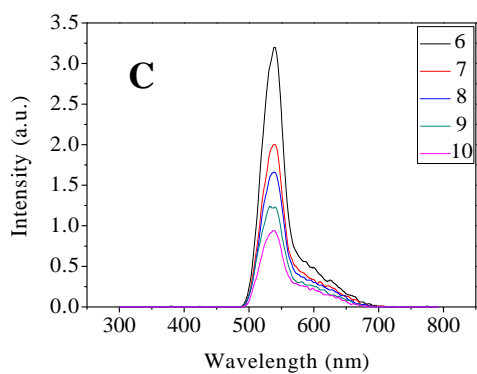
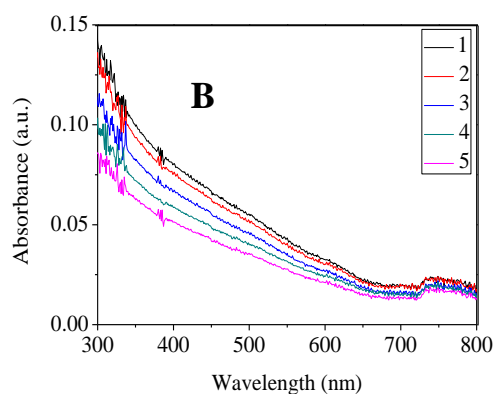
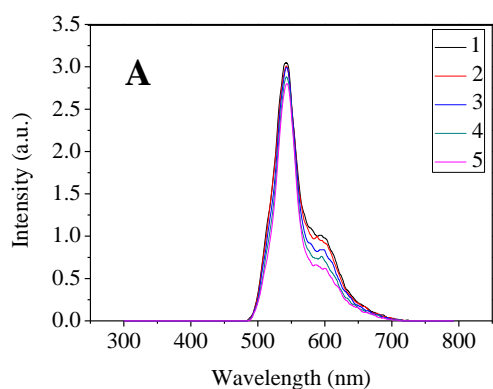
The theory values (Table 3.2) are within 95 % confidence interval (Mean \pm 2SD) of measured values (Table 3.3) accordingly. According to the table above (Table 3.3), different percentages of sodium citrate result in different particle sizes. CdSe NPs with 0.2 % sodium citrate stabilizer give the largest particle size in each of three types of CdSe NPs (10:1, 4:1 and 1:1) compare to NPs with 0.1 % and 0.05 % stabilizer. Conversely,

CdSe NPs with 0.05 % sodium citrate stabilizer has the smallest particle size in each type of CdSe NPs. Overall, the more the stabilizer in the particles the larger the particles are.

3.3 *The Quantum yield of the CdSe NPs*

Quantum yield (QY) means the ratio of photon in a photochemical reaction to the total number of absorption photons by the sample. The most reliable method for recording QY is the comparative method of Williams *et al*,²² which involves the use of well characterised standard samples with known QY values. This method compares the integrated fluorescence intensity and the absorption for unknown sample and standard using optical densities between 0.1 and 0.01. Most of papers relating to CdSe and quantum yield were use different method.^{1, 8, 20, 23-32} They use different Cd/Se ratio, heat the particles to a certain temperature to see if the band gap or change the atmosphere to affect the quantum yield.²⁰ However, the primary response of interest in the study was the fluorescence of the quantum dots caused by different ratio of Cadmium to Selenium and different percentage sodium citrate as stabilizer compare with quinine sulphate as reference. The reason why choose quinine sulphate as reference is because its absorbance range is similar to the CdSe NPs. Furthermore, the entire quantum yield results in this study depict the characteristic of the samples themselves without the influence of any other parameters.

3.3.1 CdSe NPs (1:1) with 0.05 %, 0.1 % and 0.2 % sodium citrate stabilize.



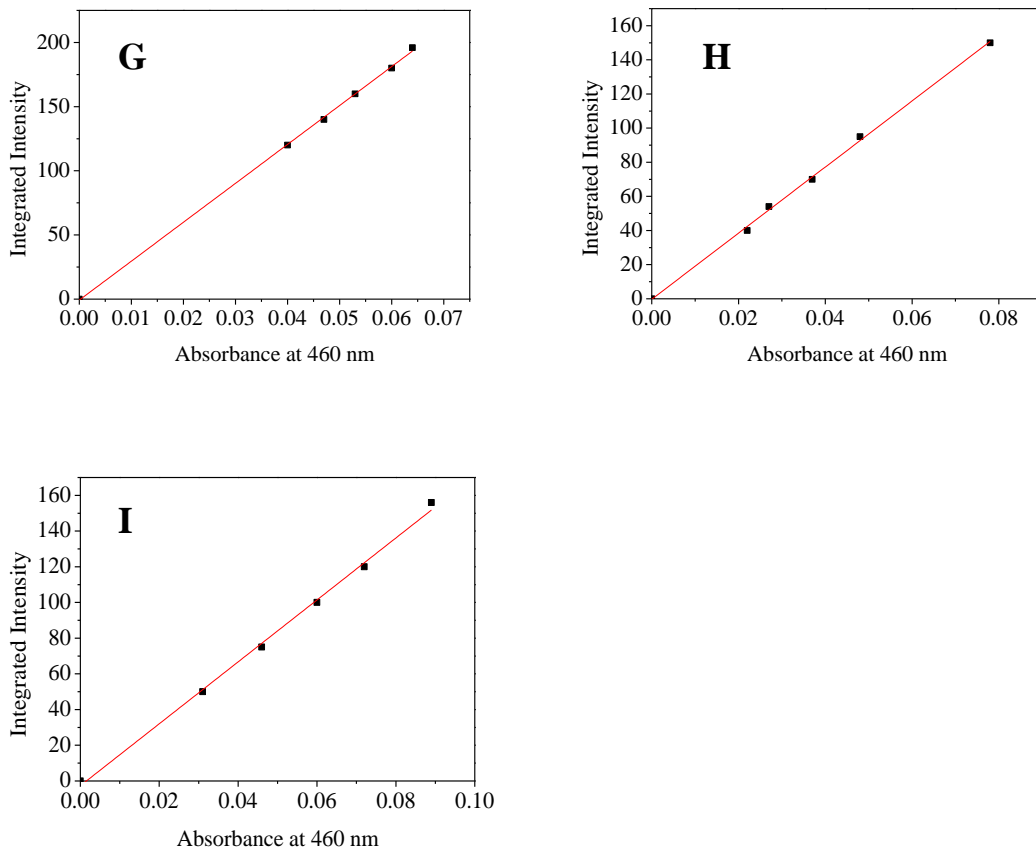


Figure 3.4 Quantum Yield results of CdSe (1:1) with 0.05 % , 0.1 % and 0.2 % sodium citrate stabilizer.

Graph A, C, E show emission spectra obtained for CdSe NPs (1:1) with 0.05 % , 0.1 % , 0.2 % sodium citrate stabiliser, respectively. Excitation was 460 nm, filter 515 nm cut off. Graph B, D, F demonstrate absorption spectra obtained for CdSe NPs (1:1) with 0.05 % , 0.1 % and 0.2 % sodium citrate stabiliser. Excitation was 460 nm. Graph G, H, I show scatter plot of absorbance at 460 nm against integrated intensity for CdSe NPs (1:1) 0.05 % , 0.1 % , 0.2 % sodium citrate stabiliser, respectively. The numbers from 1-15 was different concentrations dilute from each samples.

Table 3.3.1 Linear line absorbance vs integrated intensity of CdSe (1:1) with 0.05 %, 0.1 % and 0.2 % sodium citrate stabiliser.

CdSe NPs with different percentage of sodium citrate stabiliser	Concentrations	Absorbance at 460 nm	Integrated Intensity
CdSe (1:1) with 0.05 % sodium citrate stabiliser	1	0.064	196
	2	0.060	180
	3	0.053	161
	4	0.047	142
	5	0.041	120
CdSe (1:1) with 0.1 % sodium citrate stabiliser	6	0.078	150
	7	0.048	95
	8	0.037	70
	9	0.027	54
	10	0.022	40
CdSe (1:1) with 0.2 % sodium citrate stabiliser	11	0.089	156
	12	0.072	120
	13	0.060	100
	14	0.046	70
	15	0.031	50

Here, the quantum yield of CdSe NPs was calculated via the following equation:

$$Q = Q_R \left(\frac{Grad}{Grad_R} \right) \left(\frac{\eta^2}{\eta_R^2} \right)$$

Where Q is the quantum yield, Grad is the gradient from the plot of integrated fluorescence intensity versus absorbance. The subscript R refers to the reference

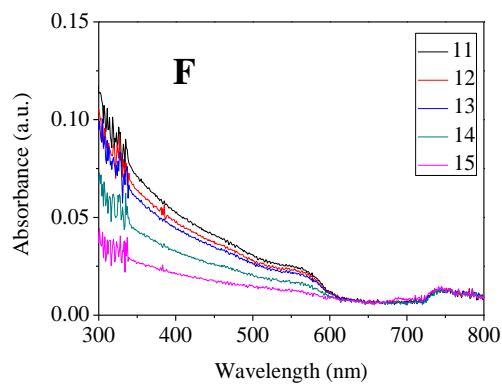
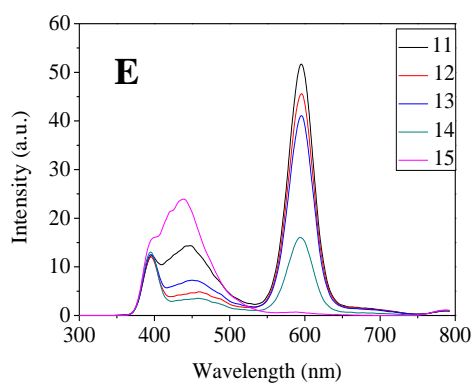
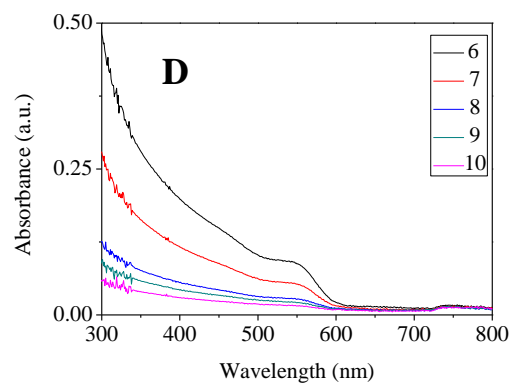
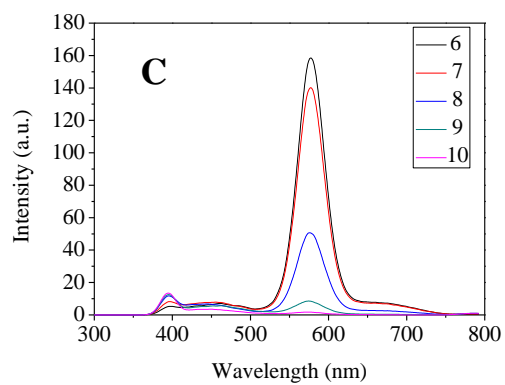
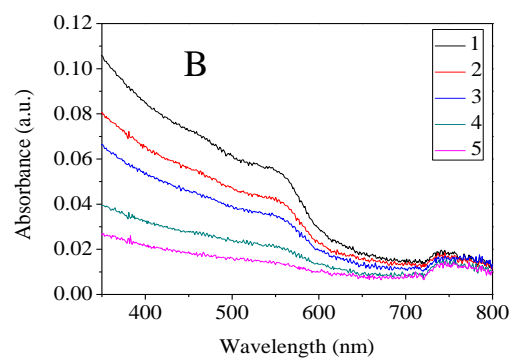
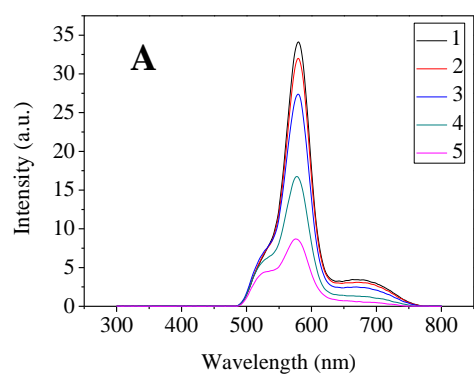
fluorophore of known quantum yield. Here Quinine Sulphate was used as reference,¹ which has a quantum yield of 54.6% when dissolved in 1N H₂SO₄. 1N (0.5M) H₂SO₄ had a refractive index of 1.346,¹ while the refractive index of water was 1.33.¹ The gradients of Quinine sulphate and CdSe NPs (1:1) with 0.05 %, 0.1 % and 0.2 % sodium citrate stabilizer were 1901980,¹ 3032 (Table 3.5, Figure 3.3.1- A, B, G), 1936 (Table 3.5, Figure 3.3.1-C, D, H) and 1735 (Table 3.5, Figure 3.3.1-E, F, I), respectively.

$$Q_{0.05\%} = 54.6\% \left(\frac{3032}{1901980} \right) \times \left(\frac{1.33^2}{1.346^2} \right) = 0.1 \%$$

$$Q_{0.1\%} = 54.6\% \left(\frac{1936}{1901980} \right) \times \left(\frac{1.33^2}{1.346^2} \right) = 0.05 \%$$

$$Q_{0.2\%} = 54.6\% \left(\frac{1735}{1901980} \right) \times \left(\frac{1.33^2}{1.346^2} \right) = 0.05 \%$$

3.3.2 CdSe NPs (4:1) with 0.05 %, 0.1 % and 0.2 % sodium citrate stabilizer



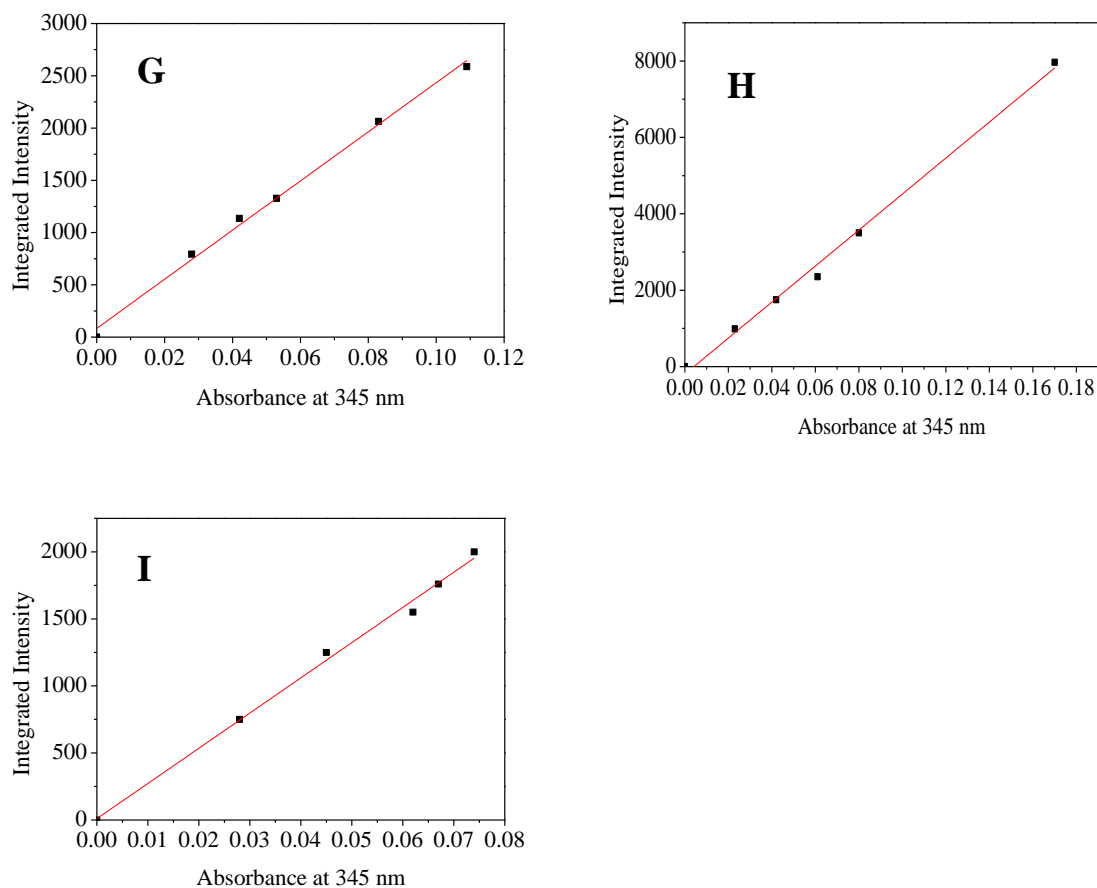


Figure 3.5 Quantum Yield results of CdSe (4:1) with 0.05 % , 0.1 % and 0.2 % sodium citrate stabilizer.

Graph A, C, E show emission spectra obtained for CdSe NPs (4:1) with 0.05 % , 0.1 % , 0.2 % sodium citrate stabiliser, respectively. Excitation was 345 nm, filter 390 nm cut off. Graph B, D, F demonstrate absorption spectra obtained for CdSe NPs (4:1) with 0.05 % , 0.1 % and 0.2 % sodium citrate stabiliser. Excitation was 345 nm. Graph G, H, I show scatter plot of absorbance at 345 nm against integrated intensity for CdSe NPs (4:1) 0.05 % , 0.1 % , 0.2 % sodium citrate stabiliser, respectively. The numbers from 1-15 was different concentrations dilute from each samples.

Table 3.3.2 Linear line absorbance vs integrated intensity of CdSe (4:1) with 0.05 %, 0.1 % and 0.2 % sodium citrate stabiliser.

CdSe NPs with different percentage of sodium citrate stabiliser	Concentration	Absorbance at 345 nm	Integrated Intensity
CdSe (4:1) with 0.05 % sodium citrate stabiliser	1	0.109	2587
	2	0.083	2064
	3	0.053	1327
	4	0.042	1136
	5	0.028	793
CdSe (4:1) with 0.1 % sodium citrate as stabiliser	6	0.170	7967
	7	0.080	3500
	8	0.061	2350
	9	0.042	1750
	10	0.023	990
CdSe (4:1) with 0.2 % sodium citrate stabiliser	11	0.074	2000
	12	0.067	1760
	13	0.062	1550
	14	0.045	1250
	15	0.028	750

Here, the quantum yield of CdSe NPs was calculated via the following equation:

$$Q = Q_R \left(\frac{Grad}{Grad_R} \right) \left(\frac{\eta^2}{\eta_R^2} \right)$$

Where Q is the quantum yield, Grad is the gradient from the plot of integrated fluorescence intensity versus absorbance. The subscript R refers to the reference

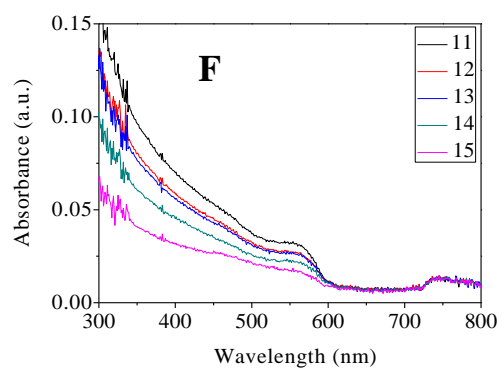
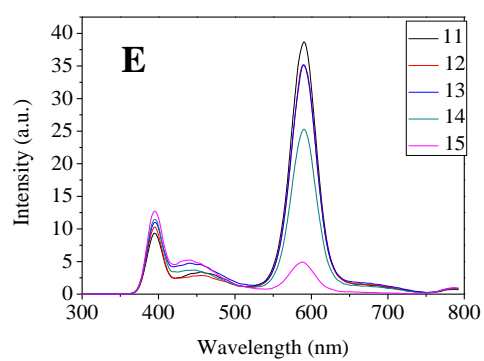
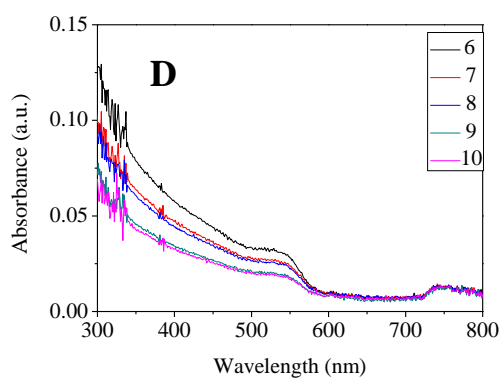
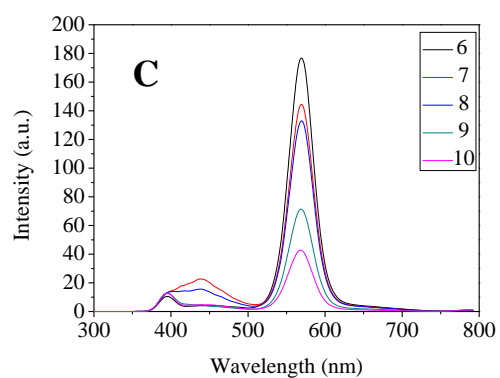
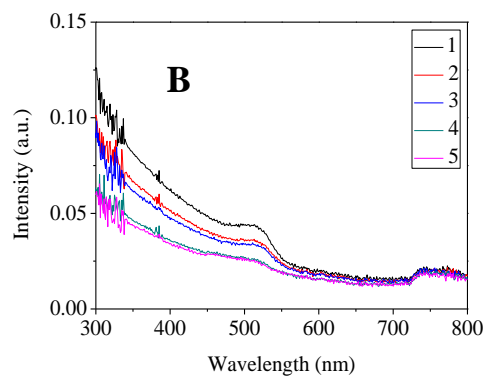
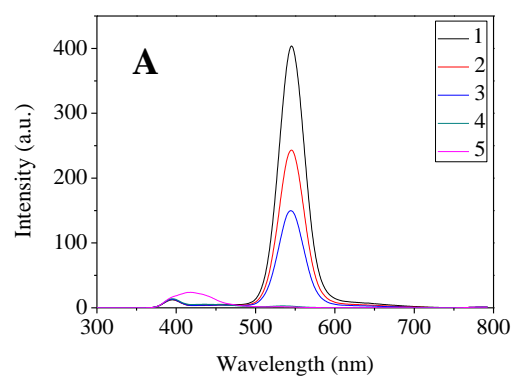
fluorophore of known quantum yield. Here Quinine Sulphate was used as reference,¹ which has a quantum yield of 54.6 %¹ when dissolved in 1N H₂SO₄. 1N (0.5M) H₂SO₄ had a refractive index of 1.346,¹ while the refractive index of water was 1.33.¹ The gradients of Quinine sulphate and CdSe NPs (1:1) with 0.05 %, 0.1 % and 0.2 % sodium citrate stabilizer were 1901980,¹ 3032 (Table 3.6, Figure 3.3.2- A, B, G), 1936 (Table 3.6, Figure 3.3.2-C, D, H) and 1735 (Table 3.6, Figure 3.3.2-E, F, I), respectively.

$$Q_{0.05\%} = 54.6\% \left(\frac{23509}{1901980} \right) \times \left(\frac{1.33^2}{1.346^2} \right) = 0.6 \%$$

$$Q_{0.1\%} = 54.6\% \left(\frac{47120}{1901980} \right) \times \left(\frac{1.33^2}{1.346^2} \right) = 1.3 \%$$

$$Q_{0.2\%} = 54.6\% \left(\frac{26265}{1901980} \right) \times \left(\frac{1.33^2}{1.346^2} \right) = 0.7 \%$$

3.3.3 CdSe NPs (10:1) with 0.05 %, 0.1 % and 0.2 % sodium citrate stabilizer



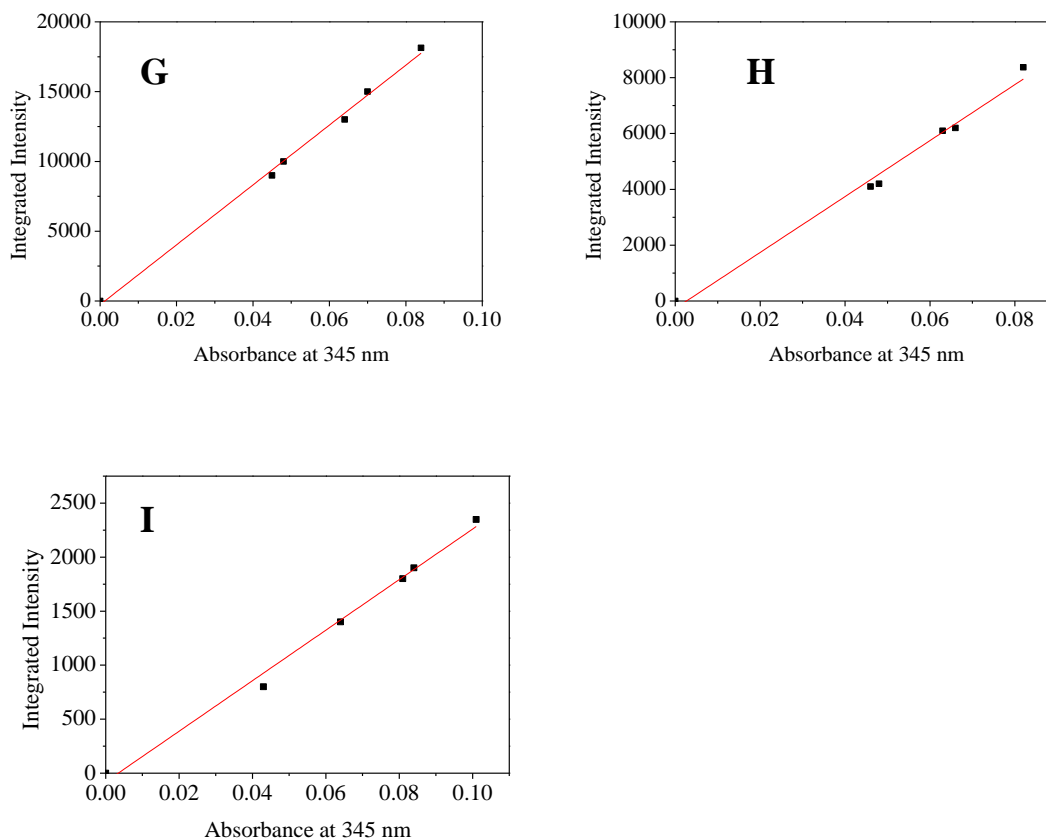


Figure 3.6 Quantum Yield results of CdSe (10:1) with 0.05 % , 0.1 % and 0.2 % sodium citrate stabilizer.

Graph A, C, E show emission spectra obtained for CdSe NPs (4:1) with 0.05 % , 0.1 % , 0.2 % sodium citrate stabiliser, respectively. Excitation was 345 nm, filter 390 nm cut off. Graph B, D, F demonstrate absorption spectra obtained for CdSe NPs (4:1) with 0.05 % , 0.1 % and 0.2 % sodium citrate stabiliser. Excitation was 345 nm. Graph G, H, I show scatter plot of absorbance at 345 nm against integrated intensity for CdSe NPs (4:1) 0.05 % , 0.1 % , 0.2 % sodium citrate stabiliser, respectively. The numbers from 1-15 was different concentration dilute from each samples.

Table 3.3.3 Linear line absorbance vs integrated intensity of CdSe (10:1) with 0.05%, 0.1% and 0.2% sodium citrate stabiliser.

CdSe NPs with different percentage of sodium citrate stabiliser	Concentrations	Absorbance at 345 nm	Integrated Intensity
CdSe (10:1) with 0.05 % sodium citrate stabiliser	1	0.084	18131
	2	0.070	15000
	3	0.064	13000
	4	0.048	10000
	5	0.045	9000
CdSe (10:1) with 0.1 % sodium citrate stabiliser	6	0.082	8370
	7	0.066	6200
	8	0.063	6100
	9	0.048	4200
	10	0.046	4100
CdSe (10:1) with 0.2 % sodium citrate stabiliser	11	0.101	2348
	12	0.084	1900
	13	0.081	1800
	14	0.064	1400
	15	0.043	800

Here, the quantum yield of CdSe NPs was calculated via the following equation:

$$Q = Q_R \left(\frac{Grad}{Grad_R} \right) \left(\frac{\eta^2}{\eta_R^2} \right)$$

Where Q is the quantum yield, Grad is the gradient from the plot of integrated fluorescence intensity versus absorbance. The subscript R refers to the reference

fluorophore of known quantum yield. Here Quinine Sulphate was used as reference,¹ which has a quantum yield of 54.6%¹ when dissolved in 1N H₂SO₄. 1N (0.5M) H₂SO₄ had a refractive index of 1.346,¹ while the refractive index of water was 1.33.¹ The gradients of Quinine sulphate and CdSe NPs (10:1) with 0.05%, 0.1% and 0.2% sodium citrate stabilizer were 1901980,¹ 214523 (Table 3.7, Figure 3.3.3- A, B, G), 100231 (Table 3.7, Figure 3.3.3-C, D, H) and 23392 (Table 3.7, Figure 3.3.3-E, F, I), respectively.

$$Q_{0.05\%} = 54.6\% \left(\frac{214523}{1901980} \right) \times \left(\frac{1.33^2}{1.346^2} \right) = 6 \%$$

$$Q_{0.1\%} = 54.6\% \left(\frac{100231}{1901980} \right) \times \left(\frac{1.33^2}{1.346^2} \right) = 3 \%$$

$$Q_{0.2\%} = 54.6\% \left(\frac{23392}{1901980} \right) \times \left(\frac{1.33^2}{1.346^2} \right) = 0.7 \%$$

Table 3.3.4 The summary of quantum yield rate of CdSeNPs.

Sodium citrate (%) Ratio (Cd:Se)	0.05	0.1	0.2
CdSe (10:1)	6	3	0.7
CdSe (4:1)	0.6	1.3	0.7
CdSe (1:1)	0.1	0.05	0.05

In conclusion, the luminescence of all CdSe NPs in this study was not as strong as expected. One reason is because luminescence of the sample itself was not strong when compared to other nanoparticles.¹ Another reason for this could be that some published experiments²⁰ exposed the samples to light in air or in nitrogen to get a quantum yield. But in this study, the results were reflected the nature of the samples without being affected by

other factors such as the light or heating. Therefore the values of the quantum yield of the samples were lower than other papers.

Basically, the CdSe NPs (10:1) has the strongest luminescent to particles with other ratios of cadmium to selenium (Table 3.7, Figure 3.3.3). In particular, CdSe NPs (10:1) with 0.05 % sodium citrate has the strongest luminescence (Table 3.7, Figure 3.3.3-A, B, G). Conversely, CdSe NPs (1:1) especially CdSe NPs (1:1) with 0.1 % and 0.2 % sodium citrate stabiliser has the lowest luminescence (Table 3.5, Figure 3.3.1).

3.4 Reference

1. Ahire JH, Wang Q, Coxon PR, et al. Highly Luminescent and Nontoxic Amine-Capped Nanoparticles from Porous Silicon: Synthesis and Their Use in Biomedical Imaging. *Acs Applied Materials & Interfaces*. 2012;4(6):3285-3292.
2. Vossmeier T, Katsikas L, Giersig M, et al. CDS NANOCCLUSERS - SYNTHESIS, CHARACTERIZATION, SIZE-DEPENDENT OSCILLATOR STRENGTH, TEMPERATURE SHIFT OF THE EXCITONIC-TRANSITION ENERGY, AND REVERSIBLE ABSORBENCY SHIFT. *Journal of Physical Chemistry*. 1994;98(31):7665-7673.
3. Zhao J, Qiu X, Wang Z, Pan J, Chen J, Han J. Application of quantum dots as vectors in targeted survivin gene siRNA delivery. *Oncotargets and Therapy*. 2013;6:303-309.
4. Pelley JL, Daar AS, Saner MA. State of Academic Knowledge on Toxicity and Biological Fate of Quantum Dots. *Toxicological Sciences*. 2009;112(2):276-296.

5. Bacon JR, Williamson G, Garner RC, Lappin G, Langouet S, Bao YP. Sulforaphane and quercetin modulate PhIP-DNA adduct formation in human HepG2 cells and hepatocytes. *Carcinogenesis*. 2003;24(12):1903-1911.
6. Fenwick GR, Heaney RK, Mullin WJ. GLUCOSINOLATES AND THEIR BREAKDOWN PRODUCTS IN FOOD AND FOOD PLANTS. *Crc Critical Reviews in Food Science and Nutrition*. 1983;18(2):123-201.
7. Brus L. ELECTRONIC WAVE-FUNCTIONS IN SEMICONDUCTOR CLUSTERS - EXPERIMENT AND THEORY. *Journal of Physical Chemistry*. 1986;90(12):2555-2560.
8. Hayes JD, McMahon M, Chowdhry S, Dinkova-Kostova AT. Cancer Chemoprevention Mechanisms Mediated Through the Keap1-Nrf2 Pathway. *Antioxidants & Redox Signaling*. 2010;13(11):1713-1748.
9. Surh YJ. Cancer chemoprevention with dietary phytochemicals. *Nature Reviews Cancer*. 2003;3(10):768-780.
10. Zhang YS, Li J, Tang L. Cancer-preventive isothiocyanates: dichotomous modulators of oxidative stress. *Free Radical Biology and Medicine*. 2005;38(1):70-77.
11. Keum YS, Jeong WS, Kong ANT. Chemopreventive functions of isothiocyanates. *Drug News & Perspectives*. 2005;18(7):445-451.
12. Mahmoud WE, Yaghmour SJ. Synthesis, characterization and luminescence properties of thiol-capped CdSe quantum dots at different processing conditions. *Optical Materials*. 2013;35(3):652-656.
13. Basten G, Bao Y, Williamson G. Sulforaphane and its glutathione conjugate but not sulforaphane nitrile induce UDP-glucuronosyl transferase (UGT1A1) and

- glutathione transferase (GSTA1) in cultured cells. *Carcinogenesis*. 2002;23(8):1399-1404.
14. Nagy A, Steinbrueck A, Gao J, Doggett N, Hollingsworth JA, Iyer R. Comprehensive Analysis of the Effects of CdSe Quantum Dot Size, Surface Charge, and Functionalization on Primary Human Lung Cells. *ACS Nano*. 2012;6(6):4748-4762.
 15. Liu W, Zhang S, Wang L, et al. CdSe Quantum Dot (QD)-Induced Morphological and Functional Impairments to Liver in Mice. *Plos One*. 2011;6(9).
 16. Chu M, Pan X, Zhang D, Wu Q, Peng J, Hai W. The therapeutic efficacy of CdTe and CdSe quantum dots for photothermal cancer therapy. *Biomaterials*. 2012;33(29):7071-7083.
 17. Rikans LE, Yamano T. Mechanisms of cadmium-mediated acute hepatotoxicity. *Journal of Biochemical and Molecular Toxicology*. 2000;14(2):110-117.
 18. Siddiqui IA, Adhami VM, Ahmad N, Mukhtar H. Nanochemoprevention: Sustained Release of Bioactive Food Components for Cancer Prevention. *Nutrition and Cancer-an International Journal*. 2010;62(7):883-890.
 19. Brus LE. ELECTRON ELECTRON AND ELECTRON-HOLE INTERACTIONS IN SMALL SEMICONDUCTOR CRYSTALLITES - THE SIZE DEPENDENCE OF THE LOWEST EXCITED ELECTRONIC STATE. *Journal of Chemical Physics*. 1984;80(9):4403-4409.
 20. Wang Y, Tang ZY, Correa-Duarte MA, et al. Mechanism of strong luminescence photoactivation of citrate-stabilized water-soluble nanoparticles with CdSe cores. *J Phys Chem B*. 2004;108(40):15461-15469.
 21. Jakubikova J, Sedlak J, Mithen R, Bao YP. Role of PI3K/Akt and MEK/ERK signaling pathways in sulforaphane- and erucin-induced phase II enzymes and

- MRP2 transcription, G(2)/M arrest and cell death in Caco-2 cells. *Biochemical Pharmacology*. 2005;69(11):1543-1552.
22. A. T. R. Williams SAWaJNM. Relative fluorescence quantum yields using a computer controlled luminescence spectrometer. *Analyst*. 1983;108:106.
 23. Mastrangelo L, Cassidy A, Mulholland F, Wang W, Bao Y. Serotonin receptors, novel targets of sulforaphane identified by proteomic analysis in Caco-2 cells. *Cancer Research*. 2008;68(13):5487-5491.
 24. Cheung KL, Kong A-N. Molecular Targets of Dietary Phenethyl Isothiocyanate and Sulforaphane for Cancer Chemoprevention. *Aaps Journal*. 2010;12(1):87-97.
 25. Dashwood RH, Myzak MC, Ho E. Dietary HDAC inhibitors: time to rethink weak ligands in cancer chemoprevention? *Carcinogenesis*. 2006;27(2):344-349.
 26. Jackson SJT, Singletary KW. Sulforaphane: a naturally occurring mammary carcinoma mitotic inhibitor, which disrupts tubulin polymerization. *Carcinogenesis*. 2004;25(2):219-227.
 27. Akhtar MJ, Ahamed M, Fareed M, Alrokayan SA, Kumar S. Protective effect of sulphoraphane against oxidative stress mediated toxicity induced by CuO nanoparticles in mouse embryonic fibroblasts BALB 3T3. *Journal of Toxicological Sciences*. 2012;37(1):139-148.
 28. Li D, Wu K, Howie AF, Beckett GJ, Wang W, Bao Y. Synergy between broccoli sprout extract and selenium in the upregulation of thioredoxin reductase in human hepatocytes. *Food Chemistry*. 2008;110(1):193-198.
 29. Herman-Antosiewicz A, Johnson DE, Singh SV. Sulforaphane causes autophagy to inhibit release of cytochrome c and apoptosis in human prostate cancer cells. *Cancer Research*. 2006;66(11):5828-5835.

30. Wu KC, Liu JJ, Klaassen CD. Nrf2 activation prevents cadmium-induced acute liver injury. *Toxicology and Applied Pharmacology*. 2012;263(1):14-20.
31. Li D, Wang W, Shan Y, et al. Synergy between sulforaphane and selenium in the up-regulation of thioredoxin reductase and protection against hydrogen peroxide-induced cell death in human hepatocytes. *Food Chemistry*. 2012;133(2):300-307.
32. Harris KE, Jeffery EH. Sulforaphane and erucin increase MRP1 and MRP2 in human carcinoma cell lines. *Journal of Nutritional Biochemistry*. 2008;19(4):246-254.

Chapter 4. Cytotoxicity and Imaging in cells

4.1 Cytotoxicity in the immortalised human hepatocytes (HHL-5) cells

Based on some studies which relates to the toxicity of CdSe NPs,¹⁻⁵ it can be indicates that the cytotoxic effect of CdSe NPs were determined by MTT (3-(4,5-dimethylthiazol-2-yl)-2,5-diphenyltetrazolium bromide) assay. Therefore, the study use MTT assay to test the cytotoxicity in HHL-5 cells. Because the CdSe NPs with 0.05 % sodium citrate in all three kinds of particles show unstable characteristics compared with those synthesised with 0.1 % and 0.2 % sodium citrate (Chapter 3), we only choose to compare the toxicity of CdSe NPs prepared with 0.1 % and 0.2 % stabiliser in HHL-5 cells.

4.1.1 CdSe NPs (10:1) with 0.1 % and 0.2 % sodium citrate stabiliser

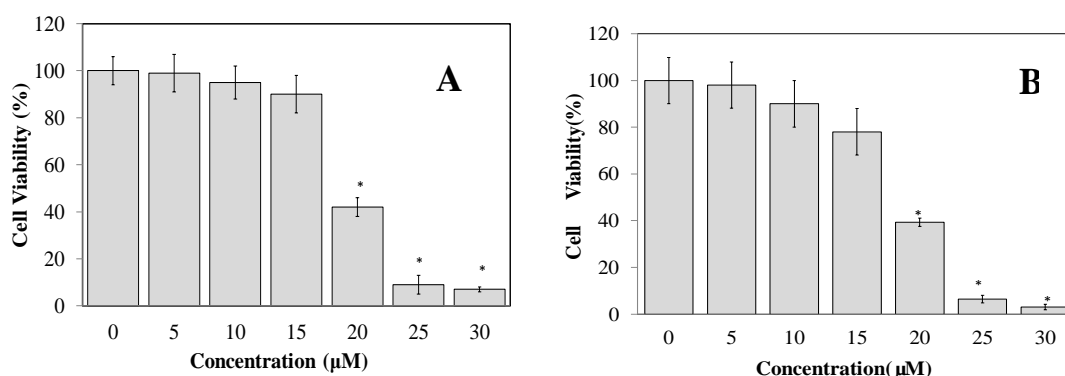


Figure 4.1 The effect of CdSe NPs on proliferation of HHL-5 cells.

HHL-5 cells in 96 well plates are treated with CdSe NPs (10:1) with 0.1 % (A) and 0.2 % (B) stabilizer of different concentrations (5, 10, 15, 20, 25 and 30 µM). Symbol * indicates a statistical significant difference compared with the media only control (0 µM) (* P<0.05)

The label with 0 in Figure 4.1.1 means the media only control. The cells which are treated with CdSe NPs show decreasing viability with an increasing concentration of particles

(Figure 4.1.1). The two bar charts above both show a dramatic decrease in cell viability (from 100 % to 40 %) when the cells are treated with 20 μM of CdSe NPs (Figure 4.1.1). When the particle concentration is increase, the observed toxicity to the cells is also increase. When the highest concentration (30 μM) of CdSe NPs is add into the HHL-5 cells, the cell viability rate drop to approximately 9%, the lowest amongst all the concentrations test (Figure 4.1.1). When the particle concentration is increase, the observe toxicity to the cells is also increase (Figure 4.1.1).

The half maximal inhibitory concentration is the half maximal (50 %) inhibitory concentration (IC) of a substance (50 % IC, or IC₅₀). IC₅₀ also means the concentration of a drug that is required for 50 % inhibition *in vitro*. The IC₅₀ values of CdSe (10:1) with 0.1 % and 0.2 % sodium citrate stabilizer are 39.1 μM and 22.2 μM , respectively. So it indicates that the CdSe NPs (10:1) with 0.2 % sodium citrate has more toxicity than 0.1 % in HHL-5 cells. The two graphs also suggest that the higher concentration of the CdSe NPs inject into the cells the lower the cell viability rate is.

Based on the results in Figure 4.1.1, most cells died when increasing the concentration to 25 and 30 μM , so concentrations of 5, 10, 15, 20 μM are choose to test cell viability in the rest of MTT experiments. In order to achieve the same toxicity by the same amount of Cadmium, to make sure each MTT results can be compared easily, concentration of Cadmium (CdSe (4:1)) is increased to 2.5 times higher than CdSe (10:1) (Figure 4.1.1), which are 12.5, 25, 37.5, 50 μM respectively (Figure 4.1.2). In Figure 4.1.3, Cadmium concentration (CdSe (1:1)) is increase to 10 times higher than CdSe (10:1) (Figure 4.1.1), which are 50, 100, 150 and 200 μM , respectively.

4.1.2 CdSe NPs (4:1) with 0.1 % and 0.2 % sodium citrate stabilizer

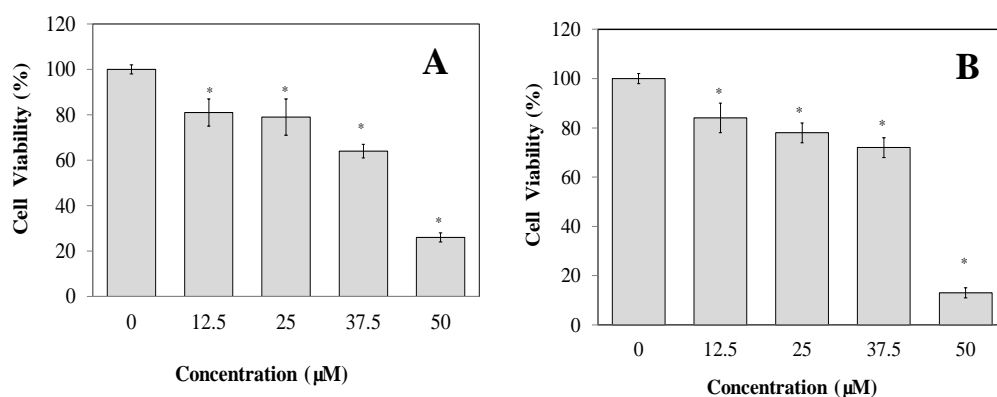


Figure 4.2 The effect of CdSe NPs on proliferation of HHL-5 cells.

HHL-5 cells in 96 well plates are treated with CdSe NPs (4:1) with 0.1 % (A) and 0.2 % (B) stabilizer of different concentrations (12.5, 25, 37.5 and 50 µM). Symbol * indicates a statistical significant difference compared with the media only control (0 µM) (* P<0.05)

The label with 0 in Figure 4.1.2 means the media only control. HHL-5 cells which are treated with CdSe NPs show decreasing viability with an increasing concentration of particles (Figure 4.1.2). These two bar charts above show a gradual decrease in cell viability (from 100 % to 80 %) when the cells are treated with 12.5 µM of CdSe NPs (Figure 4.1.2). When the highest concentration (50 µM) of CdSe NPs is added into the HHL-5 cells, the cell viability rate drop to approximately 30 % (Figure 4.1.2 A) and 18 % (Figure 4.1.2 B) which are the lowest amongst all the concentrations test in each graph, respectively. Therefore, the higher concentration of CdSe NPs inject into the cells, the lower cell viability was recorded. (Figure 4.1.2). The IC 50 values of CdSe (4:1) with 0.1 % and 0.2 % sodium citrate stabilizer are 39.7 µM and 35 µM, respectively.

4.1.3 CdSe NPs (1:1) with 0.1 % and 0.2% sodium citrate stabilizer

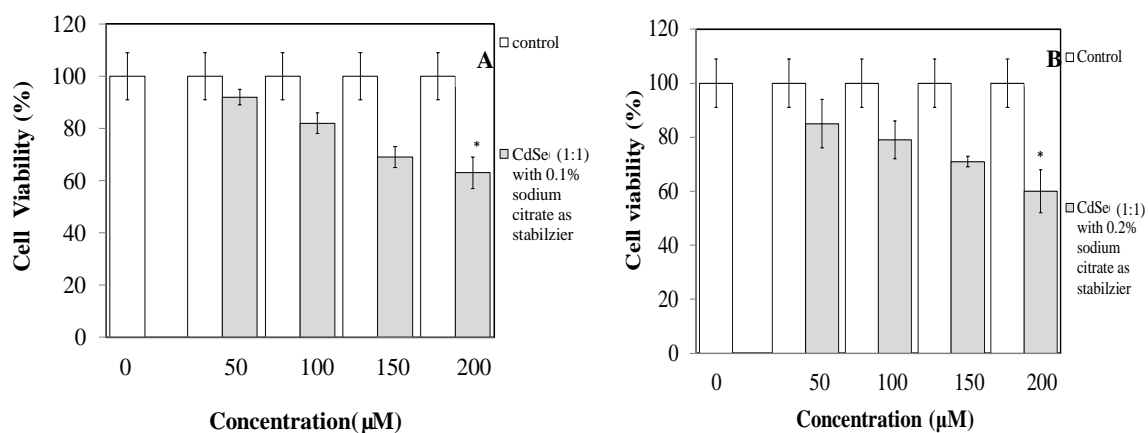


Figure 4.3 The effect of CdSe NPs on proliferation of HHL-5 cells.

The white bar shows HH-L5 cells in 96 well plates treated with 0.1 % (A) and 0.2 % (B) sodium citrate as a control. The grey bar shows the HHL-5 cells in 96 well plates which are treated by different concentrations (50, 100, 150 and 200 µM) of CdSe NPs (1:1) with 0.1 % (A) and 0.2 % (B) sodium citrate. Symbol * indicates a statistical significant difference compared with the media only control (0 µM) (*P<0.05).

The label with 0 in Figure 4.1.3 means the media only control. The rest of the control in Figure 4.1.3 is different ratio of sodium citrate which matches to each concentration of CdSe NPs. The cells which are treated with CdSe NPs show decreasing viability with an increasing particle concentration (Figure 4.1.3). Figure 4.1.3 A shows a gradual decrease in cell viability (from 100 % to 80 %) when the cells are treated with 100 µM of CdSe NPs. Figure 4.1.3 B shows a gradual decrease in cell viability (from 85 % to 75 %) when the cells are treated with 100 µM of CdSe NPs. When the highest concentration (200 µM) of CdSe NPs is added into HHL-5 cells, the cell viability rate drop to approximately 65 % (Figure 4.1.3 A) and 60 % (Figure 4.1.3 B) respectively, which are the lowest amongst all the concentrations test in each graph. Therefore, the higher the concentration of the CdSe

NPs injected into the cells, the lower cell viability is recorded. The IC 50 value of CdSe (1:1) with 0.1 % (Figure 4.1.3 A) and 0.2 % (Figure 4.1.3 B) sodium citrate stabiliser are 281.5 μM and 360.7 μM , respectively. When the concentration of the particles is increased, the toxicity observed in the cells increase according (Figure 4.1.3).

Overall, if calculating the concentration of CdSe NPs by Selenium, the total concentration of CdSe pairs in each preparation (400 μM) was determined based on the assumption that all of the Se^{2-} in the $\text{C}_3\text{H}_8\text{N}_2\text{Se}$ reacted to form CdSe pairs. If Cadmium was used to calculate the concentration, the toxicity in HHL-5 cells from high to low is CdSe (10:1) > CdSe (4:1) > CdSe (1:1) (Figure 4.1.1-4.1.3), and the toxicity of the particles with different sodium citrate concentrations from high to low was 0.2% > 0.1%. In order to compare each ratio (Cd to Se) with the same concentration, concentration of CdSe (4:1) was 2.5 times higher than CdSe (10:1) (Figure 4.1.1 and 4.1.2) and concentration of CdSe (1:1) was 10 times higher than CdSe (10:1) (Figure 4.1.3 and 4.1.2).

4.2 Confocal Imaging results in MCF-7 cells

There are many studies focus on the confocal images of different chemical structures of CdSe NPs and captured numerous useful images which proved that the CdSe NPs has great potential in biology application area.⁶⁻⁹ In this study, CdSe NPs (10:1) with 0.1 % sodium citrate stabilizer have a photoluminescence in the orange-red range (about 590 nm, Figure 3.1.3-C, D) which is useful for biological imaging. Therefore, this kind of particle has been used in the experiment. In order to study their potential for bioimaging, MCF-7 cells have been stained with CdSe (10:1) with 0.1 % sodium citrate stabilizer nanoparticles.

Simultaneous double channel detection (multi-track) was set as a combination of tunnel one and two.¹⁰ The Argon laser was set as 488 nm to detect the cells (tunnel one, Figure 4.2.1-4.2.5 b).¹⁰ The Dapi excitation was set as 325 nm (tunnel two, Figure 4.2.1-4.2.5 a).¹⁰ Figure 4.2.1-4.2.5 c was an overlap images of a and b.¹⁰ Then scan the samples under microscopy, capture the images and save images.¹⁰

4.2.1 Confocal imaging of MCF-7 cells with medium control.

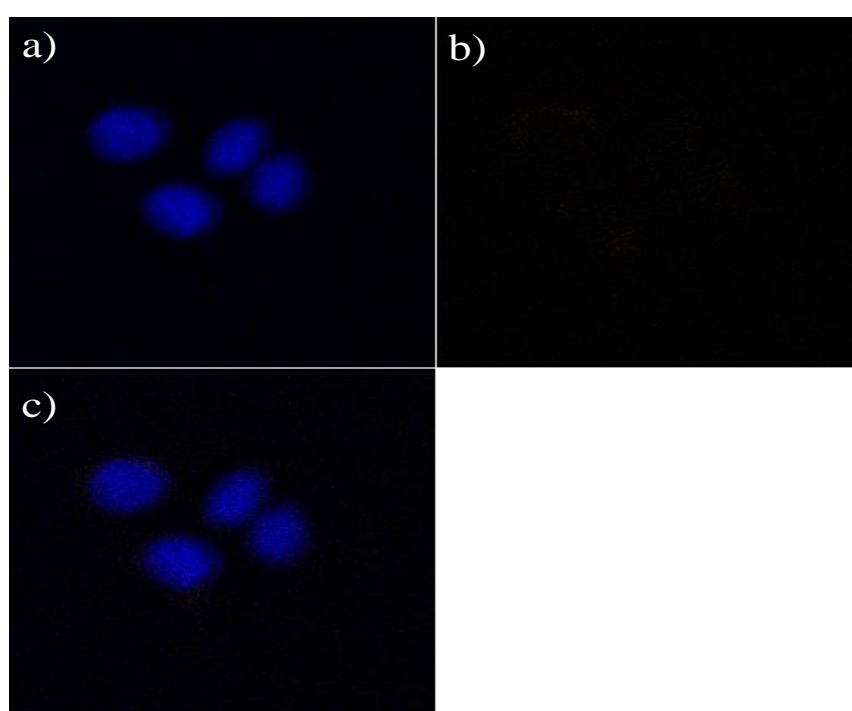


Figure 4.4 Confocal Image of MCF-7 cells with medium control only.

Fluorescent microscopy image of MCF-7 cells labeled with a) DAPI, b) nanoparticles, c) an overlap image of a) and b).

Figure 4.2.1 shows the confocal microscope image from the control of medium only. The cells were very bright and clearly without any noise or nanoparticle spots in that background. Therefore, the image can be used as the control image to compare with the cells in different concentration of CdSe NPs below.

4.2.2 Confocal imaging of MCF-7 cells in CdSe (10:1) with 0.1 % sodium citrate as stabilizer with concentration of 10 μ M without dialysis

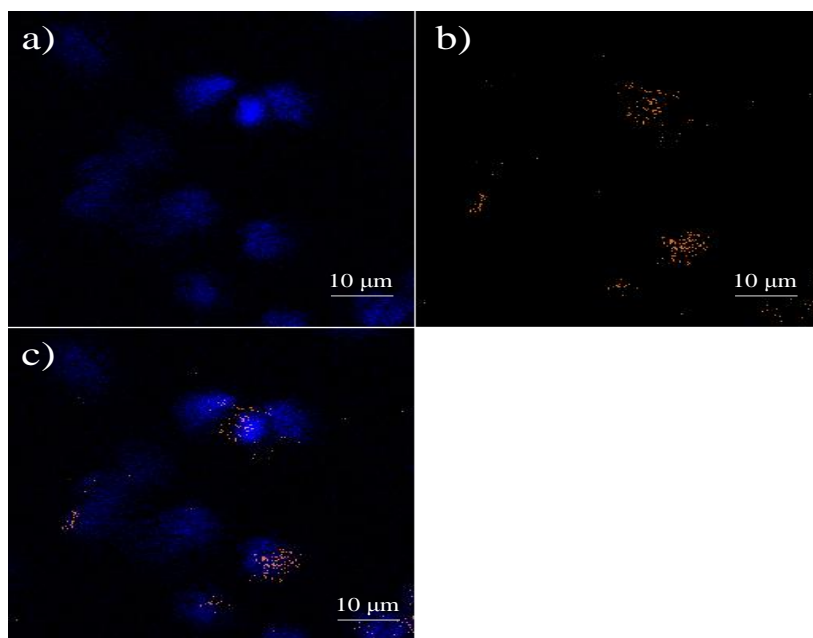


Figure 4.5 Confocal Image of MCF-7 cells after exposure in 10 μ M CdSeNPs .

Fluorescent microscopy image of MCF-7 cells labeled with a) DAPI, b) nanoparticles, c) an overlap image of a) and b).

Figure 4.2.2 a) shows the MCF-7 cells with DAPI only. The shape of each MCF-7 cells can be seen clearly and the cells are bright and well separated. Figure 4.2.2 b) shows the trend and distribution of the CdSe NPs. Figure 4.2.2 c) shows the MCF-7 cells stained with Cde NPs (10 μ m) before dialysis, it is obvious that the CdSe NPs (with orange-red photoluminescence) have surrounded and covered each live cell. Conversely, the background is clear without any particles.

4.2.3 Confocal imaging of MCF-7 cells in CdSe (10:1) with 0.1 % sodium citrate as stabilizer with concentration of 10 μ M after dialysis

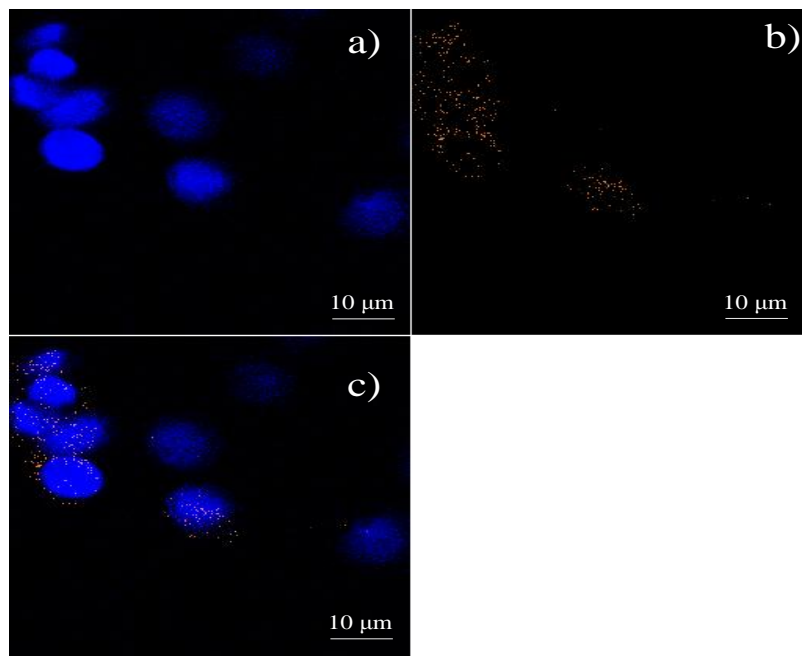


Figure 4.6 Confocal Image of MCF-7 cells after exposure in 10 μ M CdSeNPs (after dialysis) .

Fluorescent microscopy image of MCF-7 cells labeled with a) DAPI, b) nanoparticles, c) an overlap image of a) and b).

Figure 4.2.3 a) shows the MCF-7 cells with DAPI only. The shape of each MCF-7 cells can be seen clearly and the cells are bright and well separated. Figure 4.2.3 b) shows the trend and distribution of the CdSe NPs. Figure 4.2.3c) shows the MCF-7 cells stained with CdSe NPs (10 μ m) after dialysis, it was obvious that the CdSe NPs (which photoluminescence was orange-red) surrounded and covered each live cells. Conversely, the background was clear and without any particles. Compared to the same concentration of CdSe NPs without dialysis (Figure 4.2.2), it seems like there is no big difference between them.

4.2.4 Confocal imaging of MCF-7 cells in CdSe (10:1) with 0.1 % sodium citrate as stabilizer with concentration of 15 μM before dialysis

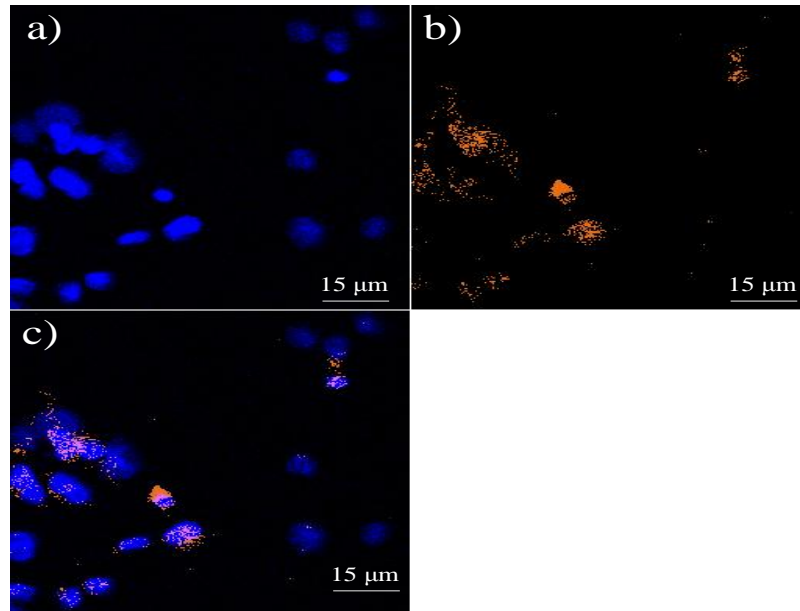


Figure 4.7 Confocal Image of MCF-7 cells after exposure in 15 μM CdSNPs (before dialysis) .

Fluorescent microscopy image of MCF-7 cells labeled with a) DAPI, b) nanoparticles, c) an overlap image of a) and b).

Figure 4.2.4 a) shows the MCF-7 cells with DAPI only. The shape of each MCF-7 cells can be seen clearly and the cells are bright and well separated. Figure 4.2.4 b) shows the trend and distribution of the CdSe NPs. Figure 4.2.4 c) shows the MCF-7 cells stained with CdSe NPs before dialysis, it is obvious that the CdSe NPs (with orange-red photoluminescence) have surrounded and covered each live cell. Conversely, the background is clear, without any particles.

4.2.5 Confocal imaging of MCF-7 cells in CdSe (10:1) with 0.1 % sodium citrate as stabilizer with concentration of 15 μ M after dialysis

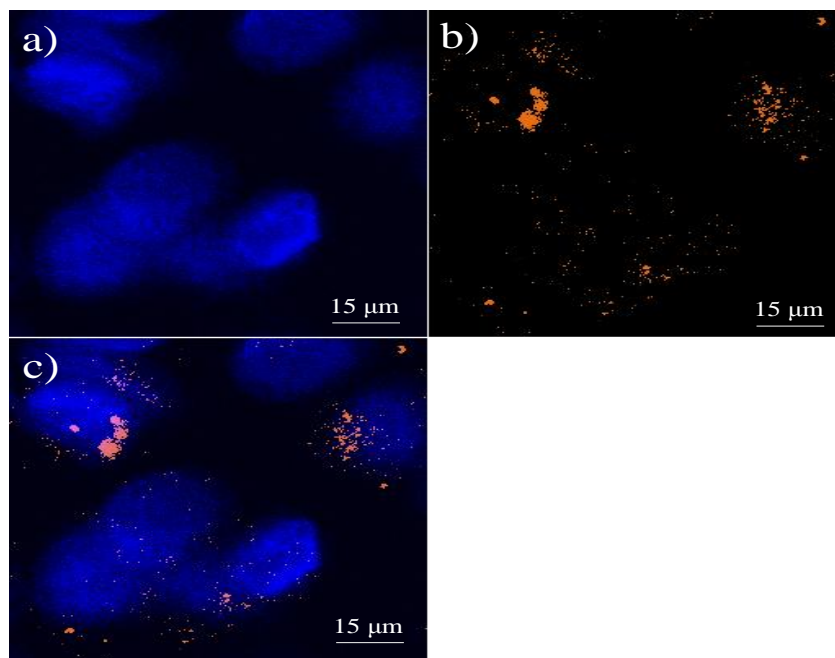


Figure 4.8 Confocal Image of MCF-7 cells after exposure in 15 μ M CdSeNPs (after dialysis) .

Fluorescent microscopy image of MCF-7 cells labeled with. a) DAPI, b) nanoparticles, c) an overlap image of a) and b).

Figure 4.2.5 a) shows the MCF-7 cells with DAPI only. The shape of each MCF-7 cells can be seen clearly and the cells are bright and well separated. Figure 4.2.5 b) shows the trend and distribution of the CdSe NPs. Figure 4.2.5 c) shows the MCF-7 cells stained with CdSe NPs after dialysis, it was obvious that the CdSe NPs (with orange-red photoluminescence) have surrounded and covered each live cell. Conversely, the background was clear and without any particles. Compared to the same concentration of CdSe NPs before dialysis (Figure 4.2.4), it seems like that is no big difference between them.

At first, we tried to test the confocal image with the same method and the same concentration of CdSe NPs in HHL-5 cells, but the results were not very good because the control background was filled with red spots of noise. If the control image was not clear, it would be difficult to distinguish which spots were noises and which spots were the real CdSe NPs. Therefore, in this study, we choose another cell line which was MCF-7. According to the results above (Figure 4.2.1-4.2.5), it is obvious that the MCF-7 cell line had a better results than HHL-5 cell line. The control image of MCF-7 was clear and without any background noise (Figure 4.2.1). Moreover the cellular toxicity observed in MCF-7 is lower for cells with 10 μM of CdSe NPs compared to those with 15 μM CdSe NPs. So it can be deduced that the higher the concentrations of CdSe NPs, the more nanoparticles the cells will take up.

4.3 Reference

1. Wang, L.; Nagesha, D. K.; Selvarasah, S.; Dokmeci, M. R.; Carrier, R. L., Toxicity of CdSe Nanoparticles in Caco-2 Cell Cultures. *Journal of nanobiotechnology*. 2008.
2. Vibin, M.; Vinayakan, R.; John, A.; Raji, V.; Rejiya, C. S.; Vinesh, N. S.; Abraham, A., Cytotoxicity and fluorescence studies of silica-coated CdSe quantum dots for bioimaging applications. *Journal of Nanoparticle Research* 2011, 13 (6), 2587-2596.
3. Chang, S. Q.; Dai, Y. D.; Kang, B.; Han, W.; Chen, D., gamma-Radiation Synthesis of Silk Fibroin Coated CdSe Quantum Dots and Their Biocompatibility and Photostability in Living Cells. *J. Nanosci. Nanotechnol.* 2009, 9 (10), 5693-5700.
4. Peng, L.; He, M.; Chen, B.; Wu, Q.; Zhang, Z.; Pang, D.; Zhu, Y.; Hu, B., Cellular uptake, elimination and toxicity of CdSe/ZnS quantum dots in HepG2 cells. *Biomaterials* 2013, 34 (37), 9545-58.

5. Zhang, T.; Jin, J. J.; Yang, C. Z.; Peng, H. Y.; Lai, L.; Han, J. Y.; Zheng, M., Microwave synthesis CdSe quantum dot clusters via ribonuclease A protein. *Micro Nano Lett* 2012, 7 (12), 1289-1291.
6. Morelli, E.; Salvadori, E.; Bizzarri, R.; Cioni, P.; Gabellieri, E., Interaction of CdSe/ZnS quantum dots with the marine diatom *Phaeodactylum tricornutum* and the green alga *Dunaliella tertiolecta*: A biophysical approach. *Biophysical chemistry* 2013, 182, 4-10.
7. Loginova, Y. F.; Kazachkina, N. I.; Zherdeva, V. V.; Rusanov, A. L.; Shirmanova, M. V.; Zagaynova, E. V.; Sergeeva, E. A.; Dezhurov, S. V.; Wakstein, M. S.; Savitsky, A. P., Biodistribution of intact fluorescent CdSe/CdS/ZnS quantum dots coated by mercaptopropionic acid after intravenous injection into mice. *Journal of Biophotonics* 2012, 5 (11-12), 848-859.
8. Zhang, S. J.; Jiang, Y. L.; Chen, C. S.; Creeley, D.; Schwehr, K. A.; Quigg, A.; Chin, W. C.; Santschi, P. H., Ameliorating effects of extracellular polymeric substances excreted by *Thalassiosira pseudonana* on algal toxicity of CdSe quantum dots. *Aquatic Toxicology* 2013, 126, 214-223.
9. Dai, G. Z.; Chen, Y.; Wan, Q.; Zhang, Q. L.; Pan, A. L.; Zou, B. S., Fabrication and optical waveguide of Sn-catalyzed CdSe microstructures. *Solid State Communications* 2013, 167, 31-35.
- 10 Confocal microscope usage manual Zeiss Lsm 510 Meta.

Chapter 5. Summary and future work

5.1 Summary

The properties and applications of different kinds of CdSe NPs have been observed in many studies. Due to different methods used to synthesize CdSe NPs, each type of CdSe NPs has their own special characteristics.¹⁻³ Some of them have a special chemical shell coating,⁴ and some of them depend on the changing of synthesis parameters such as temperature.⁵

Some research focus on the ZnS or other chemical coatings with CdSe NPs,⁴ other studies focus on the properties of CdSe NPs by changing the parameters of the NPs such as heating temperature and exposure to light.⁶ However, this study focused on natural properties (without any other parameters affect) of the CdSe NPs with different ratios of Cd to Se. In addition, each ratio was divided into three conditions with different percentage of sodium citrate as a stabiliser, in order to test optical stabilities and biological characteristics of them which have seldom been done before.

This study uses a convenient and quick wet chemical method to synthesis CdSe NPs.⁷⁻⁹ It focuses on the toxicity of Cadmium and different ratios of sodium citrate as a stabilizer in CdSe NPs which has seldom been discussed before. The important optical and biological properties of CdSe NPs which were examined in this thesis are summarized as below:

Optical properties which include Aging, TEM, and Quantum yield experiments.

Aging results: Generally speaking, all the particles were very stable (Chapter 3) Specifically, stability of CdSe NPs are increasing and colour is changing from deepest to pastel along with increased Cd to Se ratio (1:1 < 4:1 < 10:1). In the same ratio such as CdSe (10:1), the stability of CdSe NPs increase with elevated concentrations of sodium

citrate (0.05 % < 0.1 % < 0.2 %) (Chapter 3). Therefore, the more sodium citrate stabiliser or Cadmium accumulated in the CdSe NPs, the more stable the particles are. Based on the stability of photoluminescence (PL) in the CdSe NPs, it can link up with chitosan using covalent bond steadily and kept a good fluorescence¹¹ in drug delivery. Meanwhile, the nanoparticle has highly possible to apply in LED development in the future.¹⁰

TEM results: Although the size of CdSe NPs have some fluctuation between the theoretical and the real one, the average size of CdSe NPs with (10:1), (4:1) sodium citrate stabiliser is roughly the same and is bigger than the CdSe NPs with (1:1). The different size among theoretical and the real values probably because the different kinds of measurement methods between TEM and Aging, one element which could affect these results is the state of the samples (TEM samples are solid and aging samples are aqueous solution). Different size and shapes of CdSe NPs have their unique potential which probably could be used in drug delivery.¹¹

Quantum yield results: The quantum yield rates enhance along with increase Cd to Se ratio (1:1 < 4:1 < 10:1). In conclusion, the luminescence of all CdSe NPs in this study was not as strong as expected. One reason for this is because luminescence of the sample itself was not strong when compared to other nanoparticles.¹² The other reason could be that some published experiments⁶ exposed the samples to light in air or in nitrogen to get a quantum yield. But in this study, the results reflect the nature of the samples without being affected by other factors such as light or heating. Therefore the values of the quantum yield rates of the samples were lower than other papers.¹³ Based on this property, these CdSe NPs can be used as a unique and new type of biomaterial for bioimaging and other biomedical applications.¹⁴

Biology properties verify through MTT assay and confocal experiment.

MTT results: Cadmium is used to calculate the concentration, the toxicity in HHL-5 cells from high to low is CdSe (10:1) > CdSe (4:1) > CdSe (1:1) (Figure 4.1.1-4.1.3), and the toxicity of the particles with different sodium citrate concentrations from high to low was 0.2% > 0.1%. MTT assay has shown that CdSe NPs has high biocompatibility and low toxicity in vitro which can apply in biological applications and UV therapy application.¹⁵⁻¹⁷

Confocal results: The cellular toxicity observed in MCF-7 is lower for cells with 10 μ M of CdSe NPs compared to those with 15 μ M CdSe NPs, and there is no significant difference between or after dialysis. The cell viability results and Confocal images both indicated that the increase the concentration of the CdSe NPs in the cells, the greater the toxicity the cells obtained. This character of CdSe NPs can applied in biomedical area such as anti-cancer therapy,¹⁸ cell targeting¹⁹ and gene delivery.²⁰

Overall, the stability of CdSe NPs in both optical and biological properties can be applied in many areas such as it can provide power for solar cells²¹ and light-emitting diode (LED) equipment.¹⁰ It can also use as an effective drug delivery method.²⁰ In particular, it is an approach for cancer management which having the potential to inhibit the growth of the tumour cells.²¹ With the use of CdSe NPs, it is hoped that perceived toxicity concerns associated with prolonged use of anti-cancer agents can be minimized and that their bioavailability will be enhanced effectively.²¹

5.2 *Future work*

This study demonstrated the CdSe NPs in both optical and biological properties. In particular, the stable photoluminescence and low toxicity of CdSe NPs which could be applied in drug delivery in the future.²⁰ In addition to our study, a limited number of studies from other laboratories have also evaluated the usefulness of CdSe NPs which has similar properties but different chemical structures compared to this study.²¹⁻⁴³

However, there are still many properties of CdSe NPs which have not been discovered due to short of time. For instance, the optical properties of CdSe NPs could be dug out further, some studies indicate that there is a potential of CdSe NPs to use in UV therapy,¹⁷ if further research could be done, it will provide a new and energy saved method in clinical therapy. Moreover, based on the strong luminescence and good stability properties of CdSe NPs, the particle itself could be highly possible applied in power source provided, such as in solar cells²¹ and LED areas.¹⁰ For example, use semiconductor nanoparticle light source give benefits to LED source in many parts such as lower energy consumption, longer lifetime, improved physical robustness, smaller size, and faster switching.⁴⁴

One of the potential applications of CdSe NPs in biomedicine is drug delivery.^{19, 21} Based on the IC₅₀ values in MTT assay in this study, further research could test a concentration which has lowest toxicity and highest luminescence of CdSe NPs, so that the toxicity can be under control and the CdSe NPs can be traced as well. Moreover, due to the luminescence of CdSe NPs, when it encapsulated anti-cancer medicine and adheres to the target tumour cells, the whole process could be observed, recorded and controlled as well. Therefore, it could provide an effective and convenient way to cure cancer.²⁰⁻²¹

5.3 Reference

1. Teranishi T, Nishida M, Kanehara M. Size-tuning and optical properties of high-quality CdSe nanoparticles synthesized from cadmium stearate. *Chem Lett.* 2005;34(7):1004-1005.
2. Hambrock J, Birkner A, Fischer RA. Synthesis of CdSe nanoparticles using various organometallic cadmium precursors. *Journal of Materials Chemistry.* 2001;11(12):3197-3201.
3. Capek RK, Lambert K, Dorfs D, et al. Synthesis of Extremely Small CdSe and Bright Blue Luminescent CdSe/ZnS Nanoparticles by a Prefocused Hot-Injection Approach. *Chem Mater.* 2009;21(8):1743-1749.
4. Hsieh S-C, Wang F-F, Hung S-C, Chen Y, Wang Y-J. The internalized CdSe/ZnS quantum dots impair the chondrogenesis of bone marrow mesenchymal stem cells. *Journal of Biomedical Materials Research Part B-Applied Biomaterials.* 2006;79B(1):95-101.
5. Mahmoud WE, Al-Amri AM, Yaghmour SJ. Low temperature synthesis of CdSe capped 2-mercaptoethanol quantum dots. *Optical Materials.* 2012;34(7):1082-1086.
6. Wang Y, Tang ZY, Correa-Duarte MA, et al. Mechanism of strong luminescence photoactivation of citrate-stabilized water-soluble nanoparticles with CdSe cores. *Phys Chem B.* 2004;108(40):15461-15469.
7. Wang L, Nagesha DK, Selvarasah S, Dokmeci MR, Carrier RL. Toxicity of CdSe Nanoparticles in Caco-2 Cell Cultures. *Journal of nanobiotechnology.* 2008.

8. Ni T, Nagesha DK, Robles J, Materer NF, Mussig S, Kotov NA. CdS nanoparticles modified to chalcogen sites: New supramolecular complexes, butterfly bridging, and related optical effects. *Journal of the American Chemical Society*. 2002;124(15):3980-3992
9. Moghaddam MM, Baghbanzadeh M, Keilbach A, Kappe CO. Microwave-assisted synthesis of CdSe quantum dots: can the electromagnetic field influence the formation and quality of the resulting nanocrystals? *Nanoscale*. 2012;4(23):7435-7442.
10. Li D, Liu X, Xie G, Liu X. Stable and water-soluble CdTe@SiO₂ composite nanospheres: Preparation, characterization and application in LED. *Colloids and Surfaces a-Physicochemical and Engineering Aspects*. 2013;424:33-39.
11. Wang Z, Zhou C, Xia J, et al. Fabrication and characterization of CdSe conjugated magnetic carbon nanotubes: A promise of targeted and visualized drug delivery. *Cr Chim*. 2013;16(3):296-301.
12. Ahire JH, Wang Q, Coxon PR, et al. Highly Luminescent and Nontoxic Amine-Capped Nanoparticles from Porous Silicon: Synthesis and Their Use in Biomedical Imaging. *Acs Applied Materials & Interfaces*. 2012;4(6):3285-3292.
13. Wang BB, Shang H, Nie CP, Wang Q, Ma MH, Cai ZX. A novel two-step controlled basic water phase method for synthesizing size-tunable CdTe/Cd(OH)₂ core/shell quantum dots with high quantum yield and excellent stability. *Journal of Luminescence*. 2013;143:262-270.

14. Saxena M, Sarkar S. Fluorescence imaging of human erythrocytes by carbon nanoparticles isolated from food stuff and their fluorescence enhancement by blood plasma. *Mater Express*. 2013;3(3):201-209.
15. Lv Y, Li K, Li YP. Surface modification of quantum dots and magnetic nanoparticles with PEG-conjugated chitosan derivatives for biological applications. *Chem Pap*. 2013;67(11):1404-1413.
16. Zhang T, Jin JJ, Yang CZ, et al. Microwave synthesis CdSe quantum dot clusters via ribonuclease A protein. *Micro Nano Lett*. 2012;7(12):1289-1291.
17. Choi YJ, Kim YJ, Lee JW, Lee Y, Lim YB, Chung HW. Cyto-/Genotoxic Effect of CdSe/ZnS Quantum Dots in Human Lung Adenocarcinoma Cells for Potential Photodynamic UV Therapy Applications. *J Nanosci Nanotechnol*. 2012;12(3):2160-2168.
18. Yang XJ, Xiao QQ, Niu CX, et al. Multifunctional core-shell upconversion nanoparticles for targeted tumor cells induced by near-infrared light. *J Mater Chem B*. 2013;1(21):2757-2763
19. Fahmi MZ, Chang JY. Forming double layer-encapsulated quantum dots for bio-imaging and cell targeting. *Nanoscale*. 2013;5(4):1517-1528.
20. Zhao JJ, Qiu XL, Wang ZP, Pan J, Chen J, Han JS. Application of quantum dots as vectors in targeted survivin gene siRNA delivery. *Oncotargets and Therapy*. 2013;6:303-309

21. Azoz S, Jiang J, Keskar G, et al. Mechanism for strong binding of CdSe quantum dots to multiwall carbon nanotubes for solar energy harvesting. *Nanoscale*. 2013;5(15):6893-6900.
22. Siddiqui IA, Adhami VM, Ahmad N, Mukhtar H. Nanochemoprevention: Sustained Release of Bioactive Food Components for Cancer Prevention. *Nutrition and Cancer-an International Journal*. 2010;62(7):883-890.
23. Wang BB, Shang H, Nie CP, Wang Q, Ma MH, Cai ZX. A novel two-step controlled basic water phase method for synthesizing size-tunable CdTe/Cd(OH)₂ core/shell quantum dots with high quantum yield and excellent stability. *Journal of Luminescence*. 2013;143:262-270.
24. Saxena M, Sarkar S. Fluorescence imaging of human erythrocytes by carbon nanoparticles isolated from food stuff and their fluorescence enhancement by blood plasma. *Mater Express*. 2013;3(3):201-209.
25. Lv Y, Li K, Li YP. Surface modification of quantum dots and magnetic nanoparticles with PEG-conjugated chitosan derivatives for biological applications. *Chem Pap*. 2013;67(11):1404-1413.
26. Zhang T, Jin JJ, Yang CZ, et al. Microwave synthesis CdSe quantum dot clusters via ribonuclease A protein. *Micro Nano Lett*. 2012;7(12):1289-1291.
27. Choi YJ, Kim YJ, Lee JW, Lee Y, Lim YB, Chung HW. Cyto-/Genotoxic Effect of CdSe/ZnS Quantum Dots in Human Lung Adenocarcinoma Cells for Potential Photodynamic UV Therapy Applications. *J Nanosci Nanotechnol*. 2012;12(3):2160-2168.

28. Yang XJ, Xiao QQ, Niu CX, et al. Multifunctional core-shell upconversion nanoparticles for targeted tumor cells induced by near-infrared light. *J Mater Chem B*. 2013;1(21):2757-2763.
29. Fahmi MZ, Chang JY. Forming double layer-encapsulated quantum dots for bio-imaging and cell targeting. *Nanoscale*. 2013;5(4):1517-1528.
30. Zhao JJ, Qiu XL, Wang ZP, Pan J, Chen J, Han JS. Application of quantum dots as vectors in targeted survivin gene siRNA delivery. *Oncotargets and Therapy*. 2013;6:303-309.
31. Azoz S, Jiang J, Keskar G, et al. Mechanism for strong binding of CdSe quantum dots to multiwall carbon nanotubes for solar energy harvesting. *Nanoscale*. 2013;5(15):6893-6900.
32. Siddiqui IA, Adhami VM, Ahmad N, Mukhtar H. Nanochemoprevention: Sustained Release of Bioactive Food Components for Cancer Prevention. *Nutrition and Cancer-an International Journal*. 2010;62(7):883-890.
33. Ahire JH, Wang Q, Coxon PR, et al. Highly Luminescent and Nontoxic Amine-Capped Nanoparticles from Porous Silicon: Synthesis and Their Use in Biomedical Imaging. *Acs Applied Materials & Interfaces*. 2012;4(6):3285-3292.
34. Bardajee GR, Hooshyar Z, Jafarpour F. Antibacterial and optical properties of a new water soluble CdSe quantum dots coated by multidentate biopolymer. *Journal of Photochemistry and Photobiology a-Chemistry*. 2013;252:46-52.

35. Baun A, Hartmann NB, Grieger K, Kusk KO. Ecotoxicity of engineered nanoparticles to aquatic invertebrates: a brief review and recommendations for future toxicity testing. *Ecotoxicology*. 2008;17(5):387-395.
36. Behboudnia M, Azizianekalandaragh Y. Synthesis and characterization of CdSe semiconductor nanoparticles by ultrasonic irradiation. *Materials Science and Engineering B-Solid State Materials for Advanced Technology*. 2007;138(1):65-68.
37. Bellessa J, Voliotis V, Grousson R, Wang XL, Ogura M, Matsuhata H. Quantum-size effects on radiative lifetimes and relaxation of excitons in semiconductor nanostructures. *Phys Rev B*. 1998;58(15):9933-9940.
38. Bradley M, Bruno N, Vincent B. Distribution of CdSe quantum dots within swollen polystyrene microgel particles using confocal microscopy. *Langmuir*. 2005;21(7):2750-2753.
39. Brus L. electronic wave-functions in semiconductor clusters-experiment and theory. *Journal of Physical Chemistry*. 1986;90(12):2555-2560.
40. Buzea C, Pacheco II, Robbie K. Nanomaterials and nanoparticles: Sources and toxicity. *Biointerphases*. 2007;2(4):MR17-MR71.
41. Capek RK, Lambert K, Dorfs D, et al. Synthesis of Extremely Small CdSe and Bright Blue Luminescent CdSe/ZnS Nanoparticles by a Prefocused Hot-Injection Approach. *Chem Mater*. 2009;21(8):1743-1749.
42. Chaudhuri D, Orsulic S, Ashok BT. Antiproliferative activity of sulforaphane in Akt-overexpressing ovarian cancer cells. *Mol Cancer Ther*. 2007;6(1):334-345.

43. Chen FQ, Gerion D. Fluorescent CdSe/ZnS nanocrystal-peptide conjugates for long-term, nontoxic imaging and nuclear targeting in living cells. *Nano Letters*. 2004;4(10):1827-1832.
44. Coe-Sullivan S, Liu WH, Allen P, Steckel JS. Quantum Dots for LED Downconversion in Display Applications. *Ecs J Solid State Sc*. 2013;2(2):R3026-R3030.